C 51.17/12:991/12

Tech Notes

DECEMBER 1991

PB91-925912

PENNSYLVANIA STATE UNIVERSITY
FEB 04 1992
DOCUMENTS COLLECTION
U.S. Depository Copy

Technology fact sheets from Federal laboratories

NTIS
U.S. DEPARTMENT OF COMMERCE
National Technical Information Service
Center for the Utilization of Federal Technology

U.S. DEPARTMENT OF COMMERCE
Robert A. Mosbacher, Secretary of Commerce

National Technical Information Service
Joseph F. Caponio, Director

ISSN 0889-8464

COPYRIGHT WARNING
International Copyright © National Technical Information Service, 1991. All portions of this publication are protected against copying or other reproduction outside of the United States under the provisions of Article II of the Universal Copyright Convention. United States copyright is not asserted under the United States Copyright Law, Title 17, United States Code.

The Secretary of Commerce has determined that the publication of this periodical is necessary in the transaction of the public business required by law of this department. Use of funds for printing this periodical has been approved by the Director of the Office of Management and Budget through 1991.

Tech Notes

Highlighting Selected U.S. Government Technology & Resources

December 1991

Contents

Agriculture & Food 885
Computers 889
Electrotechnology 895
Energy 909
Engineering 911
Environmental Science & Technology 934
Manufacturing, Machinery & Tools 937
Materials 949
Medicine & Biology 957
Natural Resources Technology & Engineering 964
Physical Sciences 965
Transportation & Components 970

Published monthly by the National Technical Information Service (NTIS), Tech Notes bring together individual one- to two-page fact sheets prepared by Federal agencies, their laboratories, or contractors. These fact sheets highlight current Federal technology determined to have commercial or practical application. Topics cover new processes, materials, techniques, software, instrumentation, and resources.

Some of the current sources are the Department of the Navy, Department of the Army, NASA, Department of Energy, Environmental Protection Agency, Department of the Interior, and the Department of Agriculture.

Special assistance is provided by the Federal Laboratory Consortium.

Change of address or questions concerning subscriptions should be sent to:
Subscriptions Department
National Technical Information Service
Springfield, VA 22161
(703) 487-4630

Suggestions, comments, or questions concerning Tech Notes should be directed to:
Tech Notes Editor
Room 300B F
National Technical Information Service
Springfield, VA 22161
(703) 487-4805

How to Use Tech Notes

Every Tech Notes fact sheet lists a source for additional information. The source of this information may be a special support package from the originating agency, a personal contact, a licensing opportunity, or a backup report available from NTIS.

Each fact sheet also is perforated to allow for easy removal for those subscribers who may wish to keep a special fact sheet file or route to others in their organization

Sources of Further Backup Information

Below are two representative examples of how each Tech Note fact sheet provides you with a source of further information. In most cases, this information is provided directly by the agency or its laboratory.

However, there are cases where NTIS is the source for backup documentation. In these cases, use the order form at the end.

Examples:

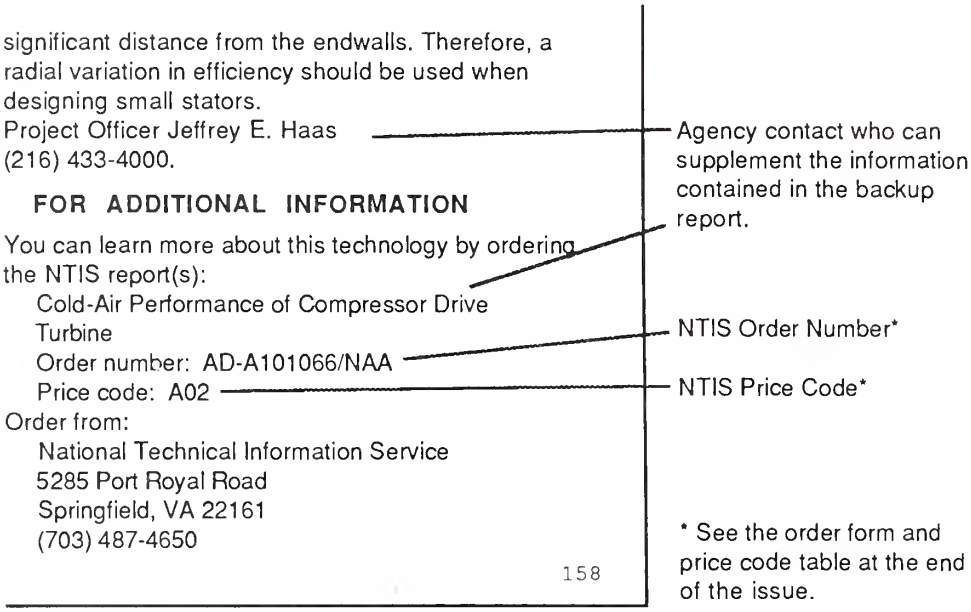
significant distance from the endwalls. Therefore, a radial variation in efficiency should be used when designing small stators.
Project Officer Jeffrey E. Haas
(216) 433-4000.
FOR ADDITIONAL INFORMATION
You can learn more about this technology by ordering the NTIS report(s):
Cold-Air Performance of Compressor Drive Turbine
Order number: AD-A101066/NAA
Price code: A02
Order from:
National Technical Information Service
5285 Port Royal Road
Springfield, VA 22161
(703) 487-4650
158
Agency contact who can supplement the information contained in the backup report.
NTIS Order Number*
NTIS Price Code*
* See the order form and price code table at the end of the issue.

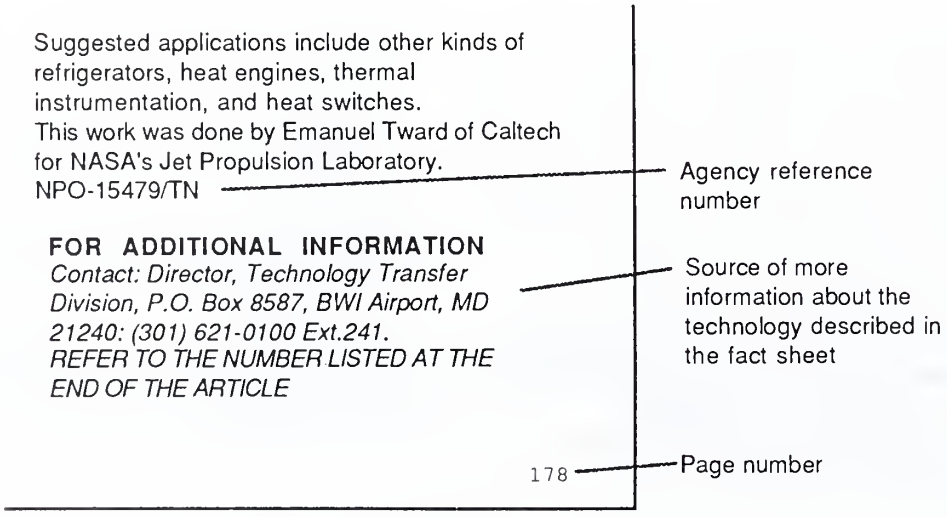
Suggested applications include other kinds of refrigerators, heat engines, thermal instrumentation, and heat switches.
This work was done by Emanuel Tward of Caltech for NASA's Jet Propulsion Laboratory.
NPO-15479/TN
FOR ADDITIONAL INFORMATION
Contact: Director, Technology Transfer Division, P.O. Box 8587, BWI Airport, MD 21240: (301) 621-0100 Ext.241.
REFER TO THE NUMBER LISTED AT THE END OF THE ARTICLE
178
Agency reference number
Source of more information about the technology described in the fact sheet
Page number

Tech Notes Title List for December 1991

Agriculture & Food

0885 Altered Biocontrol Proves Effective Against Damping-Off Disease

0886 Enzyme Could Change Sugar's Role

0887 Grasp at Straws, Irrigators are Advised

0888 Irrigation Tubing Does Double Duty

Computers

0889 Software Allows Interactive, Simultaneous Design Sessions

0890 List Processing Coprocessor Developed

0891 Distributed-Computer System Optimizes SRB Joints—Productivity is enhanced fourfold.

0892 Video Pipeline Tree for Scan Conversion of Triangles—Scenes containing many polygons could be generated in real time.

0893 Processor Reformats Data for Transmission in Bursts—The source and sink of data can operate asynchronously.

Software

0894 Design and Analysis of Linear Control Systems—Programs implement root-locus and frequency-response methods.

Electrotechnology

0895 Code Compressor for Multilevel Interleaved Multiplexed Noise Codes (Licensing Opportunity)

0896 Code Generator for Multilevel Interleaved Multiplexed Noise Codes (Licensing Opportunity)

0897 C.W. Interference Canceling System for Spread Spectrum Signals

0898 ESD Video Available

0899 Architecture for Intelligent Control of Robotic Tasks—An optimized data-abstracting hierarchy would plan, execute, and correct at acceptable high rates.

0900 Five-Segment Interconnection for Electromigration Tests—A test pattern would conform to standards.

0901 Microwave Oscillator Would Have Reduced Phase Noise—Performance would rival that of an oscillator stabilized by a quartz crystal. (Licensing Opportunity)

0902 Preventing Aim at an Undesired Target—Avoidance-control logic interrupts normal attitude-control logic when necessary. (Licensing Opportunity)

0903 Quasi-Optical Millimeter-Wavelength Resonator—The design can be scaled to wavelengths too small for conventional waveguide technology. (Licensing Opportunity)

0904 Reducing Cross-Polarized Radiation From a Microstrip Antenna—Electromagnetic modes of higher order are suppressed.

0905 Spatial Light Modulator Would Serve as Electronic Iris—The brightness of the image would be adjustable in many discrete steps. (Licensing Opportunity)

0906 Stirling-Cycle Cooling for Tunable Diode Laser—Small coolers can simplify laboratory spectroscopy and lighten airborne instruments.

0907 Switched-Capacitor Voltage Multiplier—High voltage is generated without a transformer (Licensing Opportunity)

0908 Thermal Strap and Cushion for Thermoelectric Cooler—The strap would flex in three orthogonal directions to absorb stress and vibration. (Licensing Opportunity)

Other Items of Interest

0910 Betavoltaics of Increased Power—Long-lived cells would derive power from radioactive sources.

0946 Rapid Dry Etching of Photoresists Without Toxic Gases—A room-temperature process may not damage underlying semiconductor wafers. (Licensing Opportunity)

0950 Alternative AlxGa1-xAs/GaAs Transistors for Neural Networks—Current gain is increased through reduction of bulk leakage and surface-recombination currents.

0951 GaAsP Photodiodes as X-Ray Detectors—GaAsP cells cost less than Si cells do and are less damaged by radiation.

0952 High-Gain AlxGa1-xAs/GaAs Transistors for Neural networks—Darlington pairs exhibit current gains of 4,000. (Licensing Opportunity)

0953 High-Power AlGaAs Quantum-Well Lasers on Si Substrates—Improved devices are made by migration-enhanced molecular-beam epitaxy and metalorganic vapor-phase epitaxy.

0965 Magnetic Effects Measured

0971 Electromagnetic Interference in New Aircraft—Updated standards will reflect a more severe environment and vulnerabilities of modern avionics.

Energy

0909 Improving the Thermal Efficiency of Masonry Building Walls

0910 Betavoltaics of Increased Power—Long-lived cells would derive power from radioactive sources.

Energy (Cont.)

Other Items of Interest

0892 Video Pipeline Tree for Scan Conversion of Triangles—Scenes containing many polygons could be generated in real time.

0917 Solar-Powered Cathodic Protection System Developed

Engineering

0911 Abandoned Mine Lands Program
Repairing Stream Channels to Reduce Water Loss into Underground Mines

0912 Abandoned Mine Lands Program
The Effectiveness of Surface Seals on Coal Seam Fire Control

0913 Innovative Roof Bolt Support Systems

0914 Redistributed Explosive Charges Reduce Rockfall At Surface Mines

0915 Reduction in Rockfall and Blast-Produced Overbreak in Underground Mines

0916 Correlation of Elastic-Plastic Fracture Toughness Studied

0917 Solar-Powered Cathodic Protection System Developed

0918 Accounting for Compressibility in Viscous Flow in Pipes—Variations of density and velocity across the flow cross section are included in calculations.

0919 Adaptive Grids for Computations of Three-Dimensional Flows—A spring-system analogy is extended from two to three dimensions.

0920 Algebraic Model of Turbulence for Internal Flow—An enhanced eddy-viscosity approximation simplifies calculations.

0921 Docking System Would Accommodate Misalignments—The system would also absorb kinetic energy.

0922 Experiences With the JPL Telerobot Testbed—Issues and insights are discussed.

0923 Helicity-Density and Normalized-Helicity Maps of Flows—These maps clearly indicate vortexes and other important features.

0924 Low-Speed Optical Speedometer—The delay between terrain-reflectance signals from two optical sensors indicates speed.

0925 Mathematical Model for Deposition of Soot—This model is expected to be more generally applicable than prior experimental correlations have been. (Licensing Opportunity)

0926 Self-Adjusting Choke for Nozzle—The issuing stream remains coherent for greater distances despite fluctuations in pressure and/or rate of flow. (Licensing Opportunity)

0927 Strain Center for Analysis of Forces—After yielding, forces are perpendicular to radii from the strain center.

0928 Zero-Spring-Rate Mechanism/Air Suspension Cart—A compact mechanism suspends articulating flexible structures with minimal constraints. (Licensing Opportunity)

0929 Vapor-Resistant Heat-Pipe Artery—New features of the wick improve the return of liquid in a heat pipe.

Software

0930 Program for Elastoplastic Analyses of Plane Frames—Nonlinear collapse phenomena are simulated by iterative linear analyses.

Testing & Instrumentation

0931 Fire Testing Toll Installed

0932 Holographic Interferometry To Measure Three-Dimensional Flow—Double-exposure holography is used in studies of transonic flow near rotating blades.

0933 Liquid-Crystal Coats Help Make Flows Visible—Changes of color are rapid and reversible.

Other Items of Interest

0909 Improving the Thermal Efficiency of Masonry Building Walls

0934 Sludge Dewatering by Freezing

0947 Synchronizing Rotation of a Heavy Load—A simple setup of motors, pulleys, and belts provides both torque and synchronism.

Environmental Science & Technology

0934 Sludge Dewatering by Freezing

0935 SUSV-Towed Snow Plow

0936 Radon Removal Techniques for Small Community Public Water Supplies

Manufacturing, Machinery & Tools

0937 Intelligent Machining Workstation

0938 Clean Ingot Manufacturing Technology for Superalloy Turbine Components

0939 Customized AutoCAD Develops into CRDA

0940 ADACS for Aircraft Engine Parts

0941 Diamond Turning of Stainless Steel

0942 Robot Controlled Test Bed

0943 MTI to Establish and Operate CALS Shared Resource Center

0944 Grease Inhibits Stress-Corrosion Cracking in Bearing Race—Operating life is extended at low cost.

0945 h-Parameter Analysis of Teleoperators—An electromechanical system is characterized by a mathematical model originally developed for electrical networks.

0946 Rapid Dry Etching of Photoresists Without Toxic Gases—A room-temperature process may not damage underlying semiconductor wafers. (Licensing Opportunity)

0947 Synchronizing Rotation of a Heavy Load—A simple setup of motors, pulleys, and belts provides both torque and synchronism.

Testing & Instrumentation

0948 Monitoring Welding Images and Data Simultaneously—Data on process conditions are superimposed in real time on images of the process.

Other Items of Interest

0949 Technique Developed for Fluoride Glass Windows

Materials

0949 Technique Developed for Fluoride Glass Windows

0950 Alternative AlxGa1-xAs/GaAs Transistors for Neural Networks—Current gain is increased through reduction of bulk leakage and surface-recombination currents.

0951 GaAsP Photodiodes as X-Ray Detectors—GaAsP cells cost less than Si cells do and are less damaged by radiation.

0952 High-Gain AlxGa1-xAs/GaAs Transistors for Neural networks—Darlington pairs exhibit current gains of 4,000. (Licensing Opportunity)

0953 High-Power AlGaAs Quantum-Well Lasers on Si Substrates—Improved devices are made by migration-enhanced molecular-beam epitaxy and metalorganic vapor-phase epitaxy.

0954 Stiff, Strong Splice for a Composite Sandwich Structure—Layers of alternating fiber orientation are interposed between thin ears in an adhesive joint. (Licensing Opportunity)

Testing & Instrumentation

0955 Defect Area Determines Organic Coating

0956 Device Developed to Inspect Materials

Other Items of Interest

0941 Diamond Turning of Stainless Steel

Medicine & Biology

0957 National Cell Culture Center

0958 Accelerating Protons to Treat Cancer

0959 Compact Apparatus for Growth of Protein Crystals—Growth can be initiated and terminated automatically. (Licensing Opportunity)

0960 Research Animal Holding Facility Prevents Space Lab Contamination—A healthy environment for both rodents and human researchers is maintained.

0961 Software for Design of Life-Support Systems—A special-purpose computer program combines conventional mathematical models with an expert software system.

Testing & Instrumentation

0962 Detection of Enzymes Using Agar Gel

0963 Pocket Optometer Developed for Biofeedback Training

Natural Resources Technology & Engineering

0964 Geographical Variations in Measured Lightning Fields—Features of local terrain affect electric fields.

Physical Sciences

Testing & Instrumentation

0965 Magnetic Effects Measured

0966 Self-Heterodyne Laser-Spectrum Analyzer—Spectral widths of as little as 100 kHz can be measured.

0967 Modification of Catadioptric Telescope for Laser Velocimetry—A commercially available unit can be made to work well.

0968 Scanning X-Ray or Extreme-Ultraviolet Monochromator—The angle of incidence would be varied to change the wavelength of Bragg reflection.

0969 Three-Dimensional Acousto-Optical Spectrum Analyzer—Integration in the third dimension (time) yields superfine resolution.

Other Items of Interest

0925 Mathematical Model for Deposition of Soot—This model is expected to be more generally applicable than prior experimental correlations have been. (Licensing Opportunity)

Transportation & Components

0970 Calculating Dynamics of Helicopters and Slung Loads—Motions of multiple lifting helicopters, spreader bars, cables, and loads can be simulated numerically.

0971 Electromagnetic Interference in New Aircraft—Updated standards will reflect a more severe environment and vulnerabilities of modern avionics.

Digitized by the Internet Archive
in 2012 with funding from
LYRASIS Members and Sloan Foundation

http://archive.org/details/technotes00cent

Agriculture & Food

0885 Altered Biocontrol Proves Effective Against Damping-Off Disease

0886 Enzyme Could Change Sugar's Role

0887 Grasp at Straws, Irrigators are Advised

0888 Irrigation Tubing Does Double Duty

Research Technology
Agricultural Research Service
U.S. Department of Agriculture

Altered Biocontrol Proves Effective Against Damping-Off Disease

A beneficial biocontrol fungus that controls damping-off diseases has been altered to resist a common chemical fungicide, so farmers may one day use the two side by side to control a range of soilborne crop diseases.

ARS research associate Nina Ossanna, under the supervision of geneticist Sue Mischke, genetically altered the fungus *Gliocladium virens* to resist the fungicide benomyl. Both scientists are at the Biocontrol of Plant Diseases Laboratory in Beltsville, Maryland.

In its natural, unaltered form, *G. virens* was recently approved by the Environmental Protection Agency as a greenhouse biocontrol for damping-off diseases of flowering crops.

The diseases also attack cotton, beans, carrots, and other crops, costing more than $1 billion a year. In tests, the natural *G. virens* reduces plant loss to damping-off by 80-95 percent—similar to control offered by chemical fungicides.

Meanwhile, benomyl offers excellent control of anthracnose, fusarium wilt, leafspot, powdery mildew, and other fungal diseases. And it is one of the fungicides still permitted by the Environmental Protection Agency.

But growers couldn't even hope to use the two simultaneously to control the range of soilborne diseases victimizing their crops—at least not until now. The problem, Mischke says, was that "benomyl wipes out *G. virens* entirely under normal circumstances."

So working at the ARS Biocontrol of Plant Diseases Laboratory in Beltsville, Maryland, the researchers inserted into *G. virens* a gene from another fungus that had been mutated with ultraviolet light to resist benomyl.

The result: at least one *G. virens* strain that grows well in the presence of benomyl and that inhibits damping-off organisms in a petri dish.

SCOTT BAUER

Fungus being filtered out of this molasses solution by geneticist Sue Mischke will be mixed into soil for a biological disease control for plants. (K-4168-5)

That means that genetically engineering the fungus didn't destroy its biocontrol ability.

Currently, Mischke is conducting growth chamber tests with the new *G. virens*, damping-off disease organisms, and cucumbers to see how well the new strain protects a crop from damping-off. She applies benomyl and the *G. virens* to soil containing damping-off disease and then plants the cucumbers.

Field trials—and eventual use by fa s—may be years away, because Mischke must first obtain approval from the USDA's Animal and Plant Health Inspection Service and the Environmental Protection Agency to put a genetically engineered organism into the field.

Scientists at Mischke's laboratory had previously used ultraviolet irradiation to

develop biotypes of beneficial molds. But this is the first time a biocontrol fungus has been genetically engineered with a practical trait—not just a test trait that proves the organism can be engineered.

Sue Mischke is at the USDA-ARS Biocontrol of Plant Diseases Laboratory, BARC-West, Bldg. 011A, Beltsville, MD 20705. Phone (301) 344-4003. ◆

Research Technology
Agricultural Research Service
U.S. Department of Agriculture

Enzyme Could Change Sugar's Role

A natural enzyme identified by a U.S Department of Agriculture scientist can transform sugar into nonfattening food ingredients.

That enzyme could offer a sweet bonus to the beet and cane sugar industries if they can produce the converted sugar cheaply enough for use as noncaloric fillers, binders, and extenders for food products.

Chemist Gregory L. Cote isolated and purified the enzyme, produced by the bacterium *Leuconostoc mesenteroides*, in his laboratory at the National Center for Agricultural Utilization Research at Peoria, Ill. Known as alpha-d-glucansucrase, the enzyme converts sugar to an alternan, a carbohydrate polymer.

Before alternans, chemically classed as dextrans, can be marketed for food applications, technologies for mass-producing them must be developed, says Cote, who works for USDA's Agricultural Research Service. Alternans also would have to be tested for effects on animals and humans.

According to a recent report in Agricultural Research magazine, Cote has found strains of *L. mesenteroides* that produces dextrans that resist heat deterioration or are less sticky than those now commercially used.

Cote and his colleagues are screening a collection of bacteria for strains that make an alternan-producing enzyme in such pure form it won't have to be separated chemically from other enzymes. The added expense of chemical separation now prevents alternans from being a cost-effective choice for industry, Cote said.

He said the researchers also want to clone the gene responsible for producing alternan and to genetically engineer a microorganism to produce high yields of the enzyme.

Further studies may lead to discovery of other bacterial strains of *L. mesenteroides* containing enzymes that work more efficiently than alpha-d-glucansucrase. Such enzymes might be isolated and adapted for continuous assembly-line production of dextrans. As these goals are achieved, Cote said, uses for economical dextrans could expand.

Scientists at the Peoria center conducted earlier research on dextrans that led to invention of a blood plasma extender used during the Korean conflict of the 1950s.

Cote said he had envisioned the new alternan as a substitute for the food ingredient gum arabic. But he recently found it lacks emulsifying properties to keep food components from separating.

Researchers still may find a way to mix alternans with emulsifiers to replace part of the 25 million pounds of gum arabic now imported into the United States each year from Sudan and other countries. Gum arabic costs $1 to $3 a pound.

FOR ADDITIONAL INFORMATION: Gregory L. Cote, research chemist, Biopolymer Research, National Center for Agricultural Utilization Research, Agricultural Research Service, USDA, Peoria, IL 61604. Telephone: (309)685-4011.

Research Technology
Agricultural Research Service
U.S. Department of Agriculture

Grasp at Straws, Irrigators are Advised

Scattering a little straw in furrows can save water and reduce the soil erosion that occurs when farmers irrigate their crops.

A recent study in Kimberly, Idaho, found that wasteful water runoff from the end of the furrows can be cut nearly in half, simply by scattering 1-3 pounds of straw per 100 feet of furrow.

"The straw forms mini-dams that slow the water down, so it backs up and becomes deeper in the furrows," says Melvin J. Brown, a soil scientist who worked on the study. "Soil on the sides of the furrows is porous, so the deeper water soaks in more quickly, right towards the plant's roots."

That extra water for the roots can boost yields—as much as 62 percent in dry beans, according to Brown. He's gotten similar results in fields of sugar beets, corn, and potatoes grown in southern Idaho.

The region's silty loam soils, which are fine and powdery when dry, erode easily during irrigation.

"We've documented large reductions in soil erosion by using straw," says Brown. The results are most pronounced on fields with slopes of 2 percent or greater. These fields are more prone to erosion, so improvements are more apparent.

"Farmers can use straw selectively in areas of their fields that normally don't get enough water—like steep sections and the end of the furrow," says W. Doral Kemper, an ARS soil specialist based in Beltville, Maryland.

More uniform water distribution also helps prevent nitrate fertilizer leaching caused by overirrigation, adds Kemper, who was formerly with the Kimberly research unit.

Several private companies have developed machines that deposit straw in furrows at desired rates, which should speed adoption of the practice, Brown notes.

Recognizing the value of straw mulching, as it is called, USDA's Agricultural Stabilization and Conservation Service (ASCS), with technical assistance from another USDA arm, the Soil Conservation Service (SCS), offers a cost-sharing program for farmers who want to try the technique.

"Farmers in Canyon County, Idaho, for instance, can receive from $30 to $35 per acre with this program," says James Schmollinger, at the SCS office in Caldwell, Idaho. So far, those taking advantage of the program have seen real benefits in saving both soil and water. Note, however, that the amount of government support varies from county to county.

Melvin J. Brown is with the USDA-ARS Water Management Research Unit, 3793N, 3600E, Kimberly, ID 83341. Phone (208) 423-5582. ◆

Research Technology
Agricultural Research Service
U.S. Department of Agriculture

Irrigation Tubing Does Double Duty

Farmers who grow crops under furrow irrigation could save hours of labor every time they water, using a new modification to layflat irrigation tubing recently patented by ARS agricultural engineer Allan S. Humphreys and Ed E. Oest, an irrigation equipment engineer and dealer from Fruita, Colorado.

Use of the modified tubing holds promise for conserving water, reducing leaching of agricultural chemicals, and in some cases, reducing erosion, says Humphreys, who is at the ARS Soil and Water Management Research Unit in Kimberly, Idaho.

Such problems concern farmers who raise crops on the 58 million acres of irrigated land throughout the United States. About 40 percent of that land is watered by furrows—the shallow trenches dug between crop rows that channel water across fields.

Regular layflat tubing, made with flexible materials such as rubber, vinyl, or polyethylene- or vinyl-reinforced polyester has been used by farmers for years. It's a low-cost alternative to rigid surface pipes made of metal or PVC (polyvinyl chloride). It is used to convey water to the field, or it can be fitted with outlets or gates to dispense water directly into individual furrows.

Humphreys' invention uses one layflat tube instead of the two previously required by combining conveyance and distribution into a single tube. The key is a flexible inner membrane that can move from side to side within the tube, so water can either pass through the tube or flow from outlets in the side of the tube into the furrows.

The tubing lengths vary from about 100 to 300 feet, which corresponds to an irrigation "set." Both the amount of water available—based on a farmer's

ALLAN HUMPHERYS

A membrane running lengthwise in this irrigation tubing shunts water into the furrows or with a simple move of a valve channels it through the tubing to more distant furrows or another field.

water delivery—and the capacity of the irrigation system limit the area that farmers can irrigate during a given time. So they divide their fields into segments, or sets of furrows, that are irrigated one set at a time.

Diverter valves and couplers, made from short sections of metal or PVC pipes, connect individual lengths of tubing.

Humphreys tested the new tubing on 45 acres of furrow-irrigated barley, corn, and alfalfa during the 1989-90 growing seasons. On a farm near Grandview, Idaho, the new system replaced a ditch irrigation system.

"Now, instead of moving and setting 60 siphon tubes many times during an irrigation, the irrigator simply pulls a handle on the manual valves," says Humphreys. The farmer, who had kept the ditch available in case the new system failed, recently filled it in, because the new tubing worked so well, Humphreys noted.

This spring, Humphreys began testing the system on 30 acres of cotton and 30 acres of processing tomatoes in collaboration with ARS researchers Claude J. Phené, James E. Ayars, and Harry I. Nightingale at the Water Management Research Unit in Fresno, California.

There, the researchers will use an even more advanced version of the system. The diverter valves are equipped with electric timers that automatically switch the irrigation sets. Small solar panels, about the size of a sheet of paper, sit atop the valves, providing power to run the timers.

The main advantage, says Phené, is making irrigation more uniform within a field. Changing sets manually can lead to delays, which may result in overwatering. That can increase the likelihood of erosion and leaching of agricultural chemicals.

Back in Colorado, Oest is busy working on ways to mass-produce the tubing for commercial use.

Allan S. Humphreys is with the USDA-ARS Soil and Water Management Research Unit, Route 1, 3793 N 3600 E, Kimberly, ID 83341 (208) 423-6514. Claude J. Phené, James E. Ayars, and Harry I. Nightingale are with the USDA-ARS Water Management Research Unit, 2021 S. Peach Ave., Fresno, CA 93727. Phone (209) 453-3122. ◆

Computers

0889 Software Allows Interactive, Simultaneous Design Sessions

0890 List Processing Coprocessor Developed

0891 Distributed-Computer System Optimizes SRB Joints—Productivity is enhanced fourfold.

0892 Video Pipeline Tree for Scan Conversion of Triangles—Scenes containing many polygons could be generated in real time.

0893 Processor Reformats Data for Transmission in Bursts—The source and sink of data can operate asynchronously.

Software

0894 Design and Analysis of Linear Control Systems—Programs implement root-locus and frequency-response methods.

Technology Application

Sandia National Laboratory

Software Allows Interactive, Simultaneous Design Sessions

Design engineers in different locations could work together on a design that they all can see, manipulate, and change at the same time on their computer screens, using new prototype software developed at Sandia National Laboratories.

Sandia has developed prototype interactive concurrent engineering (ICE) software for this purpose. It allows high-resolution graphics output from a computer-aided design (or any other kind of) program to be simultaneously viewed and manipulated by people in several locations. Each collaborator sees the design displayed on his or her screen and can have full control over it by using the keyboard and mouse.

The hope is that by sharing a design session, collaborators at different places can produce higher quality designs at less cost and in less time than if each were to work separately on the design.

Although the software was designed to link up engineers who use computer-aided-design (CAD) packages, it could also be used in the same way with desktop publishing or many other computer-aided tools.

"Computer-supported collaboration will change the way that people do their jobs by increasing the quantity and quality of interactions betwen co-workers," says Sandia computer scientist Craig D. Dean, developer of the prototype. "The notion is applicable to any situation where co-workers need to work together, but find it more convenient to be at different locations." He says the concept is as general and applicable as a telephone, the fax, and voice/electronic mail.

Speeds designs, cuts travel

"This capability offers significant benefits in the product engineering process—reduced time for design iterations, improved technical understanding, and less need for travel and formal changes," says Dean.

In 1989, Sandia's Engineering Network Development Division was asked to assess how or if engineers separated by distance—at laboratory or manufacturing facilities in different states, for example—could simultaneously view and modify designs using computer and communications technology. The hope was to reduce the burden and cost of travel while increasing the amount and quality of interactions between co-workers.

Computer users have already been networked, but the desire, says Dean, was to take networking a step further: to find ways that engineers could simultaneously use their separate machines just as if there really was only one physical machine that they were sharing.

The prototype interactive concurrent engineering software he has developed and demonstrated in recent months allows that.

"Fundamentally," says Dean, "we believe that ICE will change our working relationship from, 'I'll make some changes then you can review them and let me know' to something like, 'Let's look at the effect of changing this together and make a decision about such a change right now.'"

Should improve manufacturability

The method can also contribute to improved manufacturability of designs. A major problem facing high-tech manufacturers is that the designers and manufacturers usually work separately, and something about a particular design—something that might easily have been avoided—may make the product difficult to produce.

"We want to get the designers and the responsible people at the manufacturer sitting together at the design stage," says Dean.

Using interactive concurrent engineering early in the design process will allow the designer and manufacturer to go through many iterations in the design together before a design is formally agreed upon. As a result fewer changes will have to be made in formally released designs.

The ICE method links up high-resolution, window-oriented software environments now becoming commonplace in engineering. It can be implemented on any workstation supporting the so-called X Window™ environment. With X Windows, engineers can use multiple applications simultaneously in windows.

Dean's prototype ICE software proves the feasibility of simultaneously sharing applications with widely different workstations in different locations, as long as they are using X Window systems. "We leveraged the X Window up to another level," he says. A variety of different computationally intensive, graphics-oriented CAD packages have been used.

X Windows run on almost all workstation platforms. Workstations have substantially more computational power than personal computers (PCs), and they don't

have PCs' limitations on communications bandwidth, remote mouse support, hardware platform independence, and operating system independence.

Dean points out that the ICE program remains prototypical in several ways. The code was never designed with production use in mind but only as a matter of proof-of-concept. He says several person-years of work will be needed to bring it to the point where it could be made generally available as a production version. Sandia is looking for an industrial partner to share the rewards and risks; several potential ones have already indicated interest.

"Although we have produced only a laboratory prototype," concludes Dean, "it is clear that the capability will be computer-platform independent, relatively inexpensive, and will not require application software modifications or elaborate database control mechanisms." *Technical Contact: James R. Yoder (505) 845-9045.*

FOR ADDITONAL INFORMATION: Department of Energy, Sandia National Laboratories, Albuquerque, NM 87185-5800.

NAVY
Domestic Technology Transfer Fact Sheet

List Processing Coprocessor Developed

The Naval Avionics Center (NAC), Indianapolis, Indiana, has developed a list processing coprocessor, referred to as the List Chip. The chip provides a fast, low-cost method for 16-bit microprocessors to perform list processing functions in hardware. Without the use of this chip, generic 16-bit microprocessors have to perform list processing in software. In benchmark tests, the List Chip displayed a 24 times speed improvement over the best software implementation of list processing functions.

The List Chip is easily adapted to the requirements of the user. By programming the internal registers, the List Chip is configured to a particular list structure. The interface to the host microprocessor is dual-port memory, which contains the data to be processed, as well as a control block for passing instructions and results between the host and the chip.

For Additional Information:

Backup material on this effort is available from:

Navy Domestic Technology Fact Sheet Reader Reply Service
Code E211
Naval Surface Weapons Center
Dahlgren, VA 22448-5000
(703) 663-8921

Refer to 160906/TN

NASA Tech Brief
National Aeronautics and Space Administration
Langley Research Center, Hampton, Virginia

Distributed-Computer System Optimizes SRB Joints

Productivity is enhanced fourfold.

Initial calculations of a redesign of the joint on the solid rocket booster (SRB) that failed during the Space Shuttle tragedy showed that the redesign increased the weight. Optimization techniques were to be applied to determine whether the weight could be reduced while keeping the joint closed and limiting the stresses. To enable engineers to examine as many alternatives as possible, an analysis system was developed by use of existing software that coupled structural analysis with optimization computations.

The software of this system was designed to be executable on a network of computer workstations. This system took advantage of the parallelism offered by the finite-difference technique of computing gradients to enable several workstations to contribute simultaneously to the solution of the problem. The resulting system reduced the time to complete one optimization cycle from 2 hours to one-half hour, with a potential of reducing it to 15 minutes.

The major tools used for this project were the hardware (DEC MicroVAX computer workstations and DEC 11/785 minicomputer), the software (PROSSS, Programming System for Structural Synthesis), and the networks (DECnet and LaRCNET).

PROSSS, a system of computer programs that combines structural analysis and optimization, was chosen as the software tool because the majority of the code in PROSSS was independent of the type of problem being solved. In addition, PROSSS had been converted earlier to run on the workstations and had been verified with the standard test cases. EAL (Engineering Analysis Language) was chosen for the structural analysis.

The workstations and central minicomputer complex were connected by the two networks. The DECnet (the DEC software and hardware that enable different DEC operating systems to operate as a network) connected the workstations through an Ethernet circuit. The LaRCNET is the local-area network developed specifically for NASA's Langley Research Center to provide a center-wide capability for transferring data files among distributed systems of computers from multiple vendors.

Initially, PROSSS was executed sequentially on a single workstation. With a four-workstation distributed system, time was decreased by approximately a factor of 4. One workstation was used as the controlling system. The front processor, run as a stand-alone program on the controlling workstation, was modified to loop through the design variables, perturbing them one at a time and creating a separate file for each design variable with the changed shape in the form of updated joint locations. All workstations were sent a command file with checks to prevent them from executing until all of the required data were available. Once the analysis of the mathematical model with a perturbed shape was completed, an EAL library file containing the objective function, stresses, and reactions was sent to the controlling workstation. If the model was optimized, the system stopped; otherwise, it looped back to the front processor to begin a new cycle with a new shape determined by the change in the design variables.

The software system that couples structural analysis and optimization has been successfully distributed over this network of workstations. By distributing the workload over four workstations instead of just one, the time required to complete an optimization cycle decreased from 2 hours to one-half hour. Because of the enhanced productivity achieved with the distributed system, engineers were able to test more alternatives in a shorter time. The key features were the effective use of redundancies in hardware (multiple workstations and two networks) and flexible software, which enabled the optimization to proceed with minimal delay and decreased overall time to completion.

This work was done by James L. Rogers, Jr., Katherine C. Young, and Jean-Francois M. Barthelemy of **Langley Research Center**. *Further information may be found in NASA TM-89108 [N87-19022], "Distributed Computer System Enhances Productivity for SRB Joint Optimization."*

Copies may be purchased [prepayment required] from the National Technical Information Service, Springfield, Virginia 22161, Telephone No. (703) 487-4650. Rush orders may be placed for an extra fee by calling (800) 336-4700.

LAR-14311/TN

FOR ADDITIONAL INFORMATION: *Contact: Director, Technology Transfer Division, P.O. Box 8757, BWI Airport, MD 21240; (301) 621-0100 Ext. 241*

REFER TO THE NUMBER LISTED AT THE END OF THIS ARTICLE

NASA Tech Brief
National Aeronautics and Space Administration
Ames Research Center, Moffett Field, California

Licensing Opportunity

Video Pipeline Tree for Scan Conversion of Triangles

Scenes containing many polygons could be generated in real time.

A video pipeline subsystem having a branched structure would perform the scan conversion of polygons in images generated by computers. Heretofore, the conversion of computer-generated image coordinates, brightnesses, and colors of polygons to raster-scanning video signals could not be done rapidly enough for the generation of realistic images containing many polygons at the standard television rate of 30 frames per second. The new subsystem would divide the polygons into triangles, each of which would be processed rapidly in parallel, modular fashion and merged into the image. One proposed version, to consist of 127 integrated-circuit chips, could render 1,000 triangles in real time.

Figure 1 illustrates schematically a portion of the scan conversion of one triangle. The three control signals that define the raster are broadcast from a central controller to all such circuits. In synchronization with the raster video signal, this circuit would compute a color, the coordinate z (depth perpendicular to the image plane), or another linear function of the image coordinates x and y, using $z = ax + by + c$. The coefficients a, b, and c would be obtained from the computer specification of the image and would be used to compute the coefficients A, B, and C, which would be held in registers A, B, and C, respectively.

Seven such linear-function circuits would be combined into a module to produce a stream of data representative of one triangle. The seven functions would be z, red, green, blue, and three edge functions. Altogether, the data stream would be 49 bits wide: 24 bits for z, 8 bits for each color intensity, and a transparency bit that indicates whether the current picture element is inside or outside the triangle (if outside, then the other bits have no meaning and are to be ignored). The number of bits used in the internal computations of the linear-function circuit would be greater than the number of bits in the data streams.

A large number of these triangle modules would feed their 49-bit output data streams into the "leaves" of a binary tree at the standard video rate of about 10 MHz. At each branch point of the tree, a merging module would combine two of the data streams into one (see Figure 2). Of the two inputs to each merging module, one would be selected for output: If both picture elements were transparent, either could be selected. If one were opaque and the other transparent, the opaque one would be selected. If both were opaque, the one with the smallest value of z (the one in front) would be selected as in a standard z-buffer algorithm. The output of each merging module would serve as the input to a merging module at the next level of the tree.

As many triangle modules as possible would be put onto one integrated-circuit chip so that the chip would constitute a complete binary tree of merging modules with a triangle module at each "leaf." The chip would therefore have output pins for the 49-bit video-data stream emerging from the tree. The chip would also have address and data pins so that the "front-end" processor that performs the geometric transformations and calculates the coefficients for the triangles could write the coefficients into the chip.

Many such triangle chips could be built into a larger binary tree, connected by merging-module chips. Because it would contain only the merger logic, a merging-module chip would be relatively simple. However, it would require a total of 147 pins for the two 49-bit inputs and one 49-bit out-

Figure 1. A **Linear Function z of Image Coordinates x and y** is generated in synchronism with the video raster signal. Thus, $z(x,y)$ represents the function (depth or color) associated with the coordinates of the current picture element (x,y) in the video signal. The registers A, B, and C contain the coefficients of the function, which can change with time.

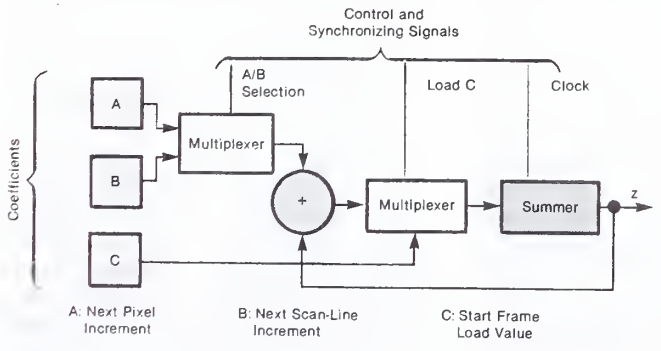

Figure 2. **Video Data From Triangle Modules Are Merged** in a binary tree by preferential selection according to transparency, opacity, and depth values. In the final merged video-data stream, the irrelevant data (representing hidden picture elements and the like) have all been suppressed, leaving only the scan-converted color and brightness signals for the visible portions of the polygons in the synthetic image. The symbols α, z, R, G, and B denote the transparency, depth coordinate, red, green, and blue signals, respectively.

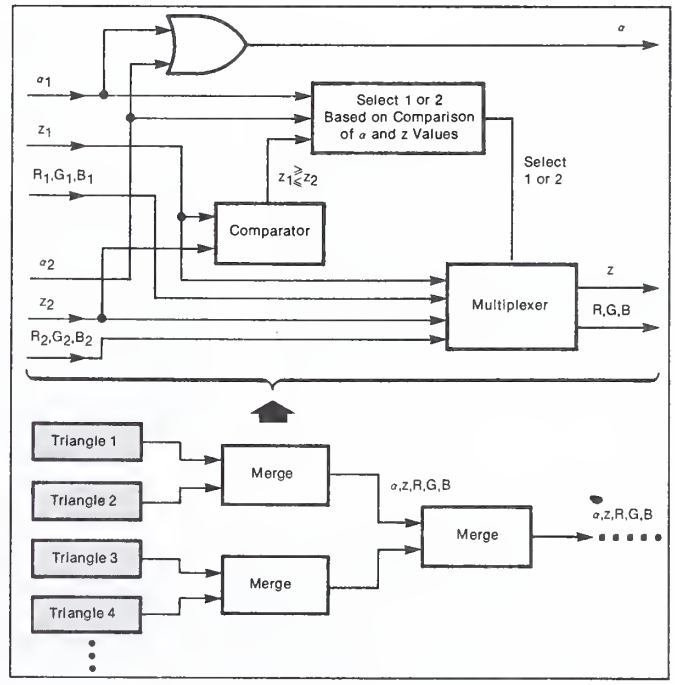

put. It might be possible to reduce the number of pins and, therefore, the cost, by time-multiplexing the data onto fewer pins at a higher bit rate.

An alternative design would be a linear pipeline of triangle chips, in which each triangle chip had a 49-bit input feeding into one leaf of its internal merge tree. The control signals would have to be staggered for the triangle chips in this linear pipeline. The merge chips would not be needed.

This work was done by Warren Robinett of **Ames Research Center.**

Inquiries concerning rights for the commercial use of this invention should be addressed to the Patent Counsel, Ames Research Center. Refer to ARC-11661/TN.

Ames Research Ctr.
Technology Utilization Officer: Laurance Milov
Mail Code 223-3
Moffett Field, CA 94035
(415) 694-4044
Patent Counsel:
Darrell G. Brekke
Mail Code 200-11
Moffett Field, CA 94035
(415) 694-5104

FOR ADDITIONAL INFORMATION: *Contact: Director, Technology Transfer Division, P.O. Box 8757, BWI Airport, MD 21240; (301) 621-0100 Ext. 241*
REFER TO THE NUMBER LISTED AT THE END OF THIS ARTICLE

NASA Tech Brief
National Aeronautics and Space Administration
Lyndon B. Johnson Space Center, Houston, Texas

Processor Reformats Data for Transmission in Bursts

The source and sink of data can operate asynchronously.

A data-processor-and-buffer electronic system receives audio signals digitized in a first standard format at a relatively low data rate (1.554 Mb/s), rearranges these data for transmission in bursts in a second standard format at a relatively high rate (150 Mb/s), stores the second-format bursts, and releases the second-format bursts at the higher rate upon request. Although the system was conceived for the asynchronous, one-way transmission of digitized speech in outer-space communications, the concept of the system could be applied in other digital communication systems in which data are transmitted from low-rate sources to high-rate sinks that are not synchronized with the sources.

The system (see Figure 1) includes an input processor (which also acts as an "input-state machine"), a dual-port random-access memory, and an output processor ("output-state machine"). The random-access memory serves as the buffer memory. It is divided into eight parts, each of which can hold one of the second-format bursts, which are called "transfer frames."

Operation begins when the input processor detects an incoming (first-format) frame of data. The input processor so notifies the buffer memory by sending it a transfer-frame header. The input processor then repeatedly encapsulates the incoming first-format frames into packets of data of the second format and packs the second-format packets into the transfer frame that is being assembled in the buffer memory. When this transfer frame has been filled, the input processor notifies the output processor that this transfer frame is available. In turn, the output processor notifies the sink of data that this transfer frame is available. Meanwhile, the input processor begins to pack a new transfer frame into the buffer memory, and this processor continues as long as the first-format data continue to come in (provided that there is still room in the buffer memory).

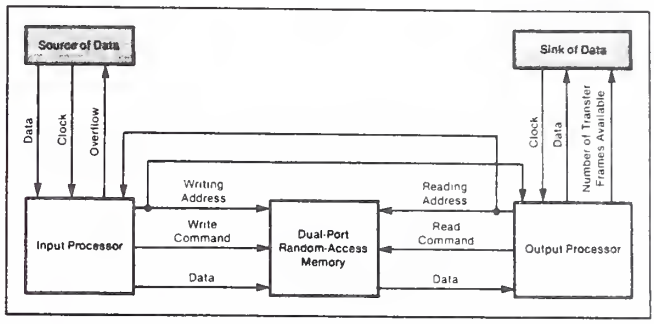

Figure 1. **Digitized Low-Rate Data** (e.g., audio) signals from the source are reformatted, buffered, and transferred to the sink in bursts called "transfer frames."

When the sink signals a request for a transfer frame, the output processor responds by transferring that frame immediately from the buffer memory to the sink and indicating to the input processor that the portion of the buffer that stored that transfer frame is now available to hold a new transfer frame.

The input processor sends, to the output processor, the number (address) of the segment of random-access memory into which it is writing data. Similarly, the output processor tells the input processor the address of the segment from which it is reading data. Both processors step through the segments of the memory in the same prescribed, repeating sequence (see Figure 2). To prevent overflow, the writing address must not be allowed to get so far ahead of the reading address that it catches up with the reading address from behind in the repeating sequence. To prevent underflow, the reading address must not be allowed to catch up with the writing address. The output processor determines how many transfer frames are available for output by noting how far the writing address is ahead of the reading address.

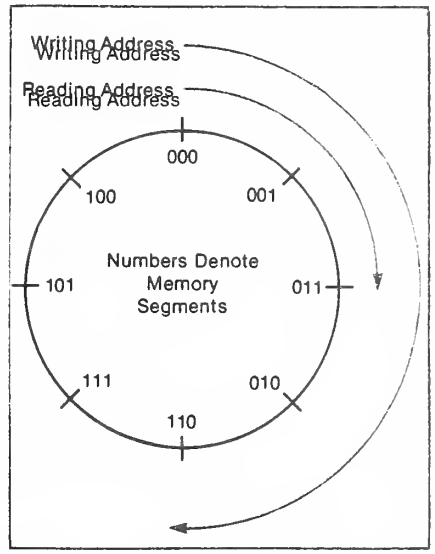

Figure 2. The **Addressing Scheme** for writing to and reading from the dual-port random-access memory is a repeating sequence. The addresses of the memory segments are put in gray code instead of normal binary sequence because this prevents the input and output processors from incorrectly perceiving asynchronous changes in the reading and writing addresses, respectively.

This work was done by Glen F. Steele of **Johnson Space Center.**
MSC-21727/TN

FOR ADDITIONAL INFORMATION: *Contact: Director, Technology Transfer Division, P.O. Box 8757, BWI Airport, MD 21240; (301) 621-0100 Ext. 241*
REFER TO THE NUMBER LISTED AT THE END OF THIS ARTICLE

Design and Analysis of Linear Control Systems

Programs implement root-locus and frequency-response methods.

A package of five computer programs was developed by the Kennedy Space Center Robotics Laboratory to assist in the design and analysis of linear control systems by the use of root-locus and frequency-response methods. The BODE program calculates magnitude and phase as a function of frequency. The Laplace transform is expressed as a ratio of factors and their reciprocals. Factors may be first- or second-order polynomial terms. The transport-lag factor and minimum- and non-minimum-phase factors are taken into account. BODE can be used to determine the general shape of the magnitude-versus-frequency curve, with options to investigate peaks of interest more closely.

The LOCUS program calculates the roots of a closed-loop characteristic equation for positive or negative gain. KTUNE, a modified version of LOCUS, allows small gain variations to establish break-in or breakaway positions and the gain corresponding to a specified damping ratio. TPEAK calculates the approximate time to peak overshoot of a closed-loop system. The program assumes that a pair of dominant complex poles characterize the system. The POLYROOT program determines the roots of polynomials. POLYROOT output aids in formulating the factored input to BODE and LOCUS. All programs require the user to set parameter switches inside the source code and alter DATA statements to specify the input.

The package is written in FORTRAN (BODE, TPEAK) and BASIC (LOCUS, KTUNE, and POLYROOT) for batch execution. The programs have been implemented on a DEC VAX computer operating under VMS with a central-memory requirement of approximately 8K of 8-bit bytes. The program was developed in 1986.

This program was written by John W. Jamison of **Kennedy Space Center.**
KSC-11376/TN

FOR ADDITIONAL INFORMATION

CONTACT

COSMIC®
112 Barrow Hall
University of Georgia
Athens, GA 30602

(404) 542-3265

Electrotechnology

0895 Code Compressor for Multilevel Interleaved Multiplexed Noise Codes (Licensing Opportunity)

0896 Code Generator for Multilevel Interleaved Multiplexed Noise Codes (Licensing Opportunity)

0897 C.W. Interference Canceling System for Spread Spectrum Signals

0898 ESD Video Available

0899 Architecture for Intelligent Control of Robotic Tasks—An optimized data-abstracting hierarchy would plan, execute, and correct at acceptable high rates.

0900 Five-Segment Interconnection for Electromigration Tests—A test pattern would conform to standards.

0901 Microwave Oscillator Would Have Reduced Phase Noise—Performance would rival that of an oscillator stabilized by a quartz crystal. (Licensing Opportunity)

0902 Preventing Aim at an Undesired Target—Avoidance-control logic interrupts normal attitude-control logic when necessary. (Licensing Opportunity)

0903 Quasi-Optical Millimeter-Wavelength Resonator—The design can be scaled to wavelengths too small for conventional waveguide technology. (Licensing Opportunity)

0904 Reducing Cross-Polarized Radiation From a Microstrip Antenna—Electromagnetic modes of higher order are suppressed.

0905 Spatial Light Modulator Would Serve as Electronic Iris—The brightness of the image would be adjustable in many discrete steps. (Licensing Opportunity)

0906 Stirling-Cycle Cooling for Tunable Diode Laser—Small coolers can simplify laboratory spectroscopy and lighten airborne instruments.

0907 Switched-Capacitor Voltage Multiplier—High voltage is generated without a transformer (Licensing Opportunity)

0908 Thermal Strap and Cushion for Thermoelectric Cooler—The strap would flex in three orthogonal directions to absorb stress and vibration. (Licensing Opportunity)

Other Items of Interest

0910 Betavoltaics of Increased Power—Long-lived cells would derive power from radioactive sources.

0946 Rapid Dry Etching of Photoresists Without Toxic Gases—A room-temperature process may not damage underlying semiconductor wafers. (Licensing Opportunity)

0950 Alternative AlxGa1-xAs/GaAs Transistors for Neural Networks—Current gain is increased through reduction of bulk leakage and surface-recombination currents.

0951 GaAsP Photodiodes as X-Ray Detectors—GaAsP cells cost less than Si cells do and are less damaged by radiation.

0952 High-Gain AlxGa1-xAs/GaAs Transistors for Neural networks—Darlington pairs exhibit current gains of 4,000. (Licensing Opportunity)

0953 High-Power AlGaAs Quantum-Well Lasers on Si Substrates—Improved devices are made by migration-enhanced molecular-beam epitaxy and metalorganic vapor-phase epitaxy.

0965 Magnetic Effects Measured

0971 Electromagnetic Interference in New Aircraft—Updated standards will reflect a more severe environment and vulnerabilities of modern avionics.

U.S. Army Fact Sheet

Licensing Opportunity

Army Communications–Electronics Command

Code Compressor for Multilevel Interleaved Multiplexed Noise Codes

The object of this invention is to provide a spread spectrum perfect noise code class that compresses to a lobeless impulse (when matched filter detected) which can easily be implemented at low cost and whose quantity is virtually inexhaustible for practical time-bandwidth products or code lengths "n". Multiplexed noise codes as a class has far reaching implications and value for numerous different applications. Systems using these codes are extremely resistant to interception and interference, operate with no self-interference, eliminate the near/far ratio problem (orthogonal CDMA is provided), operate with optimum resolution for range and velocity and yields maximum measurement accuracies, can readily employ optimum RAKE diversity to counter multipath returns, provides reliable transmission, and have inexhaustible supplies of orthogonal noise code sets from which to choose.

STATE OF DEVELOPMENT

The method has been theoretically verified and demonstrated by laboratory experiment.

APPLICATIONS

Potential uses are for improved telecommunications, local area networks, personal communication networks, mobile and multiple access systems, inter-communication systems, secure transmission, switching systems, radar, air traffic control, navigation systems, electron microscopes, remote control systems and personal burglar alarm systems.

PATENT STATUS

U.S. Patent Number 4,511,885

FOR ADDITIONAL INFORMATION: Charles Grzenda, Chief, Office of Research and Technology Applications, Center for C3 Systems, ATTN: AMSEL-RD-C3-SD, Fort Monmouth, NJ 07703, Telephone (908)544-3119. Refer to Application Assessment Number 021.

U.S. Army Fact Sheet

Army Communications–Electronics Command

Licensing Opportunity

Code Generator for Multilevel Interleaved Multiplexed Noise Codes

The object of this invention is to provide a spread spectrum perfect noise code class that compresses to a lobeless impulse which can be easily implemented at low cost and whose quantity is virtually inexhaustible for practical time bandwidth products or code lengths "n". Multiplexed noise codes as a class has far reaching implications and value for numerous practical applications. Systems using these codes are extremely resistant to interception and interference, operate with no self-interference, eliminate the near/far ratio problem, operate with optimum resolution for range and velocity, can readily employ optimum RAKE diversity to counter multipath returns, provides reliable transmission and have an inexhaustible supply of orthogonal noise code sets from which to choose.

STATE OF DEVELOPMENT

The method has been theoretically verified and demonstrated by laboratory experiment.

APPLICATIONS

Potential uses are for improved telecommunications, local area networks, personal communication networks, mobile and multiple access systems, inter-communication systems, secure transmission, switching systems, radar, air traffic control, navigation systems, electron microscopes, remote control systems and personal burglar alarm systems.

PATENT STATUS

U.S. Patent Number 4,568,915

FOR ADDITIONAL INFORMATION: Charles Grzenda, Chief, Office of Research and Technology Applications, Center for C3 Systems, ATTN: AMSEL-RD-C3-SD, Fort Monmouth, NJ 07703, Telephone (908)544-3119. Refer to Application Assessment Number 020.

U.S. Army Fact Sheet

Army Communications–Electronics Command

C.W. Interference Canceling System for Spread Spectrum Signals

It is the proposed object of the invention to completely eliminate multiple continuous wave or slowly varying continuous wave interference with no loss in the received level of the desired signal for a system that uses multiplexed noise codes. Since these codes compress to a lobeless impulse, then adding its delayed code with the undelayed code results in no loss of the signal level when the delay is equal to or greater than one code chip width. The C.W. interference is eliminated by means of a variable delay line and linear adder. By adding the delayed signal to the input signal in a linear adder, a total cancellation of the interference signal occurs while the signal level of the detected noise coded desired signal remains unchanged.

State of development: The method has been theoretically verified and demonstrated by laboratory experiment.

Applications: The invention can be applied to any type of communication system that experiences continuous wave interference or slowly varying interfering signals. The greatest potential use is for meeting electronic counter-counter measure requirements.

Patent status: U.S. Patent Number 4,472,814.

FOR ADDITIONAL INFORMATION: Charles Grzenda, Chief, Office of Research and Technology Applications, Center for C3 Systems, ATTN: AMSEL-RD-C3-SC, Fort Monmouth, NJ 07703; (908)544-3119.

ESD Video Available

The Naval Sea Systems Command (NAVSEA), Washington, D.C., has released a new videotape entitled, *ESD: The Invisible Threat.* The videotape addresses electrostatic discharge (ESD) and ESD damage prevention for electronic systems. The video would be excellent for all personnel who operate, maintain, package, handle, or supervise ESD functions for electronic parts, assemblies, or equipment.

Information on the videotape can be obtained by calling E. Dandridge at the Naval Weapons Station, Concord, California, at commercial (415) 246-5490 or DSN 253-5490.

NASA Tech Brief
National Aeronautics and Space Administration
NASA's Jet Propulsion Laboratory, Pasadena, California

Architecture for Intelligent Control of Robotic Tasks

An optimized data-abstracting hierarchy would plan, execute, and correct at acceptably high rates.

A proposed architecture for the control of such robotic devices as artificial hands calls for data-abstracting hierarchies of processing, controlling, and sensing equipment that would plan, execute, and correct the movements of the devices at acceptably high rates. The architecture combines features developed in research on artificial intelligence and control theory. It is characterized by causal connections between layers of the hierarchy, approximately equal complexities of the layers, and a directed focus of attention.

The hierarchical structure of this architecture is based partly on the analysis of human behavior during control actions. While other architectures developed previously are also hierarchical, they do not take full advantage of the possibilities offered by the hierarchical approach. In some of them, for example, the various layers represent various levels of abstraction of data, but the implementation of them with standard modules is not optimal for all levels of abstraction. Also, reflex control alone is insufficient to handle a large number of operating conditions, and expert systems are too slow for use with real-time processes.

Each level of the hierarchy would correspond to a different kind of mental process. The lowest level would interact directly with sensors and actuators, processing raw sensory feedback data and motor commands and immediately activating motor responses to important feedback signals. Middle levels could recognize typical patterns in feedback signals and command more-complicated reactions according to prescribed rules. The highest levels would be dedicated to such tasks as the recognition of sequences of patterns and general planning. In ascending the hierarchy, one would encounter increasingly symbolic types of logic, including the application of Boolean rules by artificial neural networks.

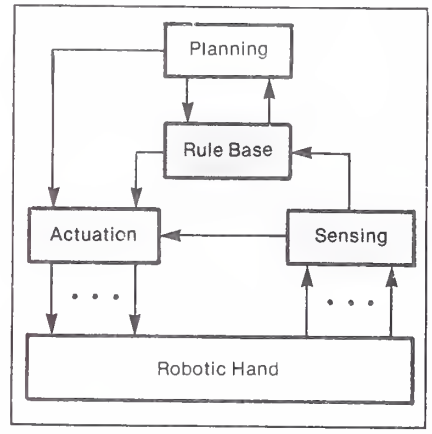

A **Three-Level Hierarchical Control System** would observe and direct the movements of an anthropomorphic artificial hand.

The figure illustrates a three-level hierarchy proposed for the control of a robotic hand. The intermediate level would be characterized by a response time and by an amount of knowledge intermediate between those of the planner (highest level) and the actuator controller (lowest level). The intermediate level would store expected relations among single feedback signals or subsets of them and would use the results to understand the evolution of a grasping task. This concept would provide for flexible reflex control in various grasping tasks and would enable the actuator controller to determine autonomously the best reaction to a given pattern of feedback signals. Both the planner and actuator controller would use feedback signals and outputs of rule-based reasoning processes to initiate modifications of actuator trajectories. When a new strategy was generated by the planner, the associated rules would be blended with the current rule base to assure a smooth transition between plans.

The use of such a hierarchical architecture to form an artificially intelligent controller has the potential for assuring immediate reactions to unexpected external conditions and for bypassing the longer processing time of the higher levels as much as possible. Such lower-level reactions would compensate for the different execution times of planning and control and fill in possible voids in the command stream. Each level would then be partly autonomous in that it could choose to continue tracking the trajectory specified by the most recently received plan or to activate a recovery procedure in case of error. Meanwhile, the error would signal the higher levels to adjust the plan.

This work was done by Paolo Fiorini and Jeffrey Chang of Caltech for **NASA's Jet Propulsion Laboratory.**
NPO-17871/TN

FOR ADDITIONAL INFORMATION: *Contact: Director, Technology Transfer Division, P.O. Box 8757, BWI Airport, MD 21240; (301) 621-0100 Ext. 241*
REFER TO THE NUMBER LISTED AT THE END OF THIS ARTICLE

NASA Tech Brief
National Aeronautics and Space Administration
NASA's Jet Propulsion Laboratory, Pasadena, California

Five-Segment Interconnection for Electromigration Tests

A test pattern would conform to standards.

A proposed integrated-circuit conductive pattern (see figure) is intended for use in electromigration lifetime testing of the interconnection lines of integrated circuits. The pattern is designed for the collection of statistics on electromigration from the smallest possible area. It includes 5 interconnection segments with Kelvin voltage taps, with a total of 12 contact pads, and provides for simultaneous measurements on all of the segments. The pattern attempts to minimize thermal gradients within each segment and conforms to the guidelines on electromigration test structures promulgated by the National Institute of Standards and Technology (NIST).

The critical design parameters are the width, W, and the length, L, of each of the test lines (the five segments); the width, W_C, and the length, L_C, of the lines that make contact with the ends of the test lines; and the width, W_I, of the current taps. From the NIST guidelines, L = 800 μm. To minimize the thermal gradients at the ends of the test lines, $W_C = 2W$, while $L_C = 10W$. To minimize both spatial and temporal nonuniformities in heating, the widths of the current taps should satisfy the relationship $W_I \geq 10W$; in the figure, $W_I = 15W$ is used.

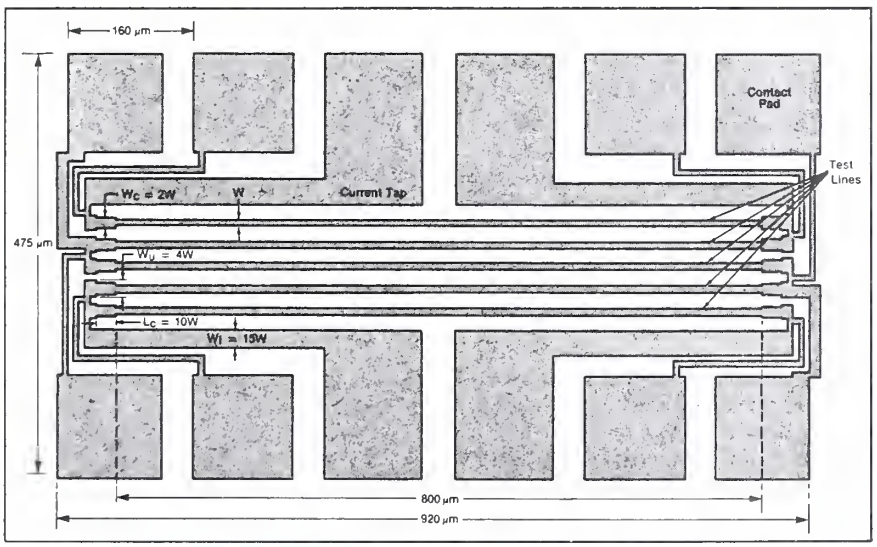

This **Integrated-Circuit Conductive Pattern** is designed for measurements that generate data on electromigration in the test lines.

The separation between adjacent test lines is not critical. The larger the separation, the smaller the thermal interaction between the test lines. However, even at separations as wide as 1,000 μm, this thermal coupling cannot be ignored and must be included in the analysis of the results of the test. In the figure, the separation between adjacent test lines is $10W$.

The U-shaped pieces that join adjacent test lines should be uniform in design to facilitate the mathematical modeling of the flow of current in resistance thermometry. A less-critical design parameter is the width, W_U, of the arms of the U-shaped pieces: W_U should equal or exceed W_C. In the figure, $W_U = 4W = 2W_C$.

The contact-pad pattern shown in the figure has twice the height of the pattern of contact-pad probes now in use at several foundries that make GaAs integrated circuits. This new pattern should facilitate both bonding and probing.

Given the size of the contact-pad pattern and the foregoing design criteria, W is constrained to be less than about 3 μm. To use wider test lines, one would have to decrease the distance between them or use fewer of them.

This work was done by David J. Hannaman and Martin G. Buehler of Caltech for **NASA's Jet Propulsion Laboratory.** *NPO-18105/TN*

FOR ADDITIONAL INFORMATION: *Contact: Director, Technology Transfer Division, P.O. Box 8757, BWI Airport, MD 21240; (301) 621-0100 Ext. 241*
REFER TO THE NUMBER LISTED AT THE END OF THIS ARTICLE

NASA Tech Brief
National Aeronautics and Space Administration
NASA's Jet Propulsion Laboratory, Pasadena, California

Licensing Opportunity

Microwave Oscillator Would Have Reduced Phase Noise

Performance would rival that of an oscillator stabilized by a quartz crystal.

Microwave oscillators of a proposed new type would incorporate a suppressed-carrier/negative-feedback feature to reduce phase noise near their carrier frequencies. Together with recent advances in the quality factors (Q's; that is, reciprocals of damping factors) of microwave resonators, the new oscillator concept could result in phase noise less than that achievable by cryogenically stabilized microwave components or by room-temperature oscillators stabilized by quartz crystals.

The new oscillator concept could be implemented in three different versions (see figure). The first version would be based partly on the established stabilized-local-oscillator concept. However, one way in which it would differ is that the signal from the resonator cavity would be returned from the input port of the cavity instead of from a second coupling port. A circulator would separate this signal from the forward driving signal. The returned signal would be fed to a phase detector in the form of a mixer. At critical coupling and on resonance, the returned signal would be identically zero. However, it would be the superposition of two nearly equal signals, one of which would emanate from the cavity and the other of which would be the reflection of the driving signal from the resonator port. At resonance, this reflected signal would not significantly affect the operation of the mixer because it would be in quadrature with the signal at the other mixer port. While the amplitude would go through zero on resonance, there would be a reversal of phase in which the in-phase signal on one side would become out of phase on the other, providing a linear dependence of the output voltage of the mixer on the frequency error, as required for effective feedback. Unlike in prior stabilized local oscillators, the returned signal would be amplified on its way to the mixer. Thus, the effective mixer phase noise would be reduced by the factor of amplifier gain. Degradation of the signal by phase fluctuations in the amplifier is prevented by carrier suppression due to the superimposed signals. Thus amplifier phase noise would also be reduced, with the amount of reduction given by the degree of carrier suppression.

The second version would resemble the first version somewhat, but the phase sensitivity would not be enhanced by amplification of the signal returned from the resonator. Instead, it would be enhanced by use of relatively high power in the high-Q resonator. The suppression of the carrier at the r port would make it possible to increase power supplied to the resonator without saturating the mixer.

The third version would be configured as a reflection oscillator with direct radio-frequency feedback. As in the first version, the signal returned from the resonator would consist of two superposed signals that would cancel at resonance if the coupling to the resonator were critical. However, here, the resonator would be slightly over-coupled, so that at resonance, the return signal would have a small, constant value. This condition can be shown theoretically to result in a reduction of the phase fluctuations by a factor that would increase with the gain of the amplifier. Because the path lengths of the circuit could give rise to large phase shifts that could cause oscillation at spurious frequencies, a band-pass filter would be incorporated to suppress such oscillations.

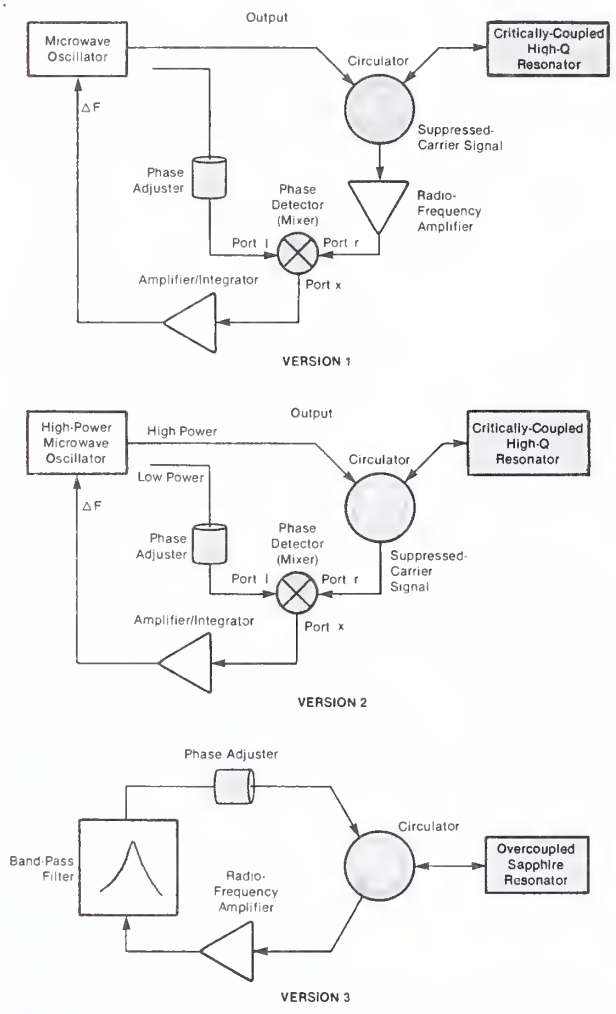

Three Versions of the Reduced-Phase-Noise Microwave Oscillator would reduce phase and frequency fluctuations via a suppressed-carrier/negative-feedback concept.

This work was done by G. John Dick and Jon Saunders of Caltech for **NASA's Jet Propulsion Laboratory.**

In accordance with Public Law 96-517, the contractor has elected to retain title to this invention. Inquiries concerning rights for its commercial use should be addressed to

Edward Ansell
Director of Patents and Licensing
Mail Stop 305-6
California Institute of Technology
1201 East California Boulevard
Pasadena, CA 91125
NPO-17945/TN

Jet Propulsion Lab.
NASA Resident Office
Technology Utilization Officer Gordon S. Chapman
Mail Stop 180-801
4800 Oak Grove Drive
Pasadena, CA 91109
(818) 354-4849
Patent Counsel Paul F. McCaul
Mail Code 180-801
4800 Oak Grove Drive
Pasadena, CA 91109
(818) 354-2734

Technology Utilization Mgr. for JPL Norman L. Chalfin
Mail Stop 156-211
4800 Oak Grove Drive
Pasadena, CA 91109
(818) 354-2240

FOR ADDITIONAL INFORMATION: *Contact: Director, Technology Transfer Division, P.O. Box 8757, BWI Airport, MD 21240; (301) 621-0100 Ext. 241*
REFER TO THE NUMBER LISTED AT THE END OF THIS ARTICLE

NASA Tech Brief
National Aeronautics and Space Administration
NASA's Jet Propulsion Laboratory, Pasadena, California

Licensing Opportunity

Preventing Aim at an Undesired Target

Avoidance-control logic interrupts normal attitude-control logic when necessary.

An electronic system that controls changes in the orientation of an optical instrument includes an avoidance-control-logic subsystem that prevents the instrument from aiming at an undesired target. For example, it could be used to protect delicate photodetectors in a servocontrolled infrared spectrometer or imaging instrument against the damage that could occur if the instrument were aimed at the Sun or another excessively bright object.

In stationary operation, another part of the overall control system controls the torque applied to the instrument in such a way as to minimize the angular error between the line of sight of the instrument and the commanded line of sight. When the instrument is commanded to turn to a new line of sight, signals from rotation-rate sensors (e.g., gyroscopes) are processed into transformed coordinates and used along with the angle-error signals to control the slew — the rapid turn through most of the angular interval between the old and new commanded orientations (see Figure 1). To obtain the shortest possible rotation, the line of sight is ordinarily slewed in the plane that contains the old and new commanded lines of sight. The desired motion is obtained by controlling the applied torques so as to make the instrument rotate about a slewing axis perpendicular to this plane.

The instrument is equipped with a Sun sensor that indicates the orientation of the line of sight to the Sun relative to the line of sight of the instrument. The avoidance control logic does not affect the motion until and unless, at some point along the slewing trajectory, these two lines of sight come within an angle θ of each other; that is, the avoidance-control logic remains inoperative until the line of sight of the instrument enters a cone of avoidance of half apex angle θ about the line of sight to the Sun.

Once activated, the avoidance control logic interrupts the normal control logic. It then calculates a succession of temporary slewing axes and associated actuator torques so as to make the line of sight follow the shorter of the two trajectories around the cone of avoidance. Once sensors indicate that the line of sight has reached the end of the trajectory around the cone of avoidance, the avoidance control logic is deactivated, the normal control logic resumes operation, and the instrument starts to turn again on the original slewing axis toward the new commanded target.

This work was done by Neil E. Goodzeit of General Electric Co. for **NASA's Jet Propulsion Laboratory.**

In accordance with Public Law 96-517, the contractor has elected to retain title to this invention. Inquiries concerning rights for its commercial use should be addressed to

William H. Meise, Patent Counsel
General Electric Co.
One Independence Wage
P.O. Box 2023
Princeton, N.J. 08540

Refer to NPO-18077/TN.

Jet Propulsion Lab.
NASA Resident Office
Technology Utilization Officer Gordon S. Chapman
Mail Stop 180-801
4800 Oak Grove Drive
Pasadena, CA 91109
(818) 354-4849
Patent Counsel Paul F. McCaul
Mail Code 180-801
4800 Oak Grove Drive
Pasadena, CA 91109
(818) 354-2734
Technology Utilization Mgr. for JPL Norman L. Chalfin
Mail Stop 156-211
4800 Oak Grove Drive
Pasadena, CA 91109
(818) 354-2240

Figure 1. The **Slew-Control System** includes avoidance-control logic, which overrides the slew-control error generator when the line of sight of the instrument comes within a cone of avoidance around the line of sight to the Sun.

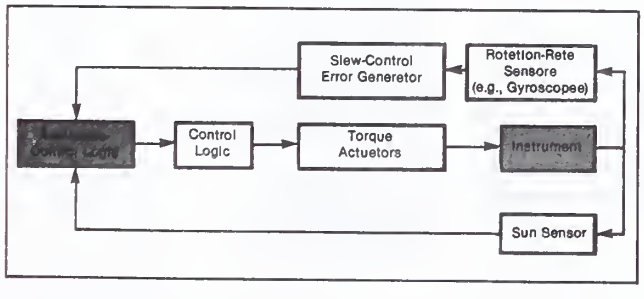

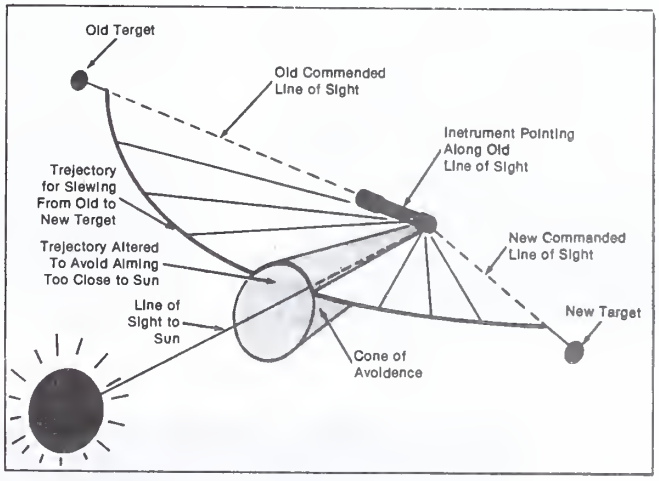
Old Terget
Old Commended Line of Sight
Inetrument Pointing Along Old Line of Sight
Trejectory for Slewing From Old to New Terget
Trejectory Altered To Avoid Aiming Too Close to Sun
New Commanded Line of Sight
Line of Sight to Sun
New Target
Cone of Avoidence

Figure 2. The **Normal Slewing Trajectory** is interrupted by the avoidance-control logic, which computes actuator torques that take the line of sight around the cone of avoidance.

FOR ADDITIONAL INFORMATION: *Contact: Director, Technology Transfer Division, P.O. Box 8757, BWI Airport, MD 21240; (301) 621-0100 Ext. 241*
REFER TO THE NUMBER LISTED AT THE END OF THIS ARTICLE

NASA Tech Brief
National Aeronautics and Space Administration
NASA's Jet Propulsion Laboratory, Pasadena, California

Licensing Opportunity

Quasi-Optical Millimeter-Wavelength Resonator

The design can be scaled to wavelengths too small for conventional waveguide technology.

A quasi-optical reflection cavity serves as a prototype resonator for oscillators at millimeter and submillimeter wavelengths. Conventional waveguide resonators for this frequency range are lossy, and it is difficult to fabricate them. The quasi-optical resonator (see figure) incorporates a folded Fabry–Perot interferometer of high Q and high finesse, another folded Fabry–Perot interferometer of lower Q and low finesse, and a Littrow-mounted diffraction grating. (Q, a measure of the sharpness of the resonant spectral peaks, is defined as 2π times the electromagnetic energy stored in the resonator divided by the electromagnetic energy dissipated in the resonator during one cycle of oscillation. Finesse is defined as Q divided by the number of wavelengths along the round-trip reflection path.)

The electromagnetic beam from the oscillator is coupled into the resonator quasi-optically; e.g., via a feed horn. At an angle of incidence of 45°, the beam first strikes metal mesh 1, which serves as one of the partially reflecting surfaces of the high-Q folded Fabry–Perot interferometer. The other partially reflecting surface is mesh 2. The reflectivity and spacing of the meshes are designed to obtain the desired comb-pattern transmission spectrum. Those parts of the spectrum of the incoming beam that are not within the narrow peaks of this transmission spectrum are reflected by mesh 1 to absorber 1.

The portion of the beam that passes through the high-Q Fabry–Perot interferometer is filtered similarly in the low-Q Fabry–Perot interferometer. The characteristics of meshes 3 and 4 and the other parameters of this interferometer are chosen so that its transmission spectrum includes at most half the peaks of the transmission spectrum of the high-Q interferometer. The rest of the spectrum incident upon mesh 3 is reflected to absorber 2.

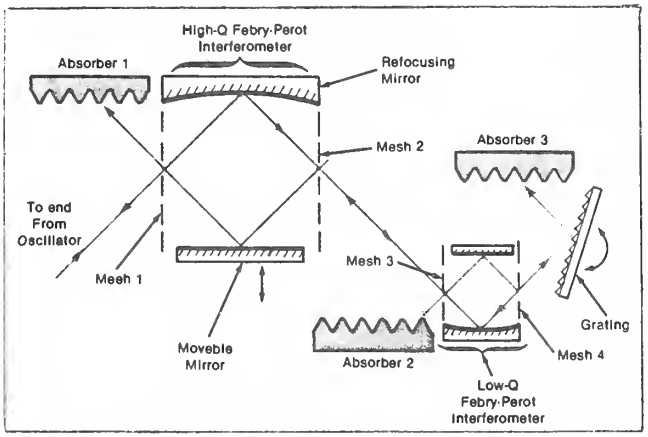

The **Quasi-Optical Millimeter-Wavelength Resonator** exploits diffraction and reflection effects to achieve high Q. This type of resonator is useful mainly at wavelengths too short for conventional waveguide techniques but too long for optical techniques.

The diffraction grating reflects the desired part of the beam back along itself toward the source and performs the final spectral filtering. The Littrow mounting is chosen to effect the desired back-reflection. The mounting angle, period, and other parameters of the grating are chosen so that only one of the spectral peaks that remain after the second grating is reflected back toward the source. The rest of the spectrum incident upon the grating is reflected onto absorber 3.

The prototype resonator was designed, fabricated, and tested at a frequency of 63 GHz. It exhiblted a Q of 6,600 and a round-trip loss of 2.52 dB. With attention to some details (e.g., nonuniform illumination, ohmic loss, and spillover loss) that were not considered in the design of the prototype, it should be possible to achieve Q's as high as 10,000. The design can be scaled easily to frequencies as high as 1 THz.

This work was done by Margaret A. Frerking and Karen A. Lee of Caltech for **NASA's Jet Propulsion Laboratory.**

This invention is owned by NASA, and a patent application has been filed. Inquiries concerning nonexclusive or exclusive license for its commercial development should be addressed to the Patent Counsel, NASA Resident Office-JPL. Refer to NPO-17919/TN.

Jet Propulsion Lab.
NASA Resident Office
Technology Utilization Officer Gordon S. Chapman
Mail Stop 180-801
4800 Oak Grove Drive
Pasadena, CA 91109
(818) 354-4849
Patent Counsel Paul F. McCaul
Mail Code 180-801
4800 Oak Grove Drive
Pasadena, CA 91109
(818) 354-2734
Technology Utilization Mgr. for JPL Norman L. Chalfin
Mail Stop 156-211
4800 Oak Grove Drive
Pasadena, CA 91109
(818) 354-2240

FOR ADDITIONAL INFORMATION: *Contact: Director, Technology Transfer Division, P.O. Box 8757, BWI Airport, MD 21240; (301) 621-0100 Ext. 241*
REFER TO THE NUMBER LISTED AT THE END OF THIS ARTICLE

NASA Tech Brief
National Aeronautics and Space Administration
NASA's Jet Propulsion Laboratory, Pasadena, California

Reducing Cross-Polarized Radiation From a Microstrip Antenna

Electromagnetic modes of higher order are suppressed.

A change in the configuration of the feed of a nominally linearly polarized microstrip-patch transmitting array antenna reduces the cross-polarized component of its radiation. It is desirable to reduce the cross-polarized component because this component can adversely affect the symmetry of the radiated beam and because it produces little or no useful signal power in another antenna aligned to receive in the expected polarization.

To make it operable over a wide frequency band, a microstrip antenna is usually constructed on a thick dielectric substrate. Unfortunately, a thick substrate supports the higher-order electromagnetic modes that give rise to asymmetry and cross polarization. Previously, all the microstrip patches in an array antenna were fed in the same phase, at the same location relative to the center of each patch (see Figure 1). This asymmetrical arrangement can result in significant excitation of higher-order modes. In the new configuration, the patches are fed on opposing sides, in opposite phases. This combination of spatial symmetry and temporal asymmetry causes the copolarized components of radiation from the fundamental modes of the patches to reinforce each other and the cross-polarized components of radiation from the higher-order modes to cancel each other.

To test this concept, two microstrip antennas like those shown in Figure 1 were constructed. The patches were 3.025-in. (7.68-cm) squares, and the substrate was 1/2-in. (12.7-mm)-thick foam with a dielectric constant of 1.05. The antennas were designed to resonate at frequencies from 1.55 to 1.66 GHz, and the distance between the elements along both principal axes was 0.6 wavelength at the middle frequency.

Figure 2 contains plots of measured and calculated intensities of the copolarized and cross-polarized components of radiation from the two antennas in the magnetic-field plane of the nominal radiated beam. These plots show clearly that the cross-polarized component is reduced by the new feed configuration.

This work was done by John Huang of Caltech for **NASA's Jet Propulsion Laboratory**. *NPO-18147/TN*

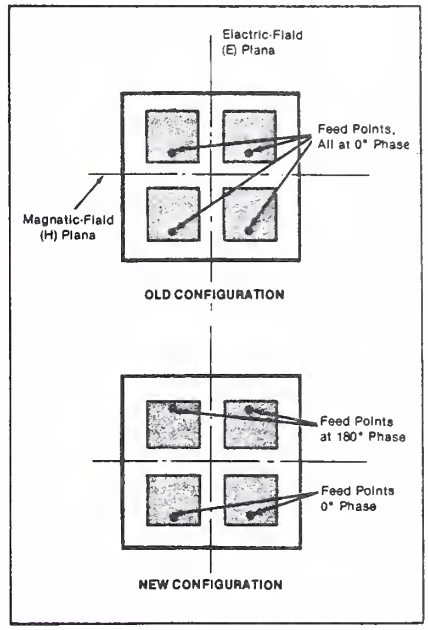

Figure 1. **Linearly-Polarized 2-by-2 Microstrip Antennas** can be fed in several alternative configurations, including the two shown here. The old configuration favored the generation of electromagnetic modes of higher order; the new configuration suppresses them.

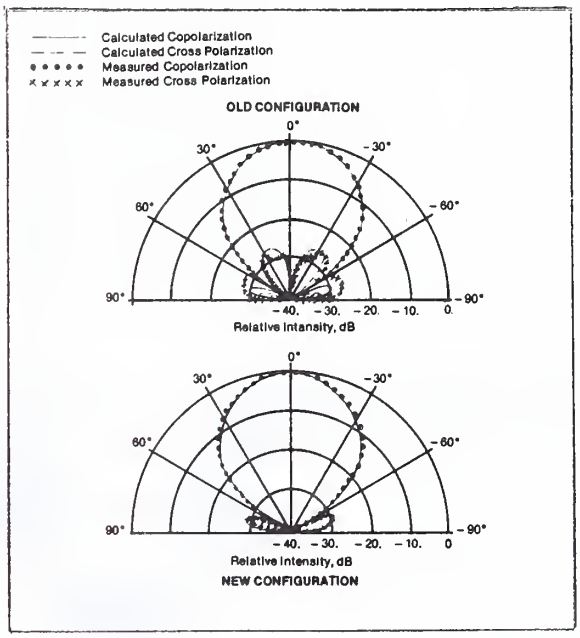

Figure 2. These **H-Plane Radiation Patterns** were produced at a frequency of 1.55 GHz by antennas like those described in Figure 1 and the text. The 0° line is perpendicular to the plane of the antenna.

FOR ADDITIONAL INFORMATION: *Contact: Director, Technology Transfer Division, P.O. Box 8757, BWI Airport, MD 21240; (301) 621-0100 Ext. 241*
REFER TO THE NUMBER LISTED AT THE END OF THIS ARTICLE

NASA Tech Brief
National Aeronautics and Space Administration
Marshall Space Flight Center, Alabama

Licensing Opportunity

Spatial Light Modulator Would Serve as Electronic Iris

The brightness of the image would be adjustable in many discrete steps.

In a proposed technique for controlling the brightness of an image formed by a lens, a spatial light modulator would serve as a segmented, electronically variable aperture. The technique offers several advantages: The spatial light modulator could be controlled remotely and would respond faster than a motorized iris or other remotely controlled mechanical iris does. Unlike an iris, the spatial light modulator could be configured so as not to vary the depth of field appreciably. Unlike a lead lanthanum zirconate titanate crystal, which could also be used to control the brightness, a spatial light modulator does not require high voltage.

A spatial light modulator is a two-dimensional array of electro-optical elements, each of which can be switched between a state of transparency or a state of opacity (intermediate states are not available). A typical device of this type contains 128 by 128 elements. In the proposed technique, the spatial light modulator would be placed in or near the principal plane of the lens (see figure).

If all the elements of the spatial light modulator were transparent, the image would be at full brightness. If one of the elements were made opaque, all of the image rays passing through that element would be stopped. Inasmuch as each point of the principal plane receives light from all points of the object plane, the opacity of that element would reduce the overall intensity of the image somewhat. Similarly, the image could be darkened further by making more elements opaque.

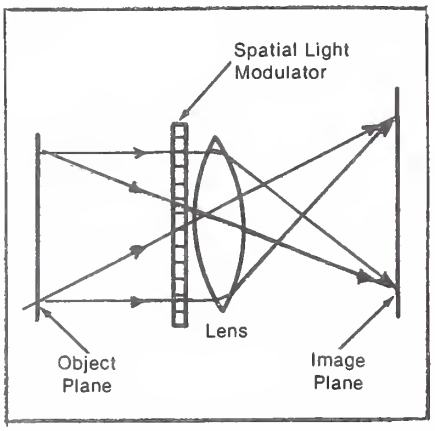

A **Spatial Light Modulator** placed at or near the principal plane of a lens would act as a segmented, electronically variable aperture.

Provided that the spatial light modulator covered the full aperture of the lens but no more, the brightness of the image could thus be reduced or increased in a large number of increments (e.g., $128^2 = 16{,}384$) from full opacity to full transparency. The depth of field would not be affected appreciably as long as the elements were turned transparent or opaque in a random spatial pattern. However, if it were desired to mimic an iris and vary the depth of field, this could be done by turning the elements on or off in a pattern that approximated an opening or closing circle of transparency surrounded by opacity.

This work was done by David A. Gutow of Rockwell International Corp. for **Marshall Space Flight Center.**

Inquiries concerning rights for the commercial use of this invention should be addressed to the Patent Counsel, Marshall Space Flight Center. Refer to MFS-29758/TN.

George C. Marshall Space Flight Center
Technology Utilization Officer Ismail Akbay
Code AT01
Marshall Space Flight Center,
AL 35812
(205) 544-2223
Patent Counsel
Leon D. Wofford, Jr.
Mail Code CC01
Marshall Space Flight Center,
AL 35812
(205) 544-0024

FOR ADDITIONAL INFORMATION: *Contact: Director, Technology Transfer Division, P.O. Box 8757, BWI Airport, MD 21240; (301) 621-0100 Ext. 241*
REFER TO THE NUMBER LISTED AT THE END OF THIS ARTICLE

NASA Tech Brief
National Aeronautics and Space Administration
NASA's Jet Propulsion Laboratory, Pasadena, California

Stirling-Cycle Cooling for Tunable Diode Laser

Small coolers can simplify laboratory spectroscopy and lighten airborne instruments.

A miniature Stirling-cycle cooler has been shown to be effective in continuously cooling a PbSnTe tunable diode laser to a stable operating temperature near 80 K. The cooler — a commercially available unit — occupies a volume of only 80 in.^{3} (1,300 cm^3) and weighs only 3 lb (1.4 kg). Such small, compact coolers can simplify laboratory diode-laser spectroscopy and instruments for use aboard aircraft and balloons.

Continuous stabilization of the temperature near 80 K and minimization of acoustic coupling are required to keep the laser output within a narrow frequency band for a long time in a typical scientific or military application. Although liquid nitrogen cools to 77 K with minimal acoustic coupling, cooling ceases when the liquid evaporates. A conventional mechanical cryogenic system can provide the required continuous cooling, but is much larger [7,500 in.^{3} (1.2×10^5 cm^3)] and heavier [170 lb (77 kg)] and produces sufficient undesired acoustic coupling to increase the half bandwidth of the laser output to the range of 30 to 50 MHz.

The combination of the PbSnTe tunable diode laser and the Stirling-cycle cooler was demonstrated in the infrared-absorption apparatus illustrated schematically in Figure 1. The laser, excited with currents ranging from 130 to 180 mA, operated at a wavelength near 8.4 μm. The laser was mounted on a copper block attached to the cold finger of the Stirling-cycle cooler. For additional stabilization of temperature, a heater wire was attached to the side of the block opposite the laser and a temperature-sensing silicon diode was mounted on the block midway between the heater wire and the laser. The cooler took about 1 h to bring the temperature from ambient down to about 80 K and about 1 additional hour to stabilize the temperature within ±1 mK of a steady value.

The short-term frequency drift of the laser was measured in the spectroscopic apparatus by use of the 1187.8787 cm^{-1} (wavelength 8.41836797 μm) spectral line of the N_2O gas in the absorption cell. Without stabilization of the temperature, this spectral line was observed to drift to lower laser currents, indicating slow warming of the laser. When the temperature was stabilized, this spectral line remained near a fixed laser current (see Figure 2). The half bandwidth of the laser output was 21 ±2 MHz — about 10 to 30 MHz narrower than that of a laser cooled by a conventional mechanical cryogenic system.

This work was done by Santo S. Durso, Randy D. May, Matthew A. Tuchscherer, and Christopher R. Webster of Caltech for **NASA's Jet Propulsion Laboratory.** *NPO-18045/TN*

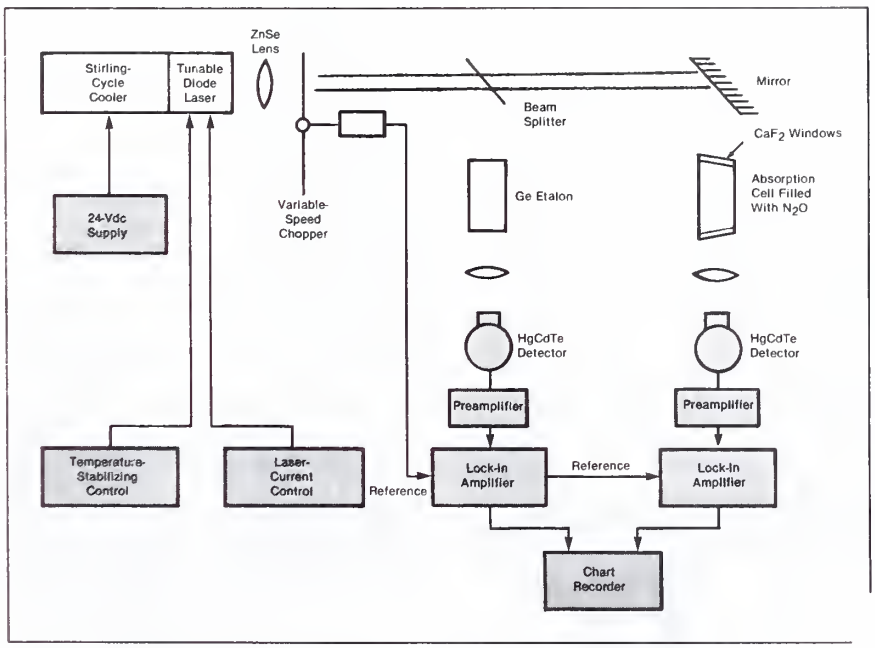

Figure 1. This **Infrared-Absorption** apparatus was used to measure the short-term frequency drift of the tunable diode laser by reference to a known spectral line of N_2O.

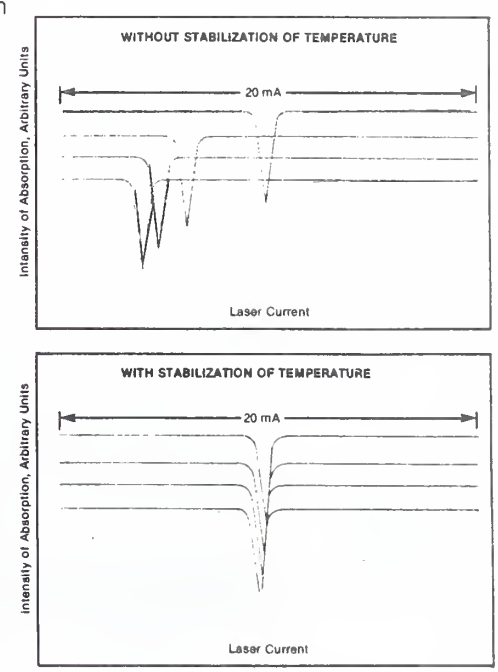

Figure 2. The **Intensity of Absorption** in the 1187.8787 cm^{-1} absorption line of N_2O was measured as a function of laser current. These scans were recorded at intervals of 2 min.

FOR ADDITIONAL INFORMATION: *Contact: Director, Technology Transfer Division, P.O. Box 8757, BWI Airport, MD 21240, (301) 621-0100 Ext. 241*
REFER TO THE NUMBER LISTED AT THE END OF THIS ARTICLE

NASA Tech Brief
National Aeronautics and Space Administration
NASA's Jet Propulsion Laboratory, Pasadena, California

Licensing Opportunity

Switched-Capacitor Voltage Multiplier

High voltage is generated without a transformer

A dc-to-dc power converter multiplies the input supply potential by a factor of nearly 40, without using a transformer. The converter is suitable for high-voltage, low-current applications. During tests, the converter stepped-up 90 V dc from a dry battery to 3.3 kV dc, at currents up to several microamperes.

The converter (see figure) includes a first bank of five capacitors, C_1 through C_5, a second bank of eight capacitors, C_6 through C_{13}, and a filter capacitor, C_f. The capacitors are connected to each other through a network of optically isolated solid-state switching devices, r_1 through r_{20} and s_1 through s_{19}. A controller that contains transistor/transistor-logic integrated circuits generates a two-phase switch-controlling signal.

At the beginning of the first half cycle, the r switches are turned off and the s switches are turned on, thereby connecting C_1 through C_5, in parallel, to the input voltage, V_i, and disconnecting these capacitors from the others. These capacitors quickly charge up to V_i. At the beginning of the next half cycle, the s switches are turned off and the r switches are turned on; this disconnects C_1 through C_5 from the power supply and connects them in series so that, in combination, they act as an intermediate source of voltage $V_i' = 5V_i$. At the same time, C_6 through C_{13} are connected in parallel to the series combination of C_1 through C_5, thereby charging C_6 through C_{13} to nearly the intermediate source voltage V_i'.

At the beginning of the next half cycle (which is the same as the first half cycle), C_6 through C_{13} are connected to each other in series, disconnected from C_1 through C_5, and connected to C_f and the load. The series combination of C_6 through C_{13} acts as a source of voltage $8V_i' = 40V_i$. This source voltage charges C_f, which in turn supplies current to the load. In practice the actual voltage gain is slightly less than 40. The reasons for this reduction are as follows: Because of non-zero conductance, a small amount of intra-circuit current exists during the off state of the solid-state relay; this gives rise to unwanted discharge of the capacitors. Secondly, the present switching frequency is rather low (125 Hz), and so the time the relays remain on or off is much higher than the charging time of the capacitors, resulting in poor utilization of the capacitors. A better gain figure and a lower percentage ripple are bound to occur if higher frequency of is used.

The proposed dc-to-high voltage dc converter has the following attributes. The design does not make use of transformers or inductors but instead effects voltage boost-up by capacitive energy transfer. The circuit is primarily made up of banks of capacitors, connected by a network of integrated-circuit relays. The converter is functionally a linear voltage amplifier with a fixed gain figure. It is truly bipolar in operation (the input voltage and the output voltage have the same polarity). The output is fully floating, and there is excellent dc isolation between the input and output terminals.

This work was done by Govind Sridharan of Caltech for **NASA's Jet Propulsion Laboratory.**

Inquiries concerning rights for the commercial use of this invention should be addressed to the Patent Counsel, NASA Resident Office-JPL. Refer to NPO-17994/TN.

Jet Propulsion Lab.
NASA Resident Office
Technology Utilization Officer Gordon S. Chapman
Mail Stop 180-801
4800 Oak Grove Drive
Pasadena, CA 91109
(818) 354-4849
Patent Counsel Paul F. McCaul
Mail Code 180-801
4800 Oak Grove Drive
Pasadena, CA 91109
(818) 354-2734
Technology Utilization Mgr. for JPL Norman L. Chalfin
Mail Stop 156-211
4800 Oak Grove Drive
Pasadena, CA 91109
(818) 354-2240

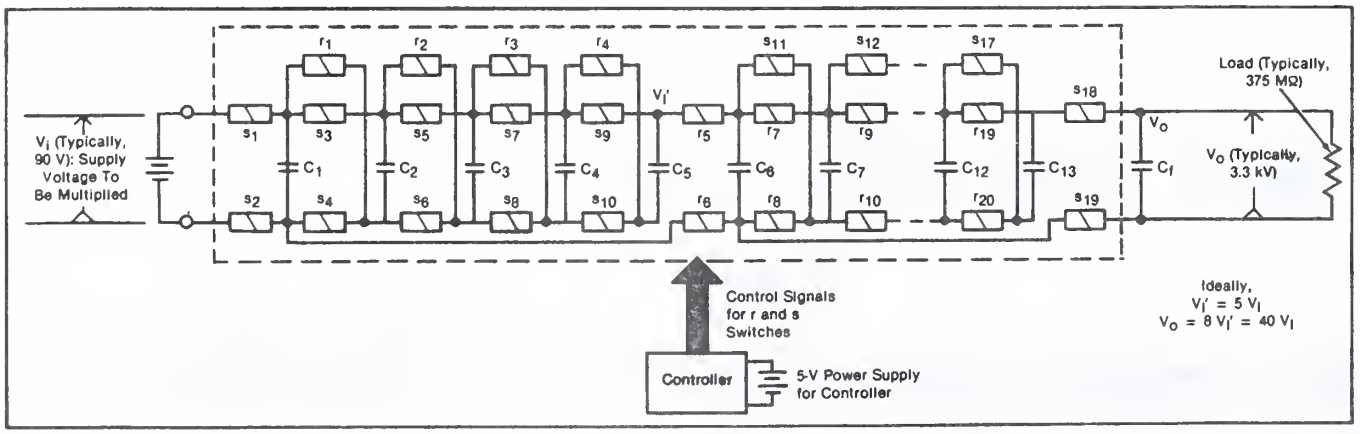
V_i (Typically, 90 V): Supply Voltage To Be Multiplied
r_1 r_2 r_3 r_4 s_{11} s_{12} s_{17}
s_1 s_3 s_5 s_7 s_9 V_i' r_5 r_7 r_9 r_{19} s_{18}
C_1 C_2 C_3 C_4 C_5 C_6 C_7 C_{12} C_{13} C_f
s_2 s_4 s_6 s_8 s_{10} r_6 r_8 r_{10} r_{20} s_{19}
V_o
Load (Typically, 375 MΩ)
V_o (Typically, 3.3 kV)
Control Signals for r and s Switches
Controller
5-V Power Supply for Controller
Ideally,
$V_i' = 5\ V_i$
$V_o = 8\ V_i' = 40\ V_i$

Capacitors in Two Banks are alternately charged in parallel and discharged in series. This switching-and-charging action multiplies the input voltage V_i by a factor of as much as 40.

NASA Tech Brief
National Aeronautics and Space Administration
NASA's Jet Propulsion Laboratory, Pasadena, California

Licensing Opportunity

Thermal Strap and Cushion for Thermoelectric Cooler

The strap would flex in three orthogonal directions to absorb stress and vibration.

A relatively inexpensive cushioning strap has been proposed for use as the thermal contact between a thermoelectric cooler and a device to be cooled, such as a laser diode, infrared detector, or charge-coupled device for imaging. The strap would provide high thermal conductance while minimizing thermal and mechanical stresses on the thermoelectric cooler, which is fragile.

The strap would be used as an alternative to a flexible thermal strap made of silver. The silver straps use usually used on flight systems whose requirements for optical alignment and thermal conductance are more stringent than for most applications. The silver straps require expensive fixtures and assembly techniques, such as custom vacuum electron-beam welding. The new thermal strap, in contrast, would have a simple design and could be fabricated easily, with relatively inexpensive materials. It would have a thermal resistance of about 1 °C/W.

The new strap would include three thin copper plates between which two corrugated foils of a thermally conductive metal — copper, aluminum, or silver — would be sandwiched (see figure). The corrugations in the two layers of foil would lie perpendicularly to each other. The layers would be bonded to the copper plates with thermally conductive epoxy resin. The corrugations would be formed during the bonding process by inserting pins under and over the foils to create the wavy pattern. The pins could be coated with a release agent so that they could be removed easily after the strap is assembled.

Insulating standoff posts would support the device to be cooled. The top and bottom copper plates of the strap would be bonded to the object to be cooled and to the cold stage of the thermoelectric cooler, respectively. The corrugations would enable the top part of the sandwich to flex between right and left and the bottom part to flex between front and back. Both halves could flex up and down. (Flexing in torsion would be limited, however.) The unit strap could thus accommodate linear motion in all three directions. This feature would help to isolate the thermoelectric cooler from thermal stress and vibration. At the same time, it would be linked to the object to be cooled by many parallel thermal paths through the plates and foils.

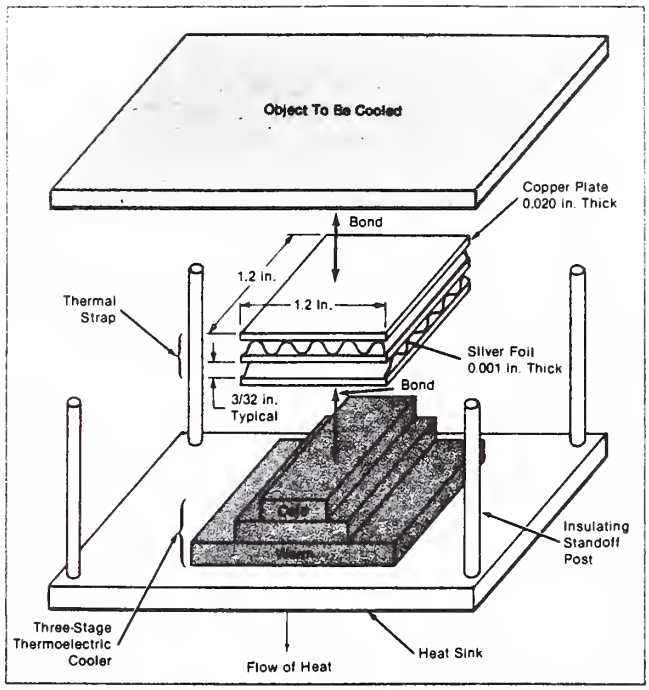

The **Double-Deck Sandwich** of flexible thermal conductors would provide many parallel paths for flow of heat from a cooled device to a thermoelectric cooler, while protecting the cooler against stress and vibration.

This work was done by Jack A. Jones, S. Walter Petrick, and Steven Bard of Caltech for **NASA's Jet Propulsion Laboratory.**

This invention is owned by NASA, and a patent application has been filed. Inquiries concerning nonexclusive or exclusive license for its commercial development should be addressed to the Patent Counsel, NASA Resident Office-JPL. Refer to NPO-17806/TN.

Jet Propulsion Lab.
NASA Resident Office
Technology Utilization Officer Gordon S. Chapman
Mail Stop 180-801
4800 Oak Grove Drive
Pasadena, CA 91109
(818) 354-4849
Patent Counsel
Paul F. McCaul
Mail Code 180-801
4800 Oak Grove Drive
Pasadena, CA 91109
(818) 354-2734
Technology Utilization Mgr. for JPL Norman L. Chalfin
Mail Stop 156-211
4800 Oak Grove Drive
Pasadena, CA 91109
(818) 354-2240

FOR ADDITIONAL INFORMATION: *Contact: Director, Technology Transfer Division, P.O. Box 8757, BWI Airport, MD 21240, (301) 621-0100 Ext. 241*
REFER TO THE NUMBER LISTED AT THE END OF THIS ARTICLE

Energy

0909 Improving the Thermal Efficiency of Masonry Building Walls

0910 Betavoltaics of Increased Power—Long-lived cells would derive power from radioactive sources.

Other Items of Interest

0892 Video Pipeline Tree for Scan Conversion of Triangles—Scenes containing many polygons could be generated in real time.

0917 Solar-Powered Cathodic Protection System Developed

U.S. Army Corps of Engineers
Cold Regions Research & Engineering Laboratory
72 Lyme Road, Hanover, New Hampshire 03755-1290

Improving the Thermal Efficiency of Masonry Building Walls

PROBLEM

Masonry buildings constructed in times of cheap, plentiful energy are now suffering a mid-life crisis. They are often poorly insulated, resulting in high heating and cooling costs and uncomfortable conditions for occupants. As landlord to many such buildings, the Army faces a dilemma: it would be too expensive to destroy these buildings before the end of their design life, yet retrofitting them for better insulation could also incur very high costs.

SOLUTION

Traditional methods of reinsulating are difficult or even impossible to use with masonry. These techniques usually add insulation between the exterior and finish walls, but with masonry blocks, for example, the same block is the outer and inner wall. A unique solution to this problem is exterior insulation. Rigid polystyrene foam insulation is adhered or mechanically fastened to the outside of the building and then an outer surface of polymer-modified cement or synthetic stucco is applied. This system not only improves the insulation value, but it also can upgrade the building's appearance.

RESULTS

The Army already had used exterior insulation systems in the 1980s when it was noticed that some did not perform as expected. The U.S. Army Cold Regions Research and Engineering Laboratory (USACRREL) and the U.S. Army Construction Engineering Research Laboratory (USACERL) conducted demonstrations to show where and how these systems would be most successful.

These demonstrations took place at Fort Devens, Massachusetts, Fort Wainwright, Alaska, and Fort Leonard Wood, Missouri, and provided important lessons for using exterior insulation systems:

- It is important to consider the traffic pattern around the building proposed for retrofitting. Buildings in high traffic areas require special considerations due to potential vandalism and impact damage.
- Proper surface preparation and installation are essential to success.

Demonstrations further showed that, besides having use as a retrofit, the insulation's price makes it competitive with other finishes for new construction.

FOR ADDITONAL INFORMATION: Contact: Stephen Fladers, U.S. Army Cold Regions Research and Engineering Laboratory, 72 Lyme Road, Hanover, New Hampshire 03755-1290; (603)646-4430, FTS 461-4302.

NASA Tech Brief
National Aeronautics and Space Administration
NASA's Jet Propulsion Laboratory, Pasadena, California

Betavoltaics of Increased Power

Long-lived cells would derive power from radioactive sources.

Batteries of newly developed betavoltaic cells have been proposed as long-lived sources of power of the order of watts. Intended for use aboard spacecraft, batteries of this type might also be used, for example, in surgically implanted devices requiring high power. Heretofore, betavoltaics have been used in surgically implanted devices — specifically, heart pacemakers, but these consume powers of no more than a few microwatts.

A betavoltaic cell functions analogously to a photovoltaic cell, except that the role of the photons is played by energetic electrons (β particles) generated by the radioactive decay of a suitable material. The β particles traverse the cell, losing kinetic energy and creating pairs of holes and electrons. Those holes and electrons that lie within a diffusion length of the p/n junction of the cell are swept across the junction and contribute to the output current of the cell. An equivalent circuit for such a cell is identical to that of a solar photovoltaic cell.

Previously, betavoltaics were not considered for supplying powers of the order of watts because available materials provided low energy-conversion efficiencies and were vulnerable to damage by the high-energy incident β particles. However, the energy-conversion efficiencies of recently developed betavoltaic cells are appreciably greater than those of the previous cells. In addition, it appears that betavoltaic cells can be produced economically in quantity by use of solar-cell technology.

The figure illustrates a conceptual betavoltaic cell and battery. The cell would be a simple p/n-junction device to which a layer of β-emitting material would be attached. There would be an optimum thickness for the β-emitting layers: each layer would have to be thick enough to emit a sufficient number of particles, but diminishing returns would be reached at thicknesses great enough to result in the reabsorption of the emitted particles. A battery would contain a stack of β-emitting layers interspersed with enough p/n-junction devices to stop most of the β particles. The battery would be encased in a suitable β-backscattering material to prevent any β particles from escaping.

A GaP betavoltaic cell has been developed. GaP is believed to be particularly suitable because it has relatively wide energy-band gaps of 2.2 eV (indirect) and 2.7 eV (direct) and because a wide gap is associated with the ability to resist damage by the β particles. The GaP cell is a p/n device, grown and diffused by liquid-phase epitaxy. The measured power-conversion efficiency for the particular cell is 8.4 percent, and the theoretically attainable power-conversion efficiency of GaP cells in general is almost 25 percent.

The most suitable source of β particles for high power applications appears to be ^{90}Sr (which has a half life of 28 years). Preliminary calculations indicate that a battery with ^{90}Sr sources could be made to have an initial specific power of about 3 W/kg. Similar calculations for cells made with ^{204}Tl β emitters (half life 4 years) indicate an initial specific power as high as 8 W/kg.

This work was done by Frederick S. Pool and Paul Stella of Caltech for **NASA's Jet Propulsion Laboratory.**
NPO-17817/TN

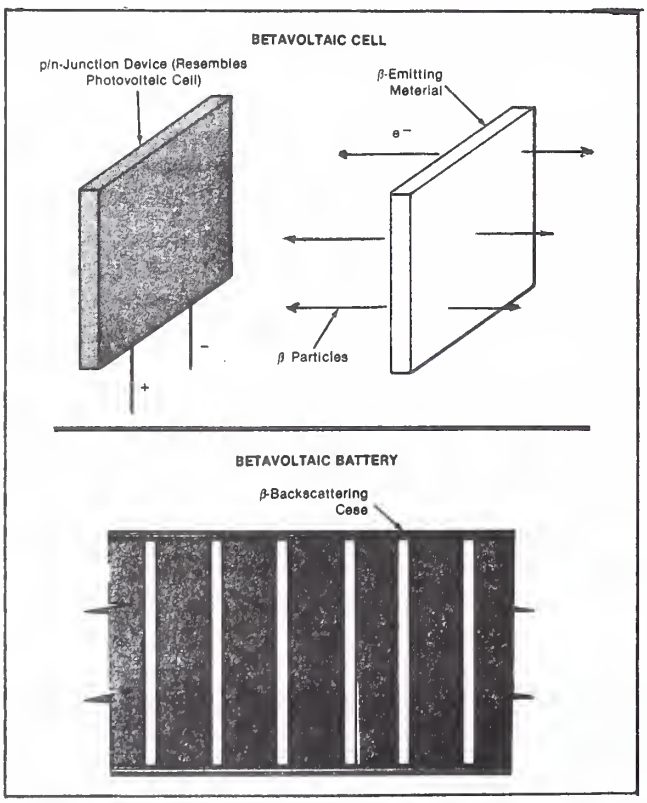

A High-Power Betavoltaic Cell of the type envisioned would resemble a solar photovoltaic cell, except that it would include a layer of β-emitting material. A betavoltaic battery would differ from a photovoltaic battery in that the cells would be stacked as in a chemical battery, and would be surrounded by a material that would contain the β rays.

FOR ADDITIONAL INFORMATION: *Contact: Director, Technology Transfer Division, P.O. Box 8757, BWI Airport, MD 21240; (301) 621-0100 Ext. 241*
REFER TO THE NUMBER LISTED AT THE END OF THIS ARTICLE

Engineering

0911 Abandoned Mine Lands Program—Repairing Stream Channels to Reduce Water Loss into Underground Mines

0912 Abandoned Mine Lands Program—The Effectiveness of Surface Seals on Coal Seam Fire Control

0913 Innovative Roof Bolt Support Systems

0914 Redistributed Explosive Charges Reduce Rockfall At Surface Mines

0915 Reduction in Rockfall and Blast-Produced Overbreak in Underground Mines

0916 Correlation of Elastic-Plastic Fracture Toughness Studied

0917 Solar-Powered Cathodic Protection System Developed

0918 Accounting for Compressibility in Viscous Flow in Pipes

0919 Adaptive Grids for Computations of Three-Dimensional Flows—A spring-system analogy is extended from two to three dimensions.

0920 Algebraic Model of Turbulence for Internal Flow—An enhanced eddy-viscosity approximation simplifies calculations.

0921 Docking System Would Accommodate Misalignments

0922 Experiences With the JPL Telerobot Testbed—Issues and insights are discussed.

0923 Helicity-Density and Normalized-Helicity Maps of Flows

0924 Low-Speed Optical Speedometer—The delay between terrain-reflectance signals from two optical sensors indicates speed.

0925 Mathematical Model for Deposition of Soot (Licensing Opportunity)

0926 Self-Adjusting Choke for Nozzle—The issuing stream remains coherent for greater distances despite fluctuations in pressure and/or rate of flow. (Licensing Opportunity)

0927 Strain Center for Analysis of Forces—After yielding, forces are perpendicular to radii from the strain center.

0928 Zero-Spring-Rate Mechanism/Air Suspension Cart (Licensing Opportunity)

0929 Vapor-Resistant Heat-Pipe Artery

Software

0930 Program for Elastoplastic Analyses of Plane Frames—Nonlinear collapse phenomena are simulated by iterative linear analyses.

Testing & Instrumentation

0931 Fire Testing Toll Installed

0932 Holographic Interferometry To Measure Three-Dimensional Flow—Double-exposure holography is used in studies of transonic flow near rotating blades.

0933 Liquid-Crystal Coats Help Make Flows Visible—Changes of color are rapid and reversible.

Other Items of Interest

0909 Improving the Thermal Efficiency of Masonry Building Walls

0934 Sludge Dewatering by Freezing

0947 Synchronizing Rotation of a Heavy Load—A simple setup of motors, pulleys, and belts provides both torque and synchronism.

New Technology from the
U.S. Bureau of Mines

U.S. Department of the Interior

Abandoned Mine Lands Program
Repairing Stream Channels to Reduce Water Loss into Underground Mines

Objective

Control surface stream loss by identifying and selectively sealing water loss zones in stream channels overlying underground mines.

Approach

Electromagnetic terrain conductivity surveys, coupled with stream gaging, are performed within a stream channel to identify saturated fracture zones associated with loss of stream water. This information is used to target locations for the injection of expandable polyurethane grout. The grout is injected two to three feet beneath the surface of the streambed, across each loss zone, to seal the fractured streambed and restore stream flow across the damaged area.

How It Works

Multiple zones of infiltration (natural and induced) normally exist in stream channels overlying mined areas, causing water handling and/or acid drainage problems in the mines as well as loss of stream flow. It is typically difficult to accurately locate these loss points. Therefore, conventional methods of stream repair, such as using plastic membranes or clay and rock rip-rapping, are applied to long lengths of a stream channel. The two-step approach developed by the Bureau of Mines first quickly and accurately locates loss zones using electromagnetic ground conductivity survey and gaging instruments. Conductivity is measured at fixed spacings (typically 25-50 ft depending on the instrument and desired observation depth). Ground conductivity increases when saturated conditions exist at depth. These apparent flow loss zones are confirmed by gaging, to eliminate possible effects due to unobservable metal debris adjacent to or buried in the stream sediment.

The second step consists of grouting designed to contain the stream water within the channel. An expandable polyurethane grout is injected so as to create a shallow and relatively impermeable barrier. Hollow steel rods approximately 3 ft in length and 3/4 in. in diameter, with hardened steel points, are manually driven into the stream sediments at 7-10 ft intervals using a sledge hammer. Where a stream flows over bedrock, a small drill hole serves to emplace the steelrod. The top of each rod has a hardened steel cap to allow mechanical injection of the grout (Figure 1). Several 1/8 in diameter holes are drilled in the side of the rod, near the bottom, providing ports for lateral grout injection. Five gallons of a two-component grout (2.5 gallon of each component) are injected into each grout hole using injection pressures of 400 to 1200 lb/in^2. Grout is injected at the maximum pressure obtainable until a surface leak developed, whereupon the injection pressure is reduced to 50 lb/in^2 until the leak is sealed by grout curing. The pressure is then slowly increased until another leak occurs or until 5 gallons of grout has been injected. Grouting is repeated, as necessary, until stream flow across the area is restored.

Results

Field tests were conducted in northwestern Maryland in a section of Staub Run, where it flows over an abandoned underground mine, and in Guyses Run in northern West Virginia, which overlies an active longwall operation. At both sites, terrain conductivity proved to be a simple, inexpensive and accurate way to pinpoint loss zones. At Guyses Run, a conductivity survey conducted before subsidence indicated a fracture zone that was providing ground water to the stream; after subsidence, this zone became the principal area of water loss. This indicates that terrain conductivity may prove to be useful for predicting stream loss zones as well as locating them after subsidence occurs.

Test results from the two sites revealed that grouting resulted in a 95-100% recovery of stream flow, at a cost of $2.50-$3.00 per sq ft of stream, approximately half that of clay and riprapping. Accurate pinpointing of loss zones resulted in much greater actual savings. The new stream sealing technique also proved to have other advantages: it was quick and easy, caused very little disturbance to the natural stream, did not require construction of access roads, and should prove to be more permanent, since the grout materials are protected from flood or drought damage by the stream bottom.

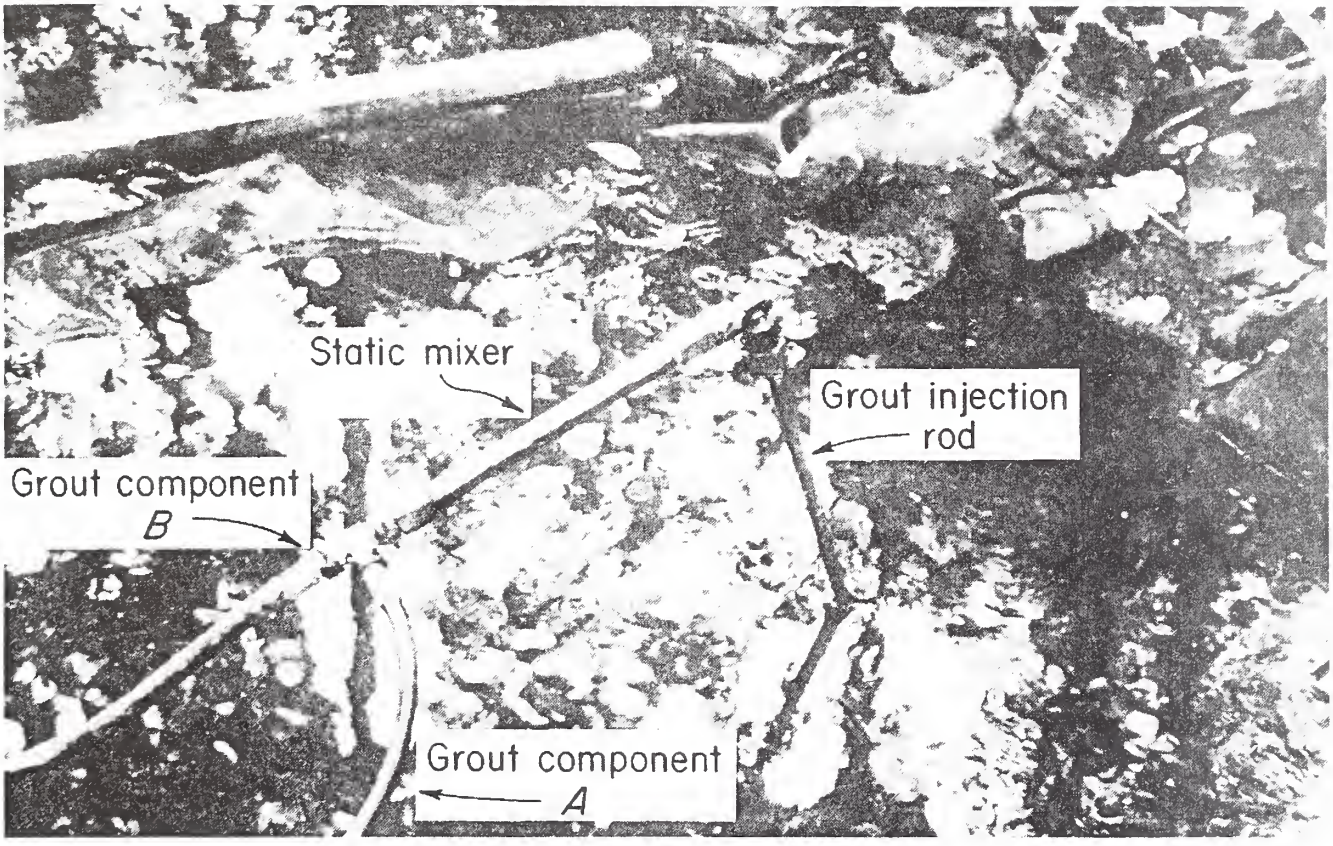

Components of stream sealing technique as it is being used to seal off a fracture zone in a streambed.

Based on the results at Staub Run, the state of Maryland has incorporated the Bureau's technique as part of its abandoned mined land reclamation efforts. Southern Ohio Coal Company's Martinka mine, which cooperated with the Bureau on the Guyses Run test, received an award for outstanding reclamation from the Office of Surface Mining, Reclamation and Enforcement (OSM). The company used this novel stream sealing approach as part of its award-winning reclamation effort.

Patent Status

The U. S. Department of the Interior is not applying for a patent on this technology.

For More Information

Additional information can be obtained by contacting

Terry Ackman or Craig Hustwitt
U.S. Bureau of Mines
Pittsburgh Research Center
P. O. Box 18070, Pittsburgh, PA 15236
Tel: (412) 892-6566.

New Technology from the U.S. Bureau of Mines

U.S. Department of the Interior

Abandoned Mine Lands Program The Effectiveness of Surface Seals on Coal Seam Fire Control

Objective

Develop a method to evaluate the effectiveness of coal seam fire surface seals so that potential problems may be corrected at an early stage, before the integrity of the surface seal is lost.

Background

Surface seals are the primary coal seam fire abatement method being used in the western United States. Surface seals smother a fire by denying it oxygen. The seal is usually constructed by placing a mantle of soil, four to ten feet thick, over a coal seam fire area to exclude air from the fire. The soil is compacted to increase effectiveness, and a soil cement may be used to augment the soil. In some cases, burning coal may be excavated and separately smothered or otherwise extinguished in another area; in other cases, a trench may be excavated and backfilled with incombustible material to isolate a fire. More often, a surface seal is simply applied over and around the entire known burning area.

In the 1950's, the Bureau of Mines administered a large program to treat numerous coal seam fires across the western United States. Methods used in this program were described in Bureau of Mines Information Circular (IC) 7932, dated 1959. More recently however, various coal seam fires have been treated with surface seals under the direction of state Abandoned Mine Land Reclamation authorities. It has frequently taken years to evaluate the effectiveness of surface seals. By the time problems become evident, it has often been too late to take corrective action within the scope of the original abatement project. For this reason, the Bureau of Mines developed a means for tracking temperature trends at coal seam fire projects to obtain a better and earlier handle on the effectiveness of surface seals.

Approach

Under an Abandoned Mine Land (AML) research contract, the effectiveness of coal seam fire seals were evaluated at thirteen sites in Montana. Nine of these sites were sealed during the 1950's and four were sealed during the 1980's. Underground temperature data and soil test data collected for the sites were correlated to determine information that might serve as indicators of successful surface seal methods. A change in the rate of underground temperature change at a given borehole was found to be an indicator of the local effectiveness of a surface seal.

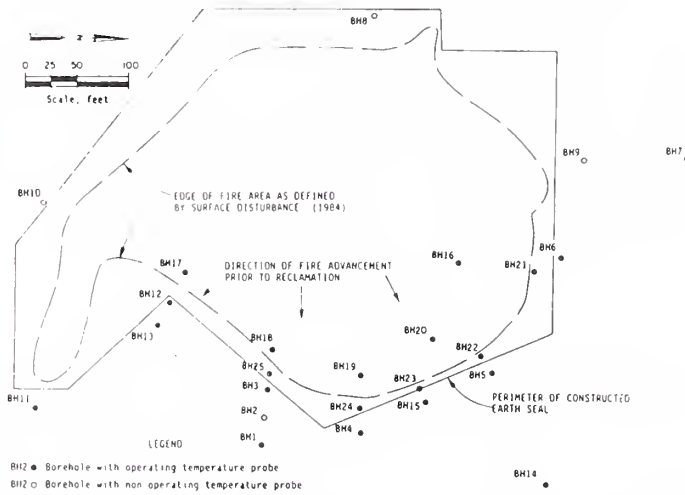
0 25 50 100
Scale, feet
EDGE OF FIRE AREA AS DEFINED BY SURFACE DISTURBANCE (1984)
DIRECTION OF FIRE ADVANCEMENT PRIOR TO RECLAMATION
PERIMETER OF CONSTRUCTED EARTH SEAL
LEGEND
BH2 Borehole with operating temperature probe
BH2 Borehole with non operating temperature probe

Figure 1.—Typical Surface Seal Monitoring Configuration.

How the Evaluations Were Made

To conduct the evaluations, boreholes were drilled to install temperature monitoring probes. The temperature monitoring probes consist of a thermocouple sealed with Teflon fluorocarbon polymer tape and heat shrink tubing. The probes were lowered into the boreholes, connected to the surface with extension wires, and backfilled with grout or soil to exclude oxygen. Temperatures, read with a potentiometer, are influenced by a relatively small area within three to four feet of the probe.

Test Results

Temperatures were monitored over time to determine temperature trends. The measured temperatures were also compared to the baseline normal ground temperatures for the area and were correlated to visual indications of possible ongoing fire activity. For the sites treated during the 1950's, present temperature readings were far below active burning temperatures, but in some cases were still somewhat above normal ground temperatures. This indicated that the seals had been successful in containing the fires but that complete extinguishment may not yet have been achieved. For the sites treated during the 1980's, temperatures were monitored during the critical period of a year or two after the seals had been installed. It was found that a decrease in the rate of temperature rise or an acceleration of temperature reduction was an early indicator of a successful surface seal.

For More Information

A Bureau of Mines Open File contract report (OFR 12-91) entitled, "Determining Effectiveness of Past Mine Fire Surface Seal Abatement Methods," by L. C. Hanson, J. E. Hodges, and K. M. Redmond, will soon be made available through the National Technical Information Service (NTIS). For additional information about this contract, and the status of its availability through NTIS, please contact the Technical Project Officer:

Mr. Les A. Beckett
U. S. Bureau of Mines
Denver Research Center
Building 20, Denver Federal Center
Denver, CO 80225-0086
Tel: (303) 236-0726

New Technology from the
U.S. Bureau of Mines

U.S. Department of the Interior

Innovative Roof Bolt Support Systems

Objective

Improve underground mine roof bolt support systems by alleviating problems associated with certain ground support systems currently being used.

Approach

Convert a passive resin-grouted roof bolt system into a uniform, tensionable roof bolting system.

Background

Resin-grouted roof bolts are one of the most common forms of ground support in U.S. underground coal mines. These support systems can be installed with a full-column of grout and be loaded with subsequent roof movements after installation. This is called a "passive" support system. An alternative to the passive support system is the mechanically-anchored, tensioned roof bolt system. This system is installed with resin grout. This system is designed to load or tension the support during installation by using a mechanical anchor, coupling, or threaded nut after the resin has properly cured. It is called an "active" support system and is used extensively for improved strata control in a laminated geologic deposition or in difficult ground conditions.

To ensure that active bolts have been properly installed, the bolt loads must be checked by using a torque wrench or other suitable equipment. Unfortunately, this practice presents potential safety hazards and has limited accuracy. Laboratory and field experiments also reveal that the torque-to-tension ratio developed on active support systems can vary by 50% from bolt-to-bolt. Variations in bolt load installations can induce stress concentrations and lead to roof degradation or failure.

To alleviate problems associated with tensionable "active" bolt installations, the Bureau of Mines has developed a support system that is independent of mechanical tensioning devices subject to frictional losses and system bleed-off. This support system also offers added advantages of providing pre-determined uniform installation load, and reducing support cost by at least 30%.

How It Works

The Bureau-developed support system utilizes resin-grouted rebar bolts installed in such a manner that the system becomes "active" immediately upon insertion. The system requires minor bolter modifications, special bolt installation stingers, and a calibrated load cell. The roof bolt machine is modified by installing a valve that permits 10,000 lb of upward force to be developed at the installation head, on demand, through the operation console. The stingers were designed to withstand enormous repetitious axial and bending loads generated between the installation head and the roof bolt. The calibrated load cell is utilized to calibrate the upward thrust to any desired level prior to support installation.

To install the support system, the following method is prescribed: Drill the hole for the roof bolt as the manufacturer recommends for the particular diameter and length of support, ensuring that the hole is 1-inch longer than the bolt tendon. Install a cartridge tube of 15-second resin into the hole and insert the bolt in compliance to the manufacturer's specifications. After the resin has been adequately mixed, the roof bolt operator throws the lever on the bolter that pushes the bolt upward with the full predetermined "thrust" and maintains the pressure until the resin has cured. When the upward force is removed, the support system is immediately placed into the predetermined tension. Additionally, the bolt operator is no longer subjected to the hazards associated with required tension determinations.

Test Results

Laboratory testing and massive underground tests at sites in room-and-pillar and longwall gateroads have demonstrated that this method is capable of installing bolts under uniform tensions equivalent to levels as high as 300 ft-lb of torque. The test site support systems were subjected to adverse underground conditions such as high levels of pillar sloughage, floor heave, and stress concentrations from an adjacent full-extraction pillar section. The support systems maintained the immediate

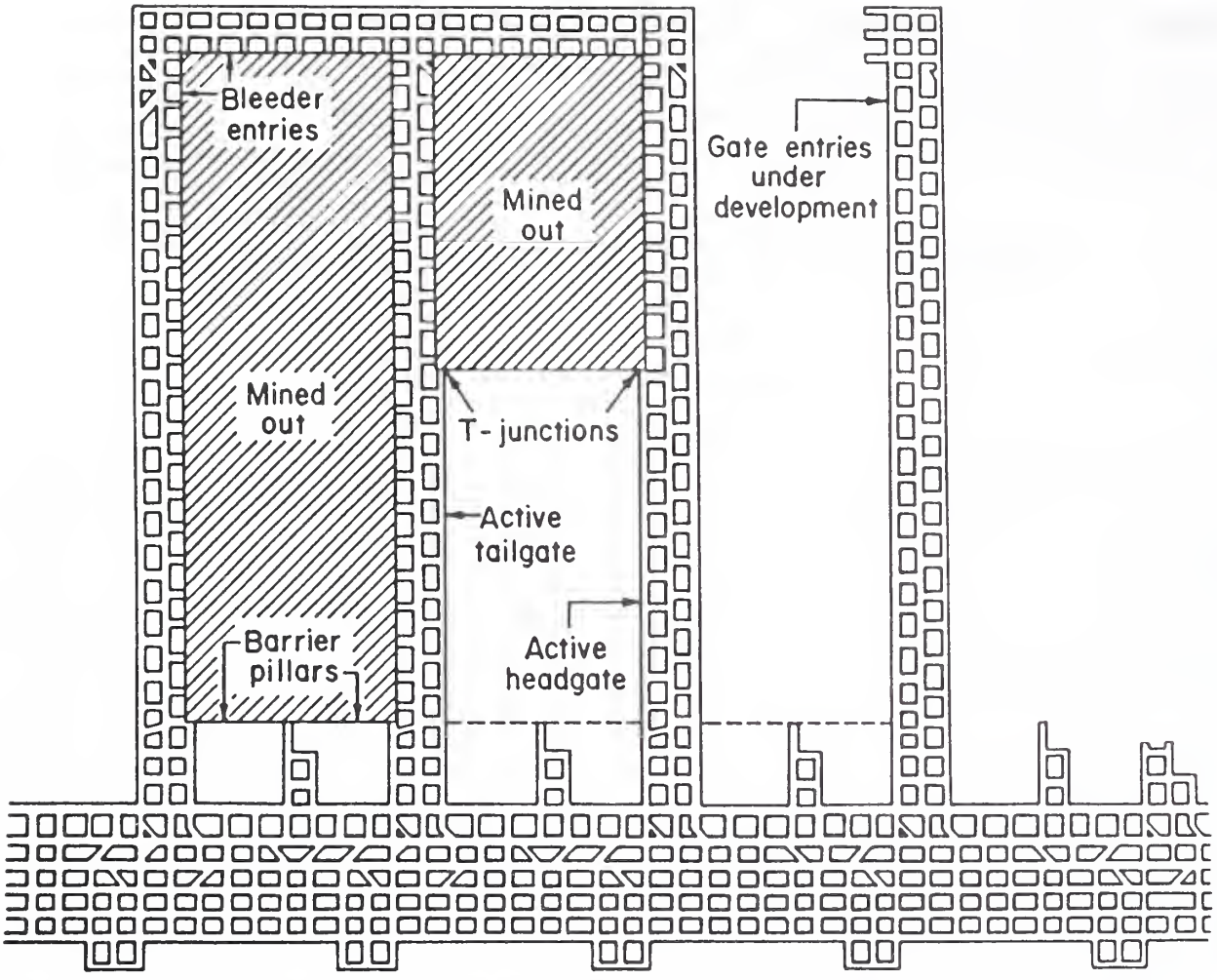

Thrust is applied to the head of the bolt forcing the immediate roof upward (exaggerated for explanation) before the resin cures. The roof tries to deflect downward after the thrust is removed, creating tension in the bolt and an "active" force between the bearing plate and the immediate roof.

roof, and no indications of strata separation or excessive deterioration were measured.

Patent Status

United States and foreign patents have been applied for by the Bureau of Mines. The term "Thrust Bolting" is being copyrighted.

For More Information

For more information regarding this development, or for answers to technical questions, contact:

Mr. Stephen C. Tadolini
U.S. Bureau of Mines
Denver Research Center
Denver Federal Center,
Bldg. #20
Denver, CO 80225
Tel: (303)236-0751

New Technology from the
U.S. Bureau of Mines
U.S. Department of the Interior

Redistributed Explosive Charges Reduce Rockfall At Surface Mines

Objective

Reduce rockfall fatalities and injuries by using innovative blasting practices to reduce damage to the rock at the excavation limits with little or no increase in cost.

The Problem

Falls of highwall have been a leading cause of fatalities, injuries, and equipment damage in the surface mining industry. Although the number of highwall falls is not great, when such an incident does occur it is about 14 times more likely to be fatal or result in severe injury and damage to equipment than other types of surface mine accidents. Overbreak or damage to the rock from poor or improper blasting practices is a major factor contributing to rock falls.

Presplitting or cushion blasting is the technique most often recommended for improved wall control. This type of blasting however, adds to drilling and blasting costs and is not universally accepted by the industry. Air gap presplitting techniques, also called air decks, are currently being used in some mines as a less costly alternative to conventional presplitting.

Approach

Blasting can cause highwall damage, but proper blasting techniques have been shown to reduce the magnitude of rockfall problems. In preventing rock falls, it is important to maintain the natural strength of the rock structure to the greatest extent possible. Improved blasting practices have three main advantages: 1) they are preventive rather than corrective in nature; 2) they are cost effective; and 3) they have a very low impact on the mining operation when properly implemented. New ways of evaluating highwall integrity, such as seismic refraction tomography, were investigated.

Test Results

Bureau projects demonstrated that simple changes in blast design, such as repositioning and redistribution of explosive loads, can significantly improve highwall condition and reduce rockfalls in both production and presplit blast designs. Full scale tests were conducted at a surface coal mine using the presplitting technique before production blasting and at a quarry using production blast designs only. Air gap presplitting using repositioned and/or decoupled explosives was the technique used during the coal mine tests. Current research by the Bureau suggests that using air gap techniques with a fully-coupled charge produces overbreak and rockfall in weak rock situations. The Bureau's air gap tests involved additional decoupling from cardboard tubes, suspending bagged ANFO, and relocating the toe charge from a weak to a more competent rock layer. Periodic visual examinations and photographic surveys of the highwalls in all test areas revealed that as a result of these changes the amount of rockfall was reduced and the time before rockfalls began was increased. In the case of the quarry production blasts, a decoupled charge

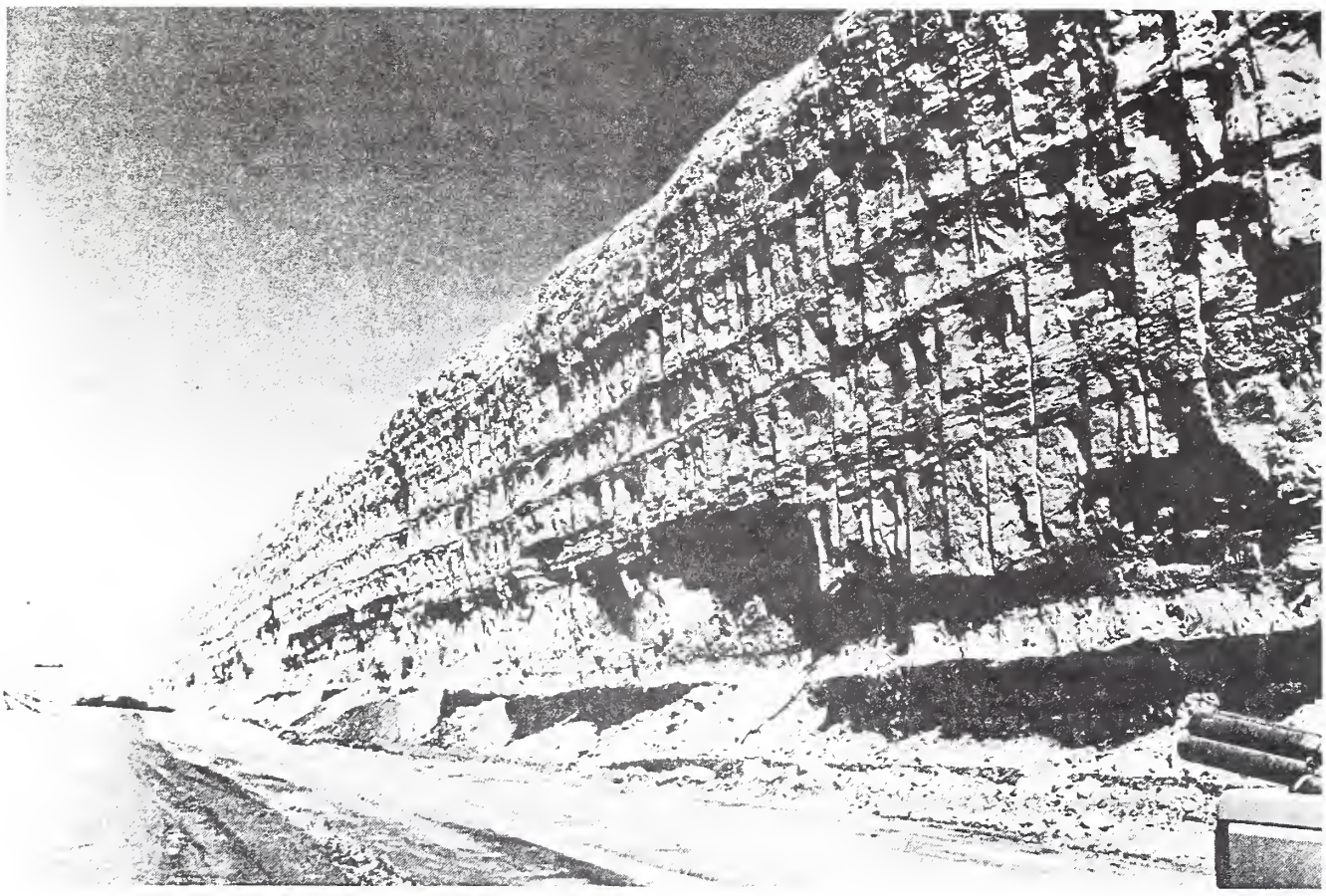

Figure 1.—The severe undercutting of this presplit highwall could be reduced by minor changes to the air gap blast design.

was used in the stemming zone of the blastholes that form the highwall. This was accomplished by using small diameter cartridged explosive in the stemming zone which promoted shearing between holes.

For More Information

U.S. Bureau of Mines researchers have written two publications reporting on the quarry studies performed in 1989 and on the surface coal mine work conducted in 1991. Both papers were published in Society of Explosive Engineers conference proceedings. The publications are also available from research personnel at the Bureau of Mines' Twin Cities Research Center, 5629 Minnehaha Avenue South, Minneapolis, MN 55417. Virgil J. Stachura (612) 725-4727, Larry R. Fletcher (612) 725-4533 or David E. Siskind (612) 725-4598 can answer questions on this work and supply copies of papers.

New Technology from the
U.S. Bureau of Mines

U.S. Department of the Interior

Reduction in Rockfall and Blast-Produced Overbreak in Underground Mines

Objective

Use controlled blasting techniques to reduce blast-produced overbreak damage to underground mine ribs and back for both safer working conditions and improvements in productivity.

The Problem

Blasting is used in metal and non-metal underground mine stopes, drifts and crosscuts to fracture rock to be excavated and further processed. Standard blasting also produces fractures in the rock beyond the desired excavation area. This is sometimes evident by rough surfaces, undercutting and other signs of excessive damage. This damage contributes to rockfalls in the mines, a major cause of injuries and fatalities and equipment damage.

A variety of controlled blasting techniques has been developed for civil engineering projects where long-term stability is essential. For several reasons, these methods are not widely used in mining. For example, these methods incur additional costs and time; there is little need to maintain stable openings over long periods of time; and there is the perception that corrective remedial techniques, such as rock bolting, are more practical. Basically the benefits of these methods are not demonstrably clear for application in underground mines.

Approach

Bureau of Mines researchers evaluated controlled blasting techniques at two underground mines: the White Pine room-and-pillar copper mine in upper Michigan, and the stoping operation of the Homestake gold mine in Lead, SD. Designs were intended to reduce overbreak while still producing adequate fragmentation and throw. In addition, practical factors were emphasized, since researchers realized that if overly complex approaches were used, the methods would probably not be adopted. At both mines, the general approach was to reduce and control blast energy in perimeter holes.

Test Results

At White Pine, the major hazard is the spalling of sandstone from high on the ribs. Two approaches were tested: decoupling by string-loading undersized, low-energy cartridges, and the use of millisecond (ms) delays

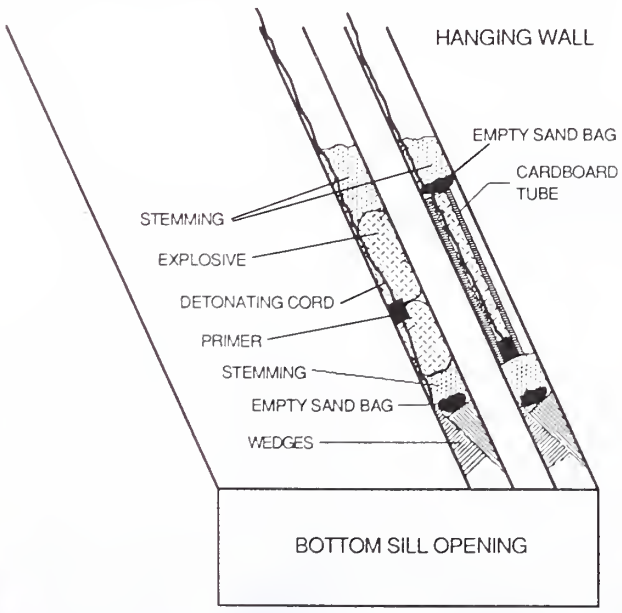

Figure 1.—Decoupled blastholes along hanging wall in Homestake mine VCR stope.

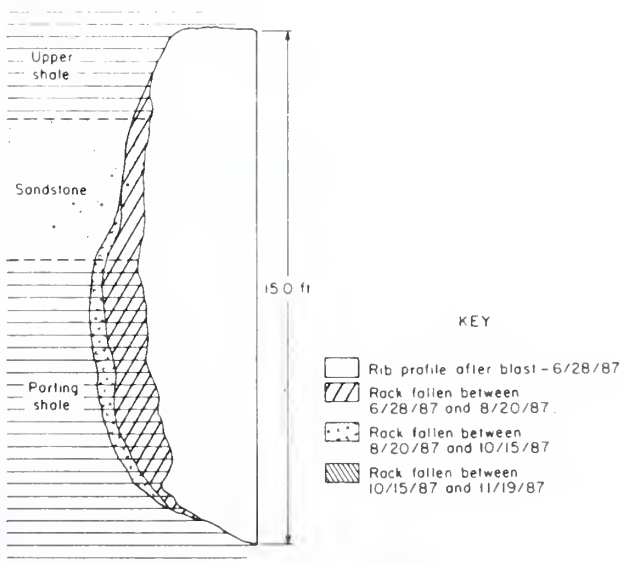

Figure 2.—Composite line drawing showing rockfall from left rib of decoupled rib holes and fast delays at White Pine room and pillar mine.

to reduce initiation time scatter. Of the four permutations of short and long delays and coupled versus decoupled, the best results were obtained with ms (short) delays and decoupling.

At Homestake, mining is performed using vertical crater retreat (VCR) and the concern is about rockfall from hanging walls in the production stopes. The Bureau-developed technique involved decoupling using cardboard tubes in the 6-1/2 inch blast holes against the hanging wall. These 4-inch ID tubes were loaded with 27 lbs of ANFO instead of the standard 60 lbs of emulsion or watergel normally used.

Because immediate improvement was noted at Homestake, the mine continued to experiment after the Bureau's efforts ended. The mine has tried or is proposing to try smaller tubes, low-energy explosives, air gaps, presplitting, timing control and combinations of these. Such methods not only provided safer and more stable stopes, but clearly decreased ore dilution.

In addition to experimental blast designs, Bureau of Mines' researchers applied a variety of techniques to measure and evaluate overbreak, including seismic refraction, photographic profiling, water integrity and long-term indices, such as ore dilution. Generally, photography and ore dilution worked the best. The seismic methods were not as useful as they had been in surface studies using tomographic mapping.

For More Information

Bureau of Mines researchers have written two papers and published them through the Society of Explosives Engineers. The papers describe the White Pine project in 1989 and the Homestake research in 1991. Both are published in Society conference proceedings. They are also available from research personnel at the Bureau's Twin Cities Research Center, 5629 Minnehaha Avenue South, Minneapolis, MN 55417. David E. Siskind (612) 725-4598 or Larry R. Fletcher (612) 725-4533 can answer questions about this work and supply copies of papers.

Correlation of Elastic-Plastic Fracture Toughness Studied

The David Taylor Research Center (DTRC), Bethesda, Maryland, has been studying the correlation of elastic-plastic fracture toughness. Single edge-notched bend (SENB) specimens containing shallow cracks ($a/W < 0.2$) are commonly employed for fracture testing of ferritic materials in the lower-transition region where extensive plasticity (but no significant ductile crack growth) precedes unstable fracture.

Critical J-values (J_c) for shallow-crack specimens are significantly larger (factor of 2-3) than the J_c values for corresponding deep-crack specimens at identical temperatures. The increase of fracture toughness arises from the loss of constraint that occurs when the gross plastic zones of bending impinge on the otherwise autonomous crack-tip plastic zones. Consequently, SENB specimens with small and large a/W ratios loaded to the same J-value have markedly different crack-tip stresses under large-scale plasticity. Detailed, plane-strain finite-element analyses (Figures 2 and 3) and a local stress-based criterion for cleavage fracture are combined to establish specimen size requirements (deformation limits) for testing in the transition region, which assure

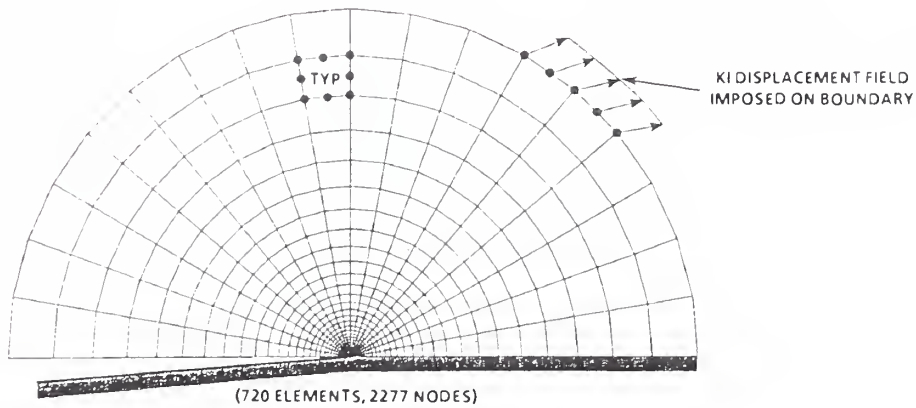

Figure 2. Finite-element mesh for the small-scale yielding computations

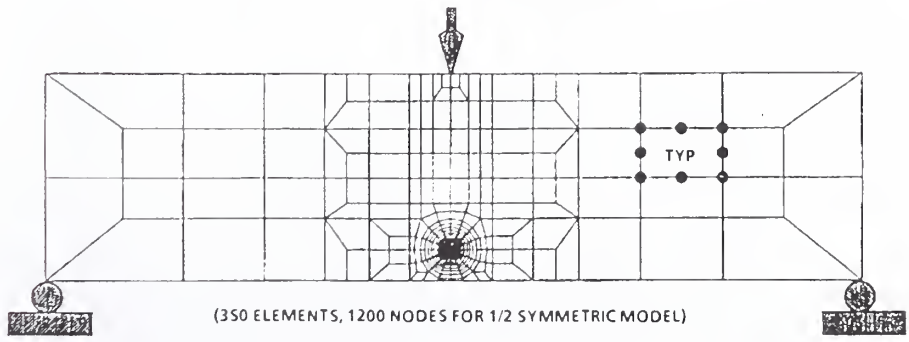

Figure 3 Typical finite-element mesh for plane strain analyses of the SENB specimens

a single parameter (J) characterization of the crack-tip stress field. Moreover, these analyses provide the first quantitative framework to correlate J_c-values with a/W ratio once the deformation limits are exceeded. The new procedures are directly applicable to estimate the toughness values for shallow-crack specimens from results of tests performed on conventional deep-crack specimens. The increased toughness values for shallow-crack specimens are required to perform realistic assessments of the surface-breaking defects most commonly encountered in structures.

The correlation procedure is applied to an extensive set of test results for an A36 steel and is shown to successfully correlate the a/W ratio effects on the measured fracture toughness values in the transition range.

For Additional Information:

Backup material on this effort is available from:

Navy Domestic Technology Fact Sheet Reader Reply Service
Code E211
Naval Surface Weapons Center
Dahlgren, VA 22448-5000
(703) 663-8921

Refer to 160502/TN

NAVY
Domestic Technology Transfer Fact Sheet

Solar-Powered Cathodic Protection System Developed

The Naval Coastal Systems Center (NCSC), Panama City, Florida, has developed a solar-powered system for cathodic protection of basic steel and iron type structures without requiring any auxiliary backup power. The impressed current type system uses a photovoltaic (PV) solar panel array to supply continuous DC operating current. The structure is initially, temporarily provided with preconditioning polarization for a predetermined extended, continuous time by a separate non-solar DC generating means; thereby, impressing it with the requisite beneficial negative potential, which completes the initial polarization. The temporary power source is then disconnected, and the solar array is promptly connected on circuit to continue to provide the requisite high negative beneficial potentials, which were achieved by the preconditioning polarization, and to thereby maintain the cathodic protection. The impressed relatively high negative potential has a relatively slow rate of decay that permits the use of a PV solar array and provides excess available power without the customary auxiliary backup power means, such as batteries. This method enables the system to easily maintain the impressed current cathodic protection system indefinitely even during inclement weather and nighttime conditions.

For Additional Information:

Backup material on this effort is available from:

Navy Domestic Technology Fact Sheet Reader Reply Service
Code E211
Naval Surface Weapons Center
Dahlgren, VA 22448-5000
(703) 663-8921

Refer to 160703/TN

NASA Tech Brief
National Aeronautics and Space Administration
Ames Research Center, Moffett Field, California

Accounting for Compressibility in Viscous Flow in Pipes

Variations of density and velocity across the flow cross section are included in calculations.

A method has been developed to account for the effects of compressibility in viscous flows through long, circular pipes of uniform diameter. The method is based on the approximation of variations in density and velocity across the pipe cross section by profile equations previously developed for boundary-layer flow between flat plates.

The concept of "fully developed" flow was originally defined for an incompressible flow in which the velocity at any given point on the cross section does not vary with position along the pipe. This concept is extended here to compressible flow in which the ratio of the velocity at any given point to the velocity at the centerline point does not vary with position along the pipe. Measurements have confirmed that subsonic flows tend to be "fully developed" in this extended sense (see figure).

The cross-sectional velocity profile is assumed to be similar to a flat-plate boundary-layer profile:

$$u/u_c = (2y/d)^n$$

where u = the velocity at radial distance y from the wall, u_c = the velocity at the centerline, and d = the diameter of the pipe. The cross-sectional distribution of temperature is constructed in a manner similar to the procedure normally used in flat-plate boundary-layer flows. The wall of the pipe is assumed to be adiabatic. In this way, the temperature at any point in the flow can be expressed in terms of the ratio of specific heats of the flow medium, the mach number at the centerline, the velocity profile, and a "recovery factor" (which is 0.88 for turbulent flows).

The **Velocity of Flow** varies along the pipe, but the power-law shape of the velocity profiles is assumed to be invariant along the pipe.

The governing equations of flow (conservation of mass, momentum, and energy) are reduced to convenient forms by introducing dimensionless variables and defining special profile integrals of velocity and temperature profiles. A method is developed to solve the equations and obtain solutions for values of flow friction in terms of measured gradients of wall static pressure.

The method was used to analyze the detailed pressure measurements made in a long pipe for flow of air at a wide range of flow speeds. Values of flow friction derived from these measurements were compared with data in the literature on incompressible flow in pipes. The effect of the mach number on flow friction was then extracted from these data by applying a special procedure that isolated the effects of the Reynolds number and the roughness of the surface. The results show that the effect of the mach number in pipe flow follows the trend previously established for flows over flat plates.

This work was done by Frank W. Steinle of **Ames Research Center**, *Ken Gee of the California Polytechnic State University, and Sreedhara V. Murthy of CALSPAN. Further information may be found in AIAA paper 88A-48888, "Compressibility Effects on Flow Friction in a Fully Developed Pipe Flow."*

Copies may be purchased [prepayment required] from AIAA Technical Information Service Library, 555 West 57th Street, New York, New York 10019, Telephone No. (212) 247-6500.
ARC-12249/TN

FOR ADDITIONAL INFORMATION: *Contact: Director, Technology Transfer Division, P.O. Box 8757, BWI Airport, MD 21240; (301) 621-0100 Ext. 241*
REFER TO THE NUMBER LISTED AT THE END OF THIS ARTICLE

NASA Tech Brief
National Aeronautics and Space Administration
Ames Research Center, Moffett Field, California

Adaptive Grids for Computations of Three-Dimensional Flows

A spring-system analogy is extended from two to three dimensions.

A self-adaptive-grid method has been devised and enhanced for the efficient computation of complicated three-dimensional flows. An extension of a method developed previously for two-dimensional flows, this method is based in part on the analogy of a fictitious system of tension and torsion springs that connect the grid points (see Figure 1).

The stiffnesses of the springs can be specified in terms of some measures of the flow-field characteristics (density, mach number, and the like) or in terms of parameters computed on the grid itself. By specifying minimum and maximum permissible spacings, the grid can be said to be "self-adaptive" or "solution-adaptive" (see Figure 2), and iterative adaptions/solutions can be performed in the effort to achieve a desired convergence.

An adaptation involves the use of variational principles to minimize the potential energy stored in the springs. For the adaptation along one coordinate line (e.g., the $\xi_{j,k}$ line in Figure 1), that line is held fixed while each grid point on the line is allowed to move freely along it in response to the tugs of the tension springs that connect it to the two adjacent grid points on the same line and to the twists of the torsion springs that connect it to the adjacent grid points on the adjacent lines that represent the same (e.g., ξ) coordinate. For a three-dimensional adaptation, the procedure is split into a sequence of adaptations, each along one coordinate axis at a time.

A user-friendly computer research code has been written to implement the adaptive-grid algorithm. In response to the maximum and minimum grid spacings specified by the user, the code automatically calculates most of the incorporated grid parameters, which affect orthogonality and smoothness. The user selects the direction of initial adaptation along a curvilinear grid line in the physical space. Grid points are then redistributed to optimal positions along a family of such lines, the collection of which sweeps a curved grid surface specified by the user. The procedure crosses, in a given marching direction, the entire physical space filled by these surfaces.

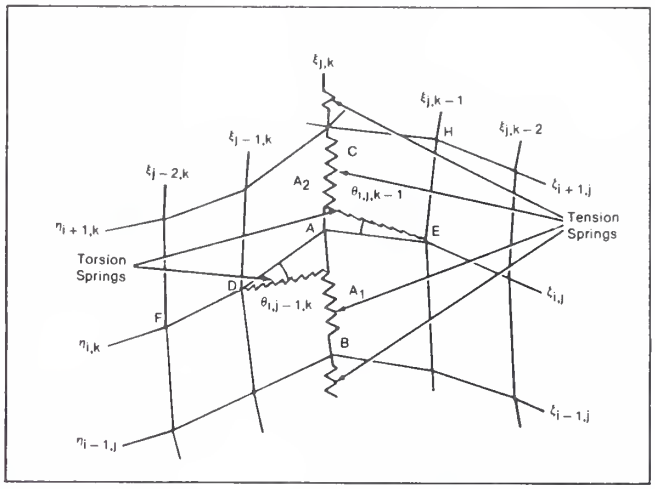

Figure 1. **Fictitious Springs** connecting the points of the computational grid are used to determine an optimum grid spacing. Each point (e.g., A) is connected to neighboring points (B through E) by tension and torsion springs. The stiffnesses of the tension springs are related to flow-field quantities. The stiffnesses of the torsion springs resist the departure of the grid from orthogonality.

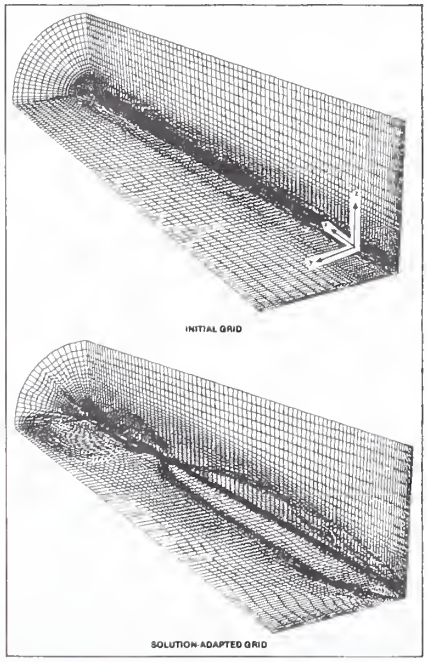

Figure 2. This **Initial Grid and Resulting Solution-Adapted Grid** were used to calculate the three-dimensional supersonic flow about a two-nozzle afterbody. In this case, the grid is adapted to the solution of mach numbers. In the adapted grid, points are clustered across the shocks and mixing layers, depicting all the features of the flow.

This work was done by M. Jahed Djomehri and George S. Deiwert of **Ames Research Center**. *Further information may be found in NASA TM-101027 [N89-11718], "Three-Dimensional Self-Adaptive Grid Method for Complex Flows."*

Copies may be purchased [prepayment required] from the National Technical Information Service, Springfield, Virginia 22161, Telephone No. (703) 487-4650. Rush orders may be placed for an extra fee by calling (800) 336-4700.
ARC-12479/TN

FOR ADDITIONAL INFORMATION: *Contact: Director, Technology Transfer Division, P.O. Box 8757, BWI Airport, MD 21240; (301) 621-0100 Ext. 241*
REFER TO THE NUMBER LISTED AT THE END OF THIS ARTICLE

NASA Tech Brief
National Aeronautics and Space Administration
Ames Research Center, Moffett Field, California

Algebraic Model of Turbulence for Internal Flow

An enhanced eddy-viscosity approximation simplifies calculations.

An algebraic approximation has been developed for use in calculating turbulent flow in a duct with a sharp 180° turn. Sharp curvatures of the surfaces at the turn increase the complexity of the flow and the equations that describe it, and previous studies of the effect of curvature on turbulence have been limited to mild curvatures. The approximation is expected to simplify the mathematical modeling of complicated turbulent flows, particularly those in air-breathing engines.

The effects of turbulence are summarized in a composite eddy viscosity ν_t. For this purpose, it is first necessary to define an effective mixing length via

$$\ell = k^2\left[1-\exp\left(-\frac{y}{k\delta_\omega}\right)\right]\delta_\omega$$

for fully turbulent internal flow, and

$$\ell = ck\left[1-\exp\left(-\frac{y}{c\delta_\omega}\right)\right]\delta_\omega$$

for partially developed turbulent flow, where y is the distance from the wall, δ_ω is the distance from the point of maximum vorticity to the point where vorticity vanishes, and c and k are adjustable parameters with typical values of 0.25 and 0.4, respectively. Next, it is necessary to define an effective vorticity length near the wall as

$$\Lambda = \frac{u_{ref}}{|\omega|_{max}}$$

where u_{ref} is the average velocity at the inlet boundary and $|\omega|$ is the magnitude of vorticity. Then, using the concept of laminar viscous spreading, an effective thickness of the viscous region is defined as

$$\delta^+ = \sqrt{\frac{\nu\Lambda}{u_{ref}}} = \sqrt{\frac{\nu}{|\omega|_{max}}}$$

The scale length y^+ of the inner sublayer is then given by

$$y^+ = \frac{y}{\delta^+}$$

where y is the distance from the wall.

Finally, one must define a factor γ, which represents the intermittency of turbulence in the outer layer:

$$\gamma = \frac{1}{2}\left\{1-\mathrm{erf}\left[5\left(\frac{y-y_{\omega max}}{\delta_\omega}-0.8\right)\right]\right\}$$

where $y_{\omega max}$ is the distance of the maximum vorticity from the wall. Then the composite eddy viscosity is given by

$$\nu_t = \gamma\left[\ell\left(1-e^{-y^+/A^+}\right)\right]^2|\omega|$$

This algebraic model of viscosity was inserted in a computer program that uses the Navier–Stokes equations to simulate three-dimensional, incompressible, steady flow. The results of the simulation agreed fairly well with the results of experiments in an axisymmetric turnaround-duct model (see figure).

The **Flow in an Axisymmetric Turnaround Duct** model was measured and compared with the flow predicted by a computer program that includes the algebraic eddy viscosity described in the text. (The experimental duct model represents a design concept for a compact turbine engine.)

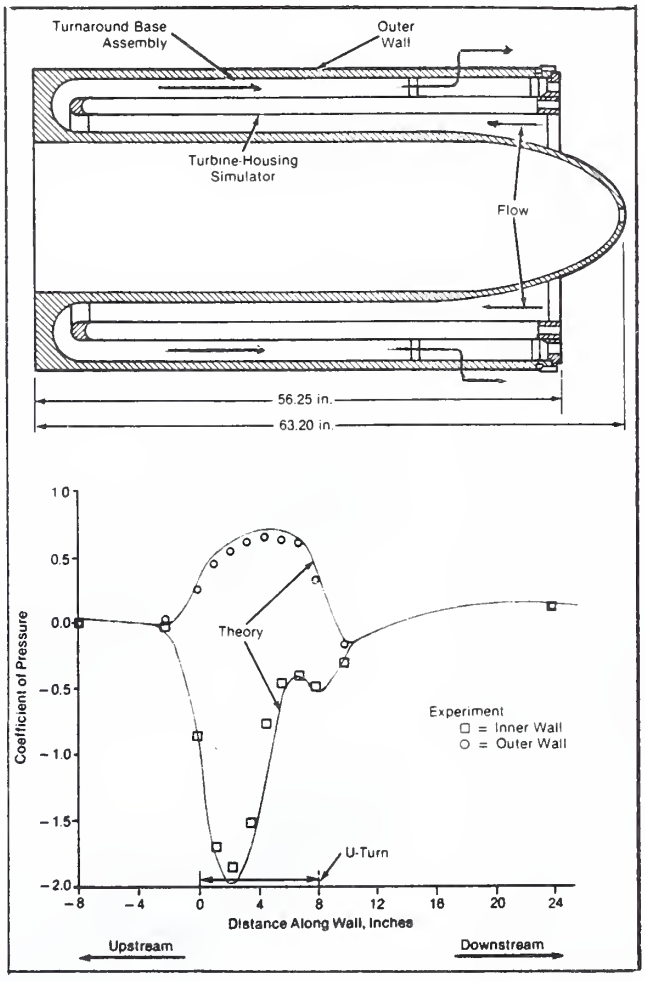

This work was done by Dochan Kwak of **Ames Research Center** *and James L. C. Chang of Rockwell International Corp. Further information may be found in AIAA paper 88A-22446, "A Numerical Study of Turbulent Internal Shear Layer Flow in an Axisymmetric U-Duct".*

Copies may be purchased [prepayment required] from AIAA Technical Information Services Library, 555 West 57th Street, New York, New York 10019, Telephone No. (212) 247-6500. ARC-12544

FOR ADDITIONAL INFORMATION: *Contact: Director, Technology Transfer Division, P.O. Box 8757, BWI Airport, MD 21240; (301) 621-0100 Ext. 241*
REFER TO THE NUMBER LISTED AT THE END OF THIS ARTICLE

NASA Tech Brief
National Aeronautics and Space Administration
Lyndon B. Johnson Space Center, Houston, Texas

Docking System Would Accommodate Misalignments

The system would also absorb kinetic energy.

A conceptual docking system would absorb kinetic energy along each of three orthogonal directions. It would accommodate large misalignments between the docking objects. Conceived for docking the Space Shuttle in the Space Station, the system may be useful in other applications in which a large moving object must be aligned with and joined to another — for example, cranes, robots, and fuel or material-loading lines.

The lightweight system would consist of a probe on one of the two docking objects and a drogue on the other object. The probe would contain a latching mechanism; pitch, roll, and yaw dampers; and centering and rigidizing mechanisms (see figure). The latching mechanism would ride on a y-axis track, which would ride on an x-axis track, which, in turn, would ride on a z-axis track. The probe could therefore translate in the x and y directions to accept misalignment with the drogue and in the z direction to enter the drogue. Three eddy-current dampers would absorb the energy of motion along the orthogonal directions, bringing the docking objects to a smooth stop.

According to the concept, as the docking objects approached, the z track would extend the probe by 9 in. (22.9 cm). At the first contact of the probe with the drogue, the x and y drives would allow such lateral translation as would be necessary to accommodate misalignment between the probe and the drogue, and the z drive would rapidly extend the probe deep into the drogue. Latches on the probe would engage the drogue.

Meanwhile, the dampers would absorb kinetic energy. The probe could rotate ±10° with respect to the x and y axes and ±11° with respect to a gimbal. When motion had been stopped, a collet on the probe would retract to lock against pitching and yawing. Actuator-driven plungers would lock the probe latches against movement in the x, y, and z directions. The z-track drive would slowly retract the probe to its storage position.

For release, the probe collet would be extended, relieving the preload between the probe and the drogue. The latch-locking piston would then be retracted, releasing the spring-loaded latches. The probe would then be disconnected from the drogue.

This work was done by Rasmik Ajemian, Earl V. Holman, and Siamak Ghofranian of Rockwell International Corp. for **Johnson Space Center.**
MSC-21596/TN

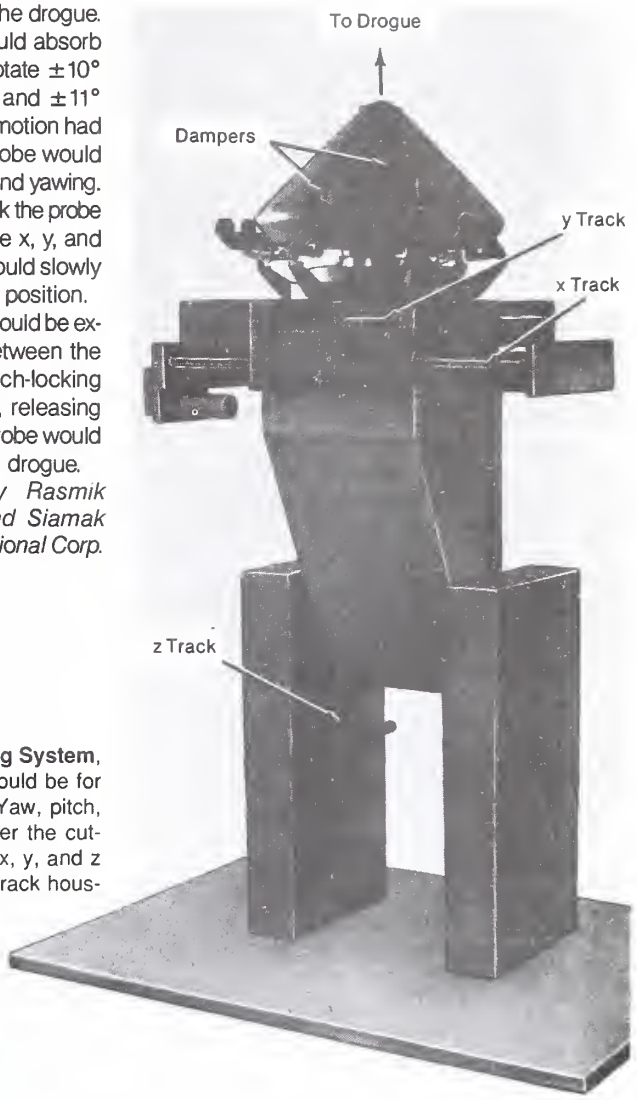

In this **Mockup of the Docking System**, the probe is extended as it would be for initial contact with a drogue. Yaw, pitch, and roll dampers appear under the cutaway shell of the probe. The x, y, and z dampers are hidden in the z-track housing.

FOR ADDITIONAL INFORMATION: *Contact: Director, Technology Transfer Division, P.O. Box 8757, BWI Airport, MD 21240, (301) 621-0100 Ext. 241*
REFER TO THE NUMBER LISTED AT THE END OF THIS ARTICLE

NASA Tech Brief
National Aeronautics and
Space Administration

Experiences With the JPL Telerobot Testbed

Issues and insights are discussed.

A report identifies problems and technological gaps that exist in robotic systems integration. It focuses upon the problems that were experienced during the development of the Telerobot Testbed System at NASA's Jet Propulsion Laboratory (JPL): an integrated robotic testbed used to develop, implement, and evaluate the performance of advanced concepts in autonomous, teleautonomous, and teleoperated control of robotic manipulators. The objective of this report is to provide information that can be used to guide and expedite the development of future integrated robotic systems. Problems are identified in calibration and world modeling, process planning, and system architecture and software engineering.

- **Calibration**. Calibration issues in an integrated multisensory, multiactuated robotic system can have a profound impact upon the design, implementation, and performance of high-level-control and task-planning algorithms. As a prime example of this, the authors cite the difficulties involved in merging information from vision and touch sensors to estimate the location of an object in the workspace.

  To merge information from disparate sensors, the information obtained by each must be transformed into a common representation to permit integration. In addition to providing a means for integration, the representation must also serve the informational needs of the rest of the system. In the Testbed, the common representation is a tree-topology connected data base describing the spatial relationships among all the objects.

  The difficulty in integrating the various sensor information has arisen, in part, from the fact that several of the sensors (i.e., two force/torque sensors and two cameras) are mounted on independent platforms. Referencing sensors on a manipulator to a common coordinate system depends on the accurate calibration of manipulator kinematics, which is extremely difficult. Inherent physical constraints have also made it difficult to determine where each manipulator is with respect to another, as in the case of the system's vision arm.

  These difficulties have had a significant impact upon several system functional components. For example, ad-hoc (i.e., engineered) methods have been employed to maintain the consistency of the system's data base.

  The authors have concluded that the design of future large-scale robotic systems must include features that permit the system's calibration in a complete and coherent fashion. In particular, accommodations must be made to facilitate the accurate identification of device spatial relationships in terms of both hardware and software.

- **Planning**. The planning of telerobot processes (i.e., actions such as move, grasp, and rotate) presented special problems because of the complex and interacting nature of a very large number of problem constraints and characteristics. Among these were the usual constraints arising from the kinematic construction of the Puma 560 manipulators, which limited manipulability over large regions. Added to these were spatial constraints in the form of interarm collision avoidance for the three arms, arm/object collision avoidance, object/object interference avoidance during manipulation, and object occlusion during vision operations. Dynamic constraints included performance degradation and even instability of compliant motion operations near singular arm configurations, and poorly known gravity and friction effects.

  The challenge in planning became that of trying to blend engineered solutions successfully with algorithmic approaches. Because a standard rule or logic-based planning system would have been very difficult to design, an alternative "generate and test" approach was used instead. This approach utilized action-selection rules and procedures based on a partial handling of the various constraints to generate candidate actions. Detailed world-model-driven simulation of the action was then used to accept or reject the candidate action.

- **Architecture**. In a well-established and -understood field, the construction of a system without first exploring its formulation and design in great detail is foolhardy. Unfortunately, this rigor is not feasible in a research environment where requirements fluctuate. In these situations, success is often determined by the ability to react rapidly to significant design changes.

  First, it was observed that space telerobotics is not a highly structured task and that efforts should be placed on the reactive, feedback portion of the architecture that allows the robot to respond to the environment.

  Second, interface "blindspots," whereby higher-level subsystems are unable to command all of the actions that the hardware devices can perform, must be avoided at all costs because they inevitably lie precisely in the regions that turn out to be crucial to the functioning of the overall system.

  Third, the ability to shift functionality easily across subsystem interfaces is crucial as the development of new algorithms with improved functionality can force the shifting of large bodies of capability from higher-level subsystems to lower ones.

  Fourth, the practice of inserting additional layers into implementations for the express purpose of decoupling external users from the internal details of a piece of software (i.e., abstraction) is essential during the development of subsystem interfaces because such practice prevents minor internal modifications from being propagated to other subsystems.

  Finally, the most important issue in large systems' software development is human rather than technological. Frequent, detailed communication among all members of a development team is required to prevent minor choices on the part of subsystems from propagating disastrously to the system.

This work was done by Henry W. Stone, J. Balaram, and John J. Beahan of Caltech for **NASA's Jet Propulsion Laboratory.** *"Experiences With the JPL Telerobot Testbed: Issues and Insights." NPO-17928/TN*

FOR ADDITIONAL INFORMATION: *Contact: Director, Technology Transfer Division, P.O. Box 8757, BWI Airport, MD 21240; (301) 621-0100 Ext. 241*
REFER TO THE NUMBER LISTED AT THE END OF THIS ARTICLE

NASA Tech Brief
National Aeronautics and Space Administration
Ames Research Center, Moffett Field, California

Helicity-Density and Normalized-Helicity Maps of Flows

These maps clearly indicate vortexes and other important features.

Maps of helicity density and normalized helicity have been shown to be useful as graphical representations of important features of three-dimensional flow fields that contain vortexes. The more conventional pressure, density, and velocity-vector maps often do not adequately represent the vortical features of interest and sometimes give ambiguous indication of swirl direction. In contrast, the helicity-density and normalized-helicity representations emphasize the complicated and, therefore, important parts of a flow field, identify the vortexes, differentiate between primary and secondary vortexes, indicate the sense of the swirling motion, locate the free singular points (those not attached to surfaces), and trace the vortex-core streamlines that emanate from these points.

The helicity density is defined as the scalar product of the velocity and vorticity vectors at a given location in the flow field. The normalized helicity is defined as the inner product of the unit vectors along the velocity and vorticity directions; that is, the normalized helicity is the cosine of the angle between the velocity and the vorticity. One of the great advantages of the helicity density and the normalized helicity is that both their magnitudes and their senses are meaningful. A large helicity density reflects a large velocity and a large vorticity when the angle between them is small. The sign of the helicity density indicates the direction of swirl of the vortex relative to the velocity. Both the relative size of the helicity density and the changing of swirl direction, emphasized by graduation in color for magnitude and by different colors for positive or negative values, facilitate the distinction between primary and secondary vortexes in a graphical representation (see Figure 1).

The effectiveness of the helicity density as an indicator of vortexes is even much greater for low-subsonic flows, for which the conventional density mapping is not sufficiently sensitive because the variations in density are almost negligible. The sensitivity of the helicity-density representation remains high because in the core regions of the vortexes, both the velocity and vorticity always reach relatively high values and the angle between them is small. All these contribute to high values of the helicity density and to a clear representation of the vortexes.

Figure 2 shows the components of the vorticity vectors relative to a local streamline. One component is parallel to the local velocity vector, and the other two are perpendicular to it. The component parallel to the velocity, which is the only component that contributes to the helicity density, vanishes everywhere in a two-dimensional flow. It also vanishes wherever the flow is locally two dimensional, as on planes of symmetry. Therefore, the normalized helicity must be zero in two-dimensional flows and must vanish locally on planes of symmetry, thus emphasizing them in the graphical representation.

Each of the two components of vorticity perpendicular to the velocity is responsible for the curvature of the streamline in the plane that is perpendicular to it and includes the velocity vector. When these two perpendicular components decrease relative to a constant parallel component, the

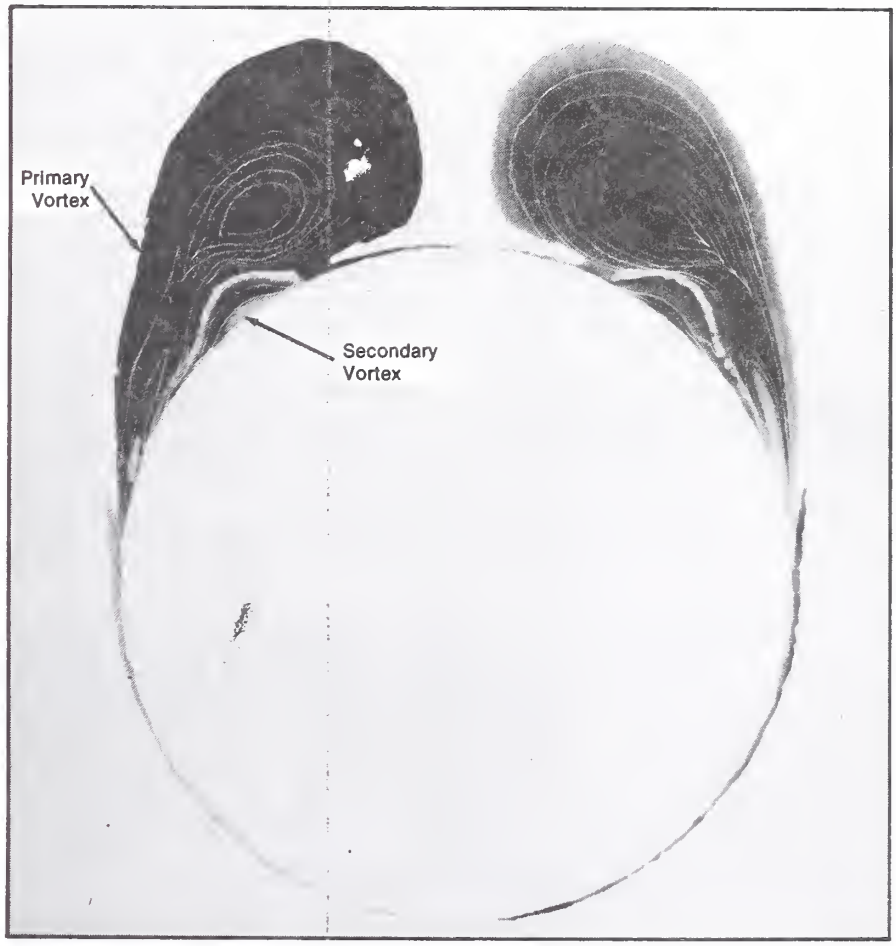

Figure 1. **A Primary and a Secondary Vortex** can be seen clearly in this plot of helicity-density contours in a cross section of the computed flow field about an ogive/cylinder body. The parameters of the flow field are free-stream mach number 0.2, angle of attack 40°, and Reynolds number 200,000.

local curvature of the streamline decreases, the angle between the vorticity and velocity vectors vanishes, and the normalized helicity tends toward unity.

The magnitude of the normalized helicity thus indicates the local curvature of the streamlines. In the limiting case, where the velocity and vorticity vectors are parallel, the normalized helicity is exactly equal to unity, and the streamline is locally straight. However, the flow is far from being two dimensional, because adjacent streamlines spiral around this streamline. The fact that the normalized helicity goes to its maximum value on a streamline of minimum curvature can be used to locate a vortex-core axis, which is such a streamline.

This work was done by Andrew D. Morrison of Caltech for **NASA's Jet Propulsion Laboratory.**

This invention is owned by NASA, and a patent application has been filed. Inquiries concerning nonexclusive or exclusive license for its commercial development should be addressed to the Patent Counsel, NASA's Resident Office-JPL. Refer to NPO-17625/TN.

Figure 2. The **Components of Vorticity** parallel and perpendicular to the streamline play an important role in the helicity-density and normalized-helicity graphical representation and are related to the local curvature of the streamline.

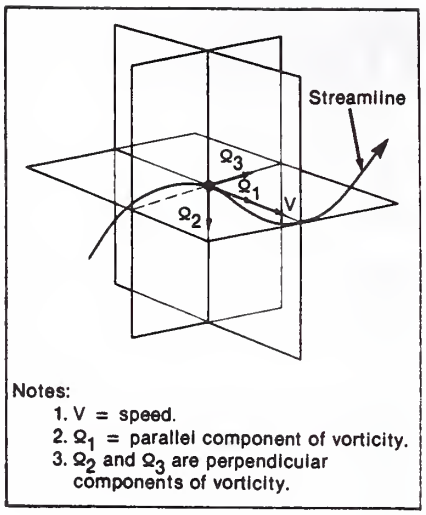

Notes:
1. V = speed.
2. Ω_1 = parallel component of vorticity.
3. Ω_2 and Ω_3 are perpendicular components of vorticity.

FOR ADDITIONAL INFORMATION: *Contact: Director, Technology Transfer Division, P.O. Box 8757, BWI Airport, MD 21240; (301) 621-0100 Ext. 241*

REFER TO THE NUMBER LISTED AT THE END OF THIS ARTICLE

NASA Tech Brief
National Aeronautics and Space Administration
NASA's Jet Propulsion Laboratory, Pasadena, California

Low-Speed Optical Speedometer

The delay between terrain-reflectance signals from two optical sensors indicates speed.

A proposed speedometer would measure the speed of a vehicle along the ground by comparing the signals from two inexpensive sensors focused on the surface passing beneath the vehicle (see figure). Unlike such sensors as Doppler radar, the proposed speedometer could be used to measure speeds as low as 10 cm/s.

Each of the two sensors would include a cylindrical lens and a single-element photodetector. Each lens would focus light from a small rectangular area of the passing ground-surface scene onto the plane that contains its detector. The sensors would be positioned so that the axes of the cylindrical lenses would be parallel to each other and perpendicular to the direction of motion.

As the vehicle moved, the sensors would follow the same path over the surface, one after the other. Thus, the two photodetectors would generate similar signals as they pass one after the other over the same surface features, but one signal would be delayed with respect to the other by an interval inversely proportional to the speed. A processor would compute a correlation between the two signals to determine the delay between them. The distance between the sensors would then be divided by this delay to determine the speed. The distance between the sensors and the focal length of the cylindrical lenses could be chosen to optimize performance for the anticipated speed range.

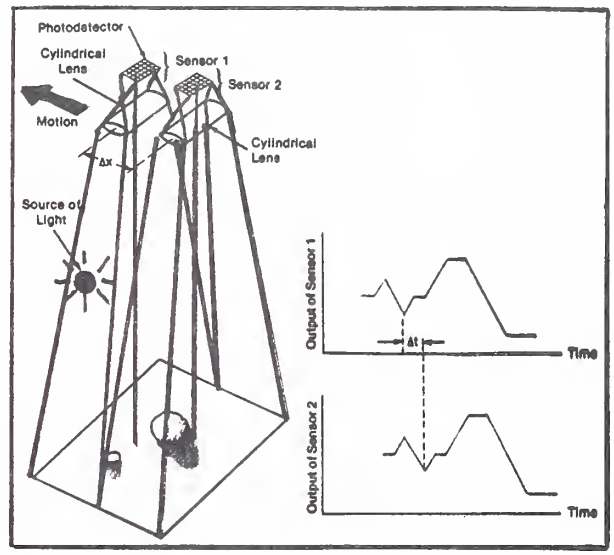

The **Optical Correlation Speedometer** would compare signals from two sensors to find the delay Δt between the passage of the first and second sensors over the same points on the ground. The two signals would be correlated to determine the value of Δt that provides the best match between them. The speed of the vehicle would be computed as $\Delta x/\Delta t$, where Δx is the distance between the sensors.

The source of light used to illuminate the area viewed by the sensors could be continuous or pulsed. With appropriate processing of the signals from the photodetectors, a pulsed or modulated source could facilitate discrimination from ambient light. An infrared source may be preferable if operation during both day and night is desired. The light source could be made to illuminate the surface obliquely to enhance ground features.

In the case of a vehicle free to move in any direction, such as a hovercraft or a vehicle equipped with pivoting wheels, there are two perpendicular components of velocity to measure. In that case, two sets of sensors mounted with their axes perpendicular to each other could measure both components.

This work was done by Katsunori Shimada of Caltech for **NASA's Jet Propulsion Laboratory**. *NPO-17702/TN*

FOR ADDITIONAL INFORMATION: *Contact: Director, Technology Transfer Division, P.O. Box 8757, BWI Airport, MD 21240; (301) 621-0100 Ext. 241*
REFER TO THE NUMBER LISTED AT THE END OF THIS ARTICLE

NASA Tech Brief
National Aeronautics and Space Administration
Marshall Space Flight Center, Alabama

Licensing Opportunity

Mathematical Model for Deposition of Soot

This model is expected to be more generally applicable than prior experimental correlations have been.

A semiempirical mathematical model predicts the deposition of soot in a tubular gas generator in which hydrocarbon fuel is burned in a very-fuel-rich mixture (equivalence ratio of the order of 10) with pure oxygen. The model was developed in response to concern over the deposition of soot in the gas generators and turbomachinery of rocket engines. The model may also be of interest in terrestrial applications that involve fuel-rich combustion or analogous processes; e.g., the purposeful deposition of soot to manufacture carbon black pigments.

Previously, the deposition of soot in rocket gas generators was studied by making crude empirical correlations between measurements of differential pressures and inferred measurements of soot. In contrast, this model is based on the physics of aerosols and is meant to be calibrated by correlation with direct measurements of the formation and deposition of soot, including measurements of the scattering of laser light from soot and laser measurements of flow fields. Once so calibrated, the model is expected to be generally applicable to gas generators of various configurations.

The principal mechanisms in the model are (1) inception of the solid soot particles from gaseous products of combustion, (2) the increase in the sizes and masses of soot particles that results from surface reactions with gas-phase hydrocarbons, and (3) deposition via thermophoresis (the transfer of mass down a gradient of temperature). The first and most important equation of the model is the one that accounts for the volume fraction of soot (the volume of soot per unit volume of flow) as a function of time. The right side of this equation consists of a term that accounts for inception and a term that accounts for growth. This equation can be used to calculate the volume fraction of soot as a function of position along the axis of a gas generator by assuming that the flow is one-dimensional and converting the time variable to the equivalent axial position.

The two critical variables in the equation are the rate of inception of particles (which is a function of injector mixing) and the rate of growth of soot on the surfaces of the particles. These variables were chosen because they can be quantified empirically via laser measurements of the soot and flow field.

The second major equation of the model is the one that accounts for the gross deposition of soot particles from the flow onto the wall. This equation uses well-defined correlations among local coefficients for the transfer of heat and mass to determine the local coefficients for the deposition of soot. One factor in this equation is the volume fraction of soot calculated in the first equation. The coefficient for the transfer of mass in the deposition of soot is found by using the conventional analogy between the transfers of heat and mass and accounting for thermophoresis. The thermophoretic influence on deposition is characterized by the ratio between the temperature of the wall and the temperature of the free-stream part of the flow.

The amount of soot ultimately deposited on the wall is calculated as the difference between the gross amount deposited (calculated as described above) and the amount of previously deposited soot that is sheared off the wall by the flow. The equation for the fraction sheared off is based on a semiempirical soot-layer-adhesion-strength criterion that has been found to be accurate in studies of the adhesion of dust and includes an assumed log-normal distribution of the force required to remove a particle of soot from the surface. The force that causes the removal of soot is assumed to correspond to the wall shear stress.

This work was done by Darby B. Makel of Aerojet TechSystems for **Marshall Space Flight Center.**

Inquiries concerning rights for the commercial use of this invention should be addressed to the Patent Counsel, Marshall Space Flight Center. Refer to MFS-28506/TN.

George C. Marshall Space Flight Center
Technology Utilization Officer Ismail Akbay
Code AT01
Marshall Space Flight Center,
AL 35812
(205) 544-2223
Patent Counsel
Leon D. Wofford, Jr.
Mail Code CC01
Marshall Space Flight Center,
AL 35812
(205) 544-0024

FOR ADDITIONAL INFORMATION: *Contact: Director, Technology Transfer Division, P.O. Box 8757, BWI Airport, MD 21240; (301) 621-0100 Ext. 241*
REFER TO THE NUMBER LISTED AT THE END OF THIS ARTICLE

NASA Tech Brief
National Aeronautics and Space Administration
NASA's Jet Propulsion Laboratory, Pasadena, California

Licensing Opportunity

Self-Adjusting Choke for Nozzle

The issuing stream remains coherent for greater distances despite fluctuations in pressure and/or rate of flow.

A self-adjusting choke for a nozzle enables the issuing stream of liquid to remain coherent, despite fluctuations in the flow, along a greater distance than is possible with the same nozzle without the choke. The resulting extended coherent stream is advantageous for firefighting, making it possible to direct a more concentrated flow of water at a flame or hotspot. It could also be used in mining and for transferring liquids.

The natural instabilities of streams leaving nozzles frequently cause the streams to disperse relatively close to the nozzles. Although a previously developed advanced nozzle produces a more-coherent issuing stream, it functions optimally at only one upstream pressure or rate of flow. The new choke, based partly on the previous nozzle concept, helps to maintain the coherence of the flow over a range of pressures and rates of flow.

The self-adjusting choke is a relatively thick, flexible membrane that contains, typically, three orifices, the outer two of which are slanted (see figure). The membrane is inserted into the opening of the nozzle. When the rate of flow is low and the membrane is not much distorted by the upstream pressure of the fluid, the liquid issuing from the outer orifices tends to separate into two diverging streams. Simultaneously, the web of fluid issuing from the middle orifice tends to pull the diverging streams together. The resulting balance of forces produces a stable spiraling stream.

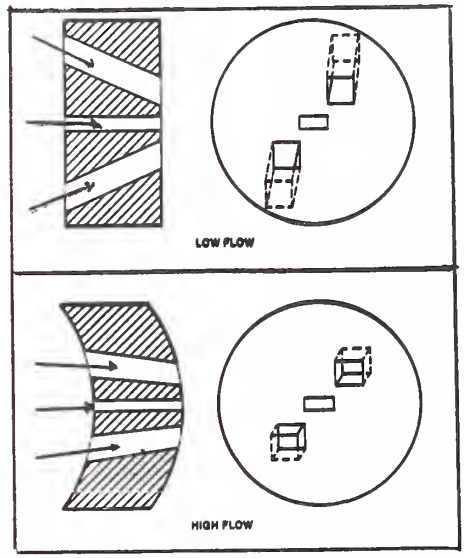

A **Flexible Membrane With Slanted Orifices** deforms according to the upstream pressure in the flowing liquid, producing a more-coherent spiraling stream.

As the upstream pressure (or, equivalently, the rate of flow) increases, the membrane flexes, redirecting the outer streams so that they have a lesser tendency to diverge. Thus, although the greater flow tends to cause the outer streams to separate more than under the unloaded condition, the smaller angle between the outer streams still enables the web to counterbalance the tendency toward divergence, and a stabler stream results.

This work was done by Andrew D. Morrison of Caltech for **NASA's Jet Propulsion Laboratory.**

This invention is owned by NASA, and a patent application has been filed. Inquiries concerning nonexclusive or exclusive license for its commercial development should be addressed to the Patent Counsel, NASA's Resident Office-JPL. Refer to NPO-17625/TN.

Jet Propulsion Lab.
NASA Resident Office
Technology Utilization Officer Gordon S. Chapman
Mail Stop 180-801
4800 Oak Grove Drive
Pasadena, CA 91109
(818) 354-4849
Patent Counsel Paul F. McCaul
Mail Code 180-801
4800 Oak Grove Drive
Pasadena, CA 91109
(818) 354-2734
Technology Utilization Mgr. for JPL Norman L. Chalfin
Mail Stop 156-211
4800 Oak Grove Drive
Pasadena, CA 91109
(818) 354-2240

FOR ADDITIONAL INFORMATION: *Contact: Director, Technology Transfer Division, P.O. Box 8757, BWI Airport, MD 21240; (301) 621-0100 Ext. 241*
REFER TO THE NUMBER LISTED AT THE END OF THIS ARTICLE

NASA Tech Brief
National Aeronautics and Space Administration
NASA's Jet Propulsion Laboratory, Pasadena, California

Strain Center for Analysis of Forces

After yielding, forces are perpendicular to radii from the strain center.

The concept of a strain center has been introduced to facilitate the analysis of forces resulting from an eccentric load after the elastic limit has been exceeded. The concept is especially useful where the loads are known and the directions of the forces are being analyzed; e.g., the limiting frictional force between a wheel and the ground.

Conventional force analysis superimposes direct forces upon separately computed torsional forces when an object is eccentrically loaded. The conventional torsional forces are perpendicular to and proportional to their radii from the center of gravity of the force pattern. This superposition gives rise to a centroid from which the vector sums are also perpendicular to and proportional to their radii from this centroid. The centroid lies on a line through the center of gravity and perpendicular to the direction of the eccentrically applied load.

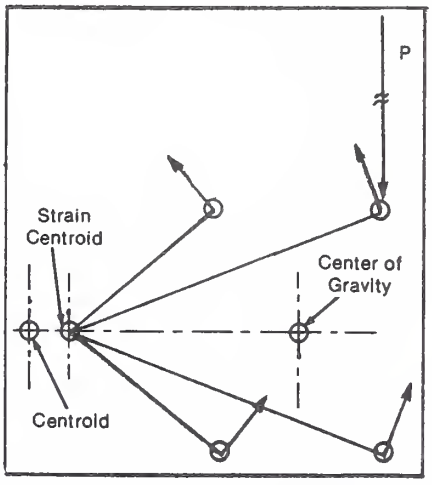

Strain Centroid has equal resisting forces.

After the elastic limit is exceeded (the wheels slip on the ground), the forces redistribute until each is at its maximum value. The forces are no longer perpendicular to radii from the centroid. They shift to being perpendicular to radii from the strain center. The strain center also lies on the line through the center of gravity and perpendicular to the direction of the eccentrically applied load.

This work was done by Donald B. Bickler of Caltech for **NASA's Jet Propulsion Laboratory**.
NPO-17966/TN

FOR ADDITIONAL INFORMATION: *Contact: Director, Technology Transfer Division, P.O. Box 8757, BWI Airport, MD 21240; (301) 621-0100 Ext. 241*
REFER TO THE NUMBER LISTED AT THE END OF THIS ARTICLE

NASA Tech Brief
National Aeronautics and Space Administration
Langley Research Center, Hampton, Virginia

Licensing Opportunity

Zero-Spring-Rate Mechanism/Air Suspension Cart

A compact mechanism suspends articulating flexible structures with minimal constraints.

New suspension techniques will be necessary for ground-testing of the flexible spacecraft anticipated in NASA's future space activity. The most complex spacecraft involve nonlinear maneuvering (i.e., large-angle slewing) with such articulating substructures as remote manipulating systems. Ultimately, the goal of research in advanced suspension systems is to simulate flight boundary conditions (weightlessness) when testing flexible space structures on the ground. To achieve such a goal, a suspension system must counteract gravitational loads while allowing a structure to move without constraint. Because vibratory motion results from the elasticity of a flexible spacecraft, the suspension problem involves the development of methods of suspending spacecraft that have vibratory motions superimposed on large rigid-body motions. Any suspension device must be considered as an integral part of the structure. However, it should be designed so that the dynamics of the device interact minimally with the dynamics of the structure.

A zero-spring-rate mechanism (ZSRM)/air suspension cart is being developed by NASA Langley Research Center. It is to be used to suspend flexible, "mass-critical" articles like lightweight spacecraft undergoing such large motions as slewing, translation, and telescoping/retraction. The novelty of the method and equipment is the ability to suspend a flexible article undergoing large rigid-body motion concurrent with vibratory motion, with minimal interaction between the suspended article and the suspending hardware. Previous suspension devices include cable suspensions, airbags, air bearings, and cables with ZSRM's. These devices are not designed for structures that undergo concurrent rigid-body and vibratory motions. The ZSRM/air suspension cart is very adaptive to active control, which would reduce undesirable effects caused by friction, nonlinearity, and mass coupling. The ZSRM/air suspension cart (see figure) is very small compared to a test article and is easily adapted to most test facilities. Because no cables are needed, minimal overhead clearance is needed. Because this device is built easily, it is practical for most suspension applications.

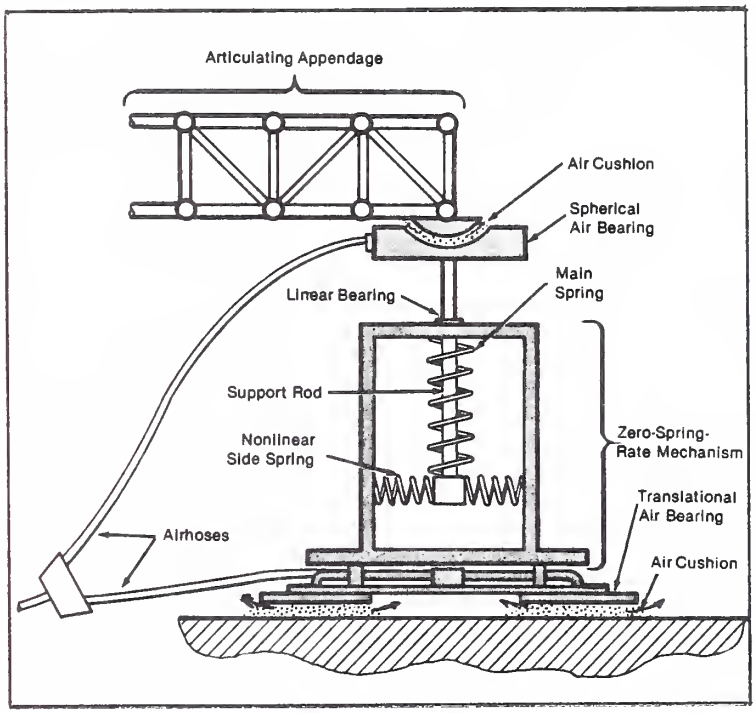

An **Articulating Appendage** is suspended from underneath by a ZSRM/air suspension cart.

The design of this device evolves from the premise that as the dynamic properties of the suspension device are diminished, the dynamic properties of the test structure dominate the structure/suspension system. By combining a translational air bearing, a ZSRM, and a spherical air bearing, the design goal can be met. An air bearing carries a load in translation with very low friction. This air bearing allows the structure to have any horizontal motion. The ZSRM, which is placed atop the air bearing, supports the weight of structure with minimal vertical stiffness. A ZSRM is a negative nonlinear spring in parallel with a positive spring such as a prestressed coil spring. The negative spring can be any prestressed member that provides a component of prestressed stiffness in the vertical direction.

The weight of a structure is supported by the main spring. A compressive side load is applied to the structure-attachment point. When the article under test is displaced vertically from the equilibrium position of the main spring, a vertical component of the side load acts in a direction opposite to that of the load produced by the main spring. Because the vertical component of the side force acts in a sense opposite to that of the main spring, it behaves effectively like a negative spring. This negative spring reduces the overall stiffness in suspending a structure. By reducing the vertical stiffness, one decreases the constraint on the motion of the structure; that is, there is very little resistance to the vibratory motion of the structure. The spherical air bearing atop the ZSRM leaves the rotational motion of the structure at the point of attachment unconstrained. The overall effect of the device is that the weight of the structure is supported while its motion is virtually unconstrained. Therefore, the structure can behave as though it were weightless.

Another basic suspension consideration is whether structures will be supported overhead or underneath. Overhead suspension is usually accomplished with cables. These are widely used, their overall vertical stiffnesses can be reduced with ZSRM's, and they offer simplicity for ground testing of structures undergoing only vibratory motions. Cable suspensions have pendular and axial stiffnesses, and if they

are used to suspend rapid slewing or articulating structures, then complicated control devices and suspension hardware must also be used. With the ZSRM/air suspension from underneath, high overhead height needed for cables (to reduce pendular and axial stiffness) is not required. Therefore, only the size of the structure will dictate how tall a test facility should be. Though the mass of the suspension hardware couples horizontally with the structure, its dynamic effect can be easily modeled analytically.

This work was done by Stanley E. Woodard and Victor M. Cooley of **Langley Research Center.**

This invention is owned by NASA, and a patent application has been filed. Inquiries concerning nonexclusive or exclusive license for its commercial development should be addressed to the Patent Counsel, Langley Research Center. Refer to LAR-14142/TN.

Langley Research Ctr.
Technology Utilization
Officer John Samos
Mail Stop 139A
Hampton, VA 23665
Patent Counsel
George F. Helfrich
Mail Code 279
Hampton, VA 23665
(804) 864-3523

FOR ADDITIONAL INFORMATION: *Contact: Director, Technology Transfer Division, P.O. Box 8757, BWI Airport, MD 21240; (301) 621-0100 Ext. 241*
REFER TO THE NUMBER LISTED AT THE END OF THIS ARTICLE

NASA Tech Brief
National Aeronautics and Space Administration
Lyndon B. Johnson Space Center, Houston, Texas

Vapor-Resistant Heat-Pipe Artery

New features of the wick improve the return of liquid in a heat pipe.

Vapor lock in a heat pipe can be delayed or prevented by modification of the liquid-return artery. In vapor lock, vapor generated in the wick penetrates the artery. Vapor lock prevents liquid from moving along the artery and thus stops the transfer of heat along the heat pipe.

Two anti-vapor-lock modifications have been developed and tested (see figure). In one, a fine-grained aluminum powder is sintered to form the portion of the wick that surrounds the artery; a coarse-grained sintered aluminium powder constitutes the rest of the wick, which lines the wall of the heat pipe. The fine-grained portion of the wick allows condensed liquid, but not much vapor, to pass through to the artery.

In the other modification, a slotted tube is placed around the artery within the wick. Condensed liquid can pass through the slot to the artery. The smooth inside surface of the tube, unlike the rough, porous interior of the wick, offers few sites for the nucleation of bubbles. Thus, a larger temperature drop is required before nucleate boiling — and, hence, the formation of appreciable amounts of vapor — can begin.

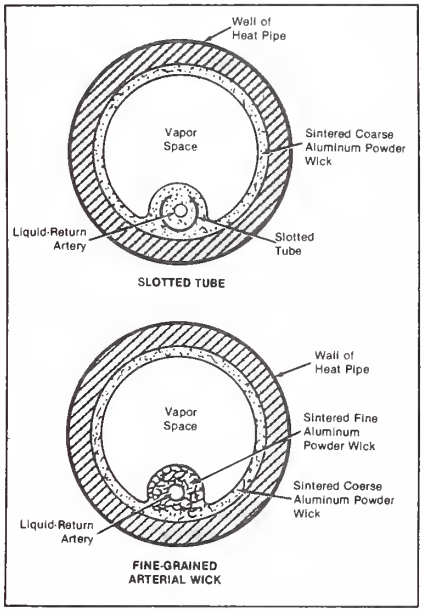

Modifications of the Wick prevent the flow of vapor into, or the formation of vapor in, the liquid-return artery. The small pores of the fine-grained sintered wick help to prevent the formation of large bubbles. The slotted tube offers few nucleation sites for bubbles.

This work was done by Peter M. Dussinger, Robert M. Shubach, and Matt Buchko of Thermacore, Inc., for **Johnson Space Center**.

In accordance with Public Law 96-517, the contractor has elected to retain title to this invention. Inquiries concerning rights for its commercial use should be addressed to

Peter M. Dusinger
Thermacore, Inc.
780 Eden Road
Lancaster, PA 17601

Refer to MSC-21492/TN, volume and number of this NASA Tech Briefs *issue, and the page number.*

FOR ADDITIONAL INFORMATION: *Contact: Director, Technology Transfer Division, P.O. Box 8757, BWI Airport, MD 21240; (301) 621-0100 Ext. 241*
REFER TO THE NUMBER LISTED AT THE END OF THIS ARTICLE

NASA Tech Brief
National Aeronautics and Space Administration

Program for Elastoplastic Analyses of Plane Frames

Nonlinear collapse phenomena are simulated by iterative linear analyses.

PLAN2D is a FORTRAN computer program for the plastic analysis of planar frame structures. Given a structure and loading pattern as input, PLAN2D calculates the ultimate load that the structure can sustain before collapse. Element moments and plastic hinge rotations are calculated for the ultimate load. The locations of hinges required for collapse mechanisms to form are also determined.

The program proceeds in an iterative series of linear elastic analyses. After each iteration, the resulting elastic moments in each member are compared to the reserve plastic moment capacity of that member. The member or members in which moments are closest to their reserve capacities determine the minimum load factor and the site where the next hinge(s) is(are) to be inserted. Next, hinges are inserted and the structural-stiffness matrix is reformulated. This cycle is repeated until the structure becomes unstable. At this point, the ultimate collapse load is calculated by accumulating the minimum load factor from each previous iteration and multiplying these factors by the original input loads.

PLAN2D is based on the program STAN, originally written by Dr. E. L. Wilson at U. C. Berkeley. PLAN2D has several limitations: (1) although PLAN2D detects the unloading of hinges, it cannot remove hinges; (2) PLAN2D does not allow the user to put in different positive and negative moment capacities; and (3) PLAN2D does not consider the interaction between axial and plastic moment capacity. Axial yielding and buckling are ignored, as is the reduction in moment capacity due to axial load.

PLAN2D is written in FORTRAN and is machine-independent. It has been tested on an IBM PC and on a DEC MicroVAX computer. The program was developed in 1988.

This program was written by C. Lawrence, and A.A. Huckelbridge of **Lewis Research Center.**
LEW-14889/TN

FOR ADDITIONAL INFORMATION

CONTACT
COSMIC®
112 Barrow Hall
University of Georgia
Athens, GA 30602

(404) 542-3265

Fire Testing Toll Installed

The David Taylor Research Center (DTRC), Carderock, Maryland, has recently completed installation of a Cone Calorimeter (Figure 2). This new test apparatus, developed by the National Institute of Standards and Technology (NIST) and modified for extended analytical capability by DTRC, provides a bench-scale test of a material's fire hazard characteristics. This will greatly aid DTRC in its responsibilities of fire testing new materials before approval for fleet use.

A Cone Calorimeter test provides a wealth of information about a material's fire behavior, unlike many standardized, small-scale test methods that provide information on just a single fire hazard characteristic. During a test, the exhaust flow is monitored for concentrations of O_2, CO_2, CO, and hydrocarbons as well as several toxic gases, such as hydrogen cyanide (HCN) hydrogen halides (HF, HC1, HBR) and oxides of nitrogen (NO, NO_2, NO_X). Burning a specimen in the Cone Calorimeter provides the following fire hazard properties: time-to-ignition, smoke generation, the heat of combustion, and the rate of heat release (RHR). The heat of combustion is based on the rate of mass lost over the course of the test, and the RHR is based on the percentage of oxygen depleted from the exhaust flow. The information gathered from this bench-scale test can accurately predict a tested material's behavior in a large-scale test.

The Cone Calorimeter is quite versatile in that it can be used to test liquids and small sections of cables as well as surface coatings (paints, primers, and sealers) on a standard 10-centimeter square

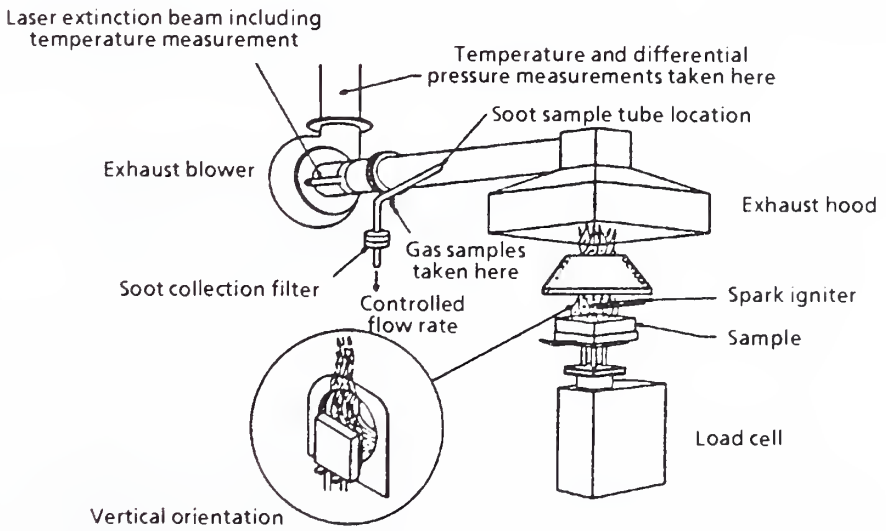

Figure 2. Cone Calorimeter

sample. The arrival of the Cone Calorimeter coincides with an influx of many new composite materials and has proved invaluable in helping DTRC keep up with their rapid pace of development. The Cone Calorimeter is also aiding in the application of embedding fiber-optic thermocouples in composite materials in order to understand structural failure modes under fire conditions. In the future, the Cone Calorimeter is expected to help direct development of composite materials with fire retardant properties.

For Additional Information:

Backup material on this effort is available from:

Navy Domestic Technology Fact Sheet Reader Reply Service
Code E211
Naval Surface Weapons Center
Dahlgren, VA 22448-5000
(703) 663-8921

Refer to 160702/TN

NASA Tech Brief
National Aeronautics and Space Administration
Ames Research Center, Moffett Field, California

Holographic Interferometry To Measure Three-Dimensional Flow

Double-exposure holography is used in studies of transonic flow near rotating blades.

A double-exposure holographic interferometry technique is used for studies of the density distribution in transonic airflow in the vicinity of a rotating helicopter blade. The interference fringes in the holographic interferograms are contours of a two-dimensional projection of the flow-field density integrated along the light path. A detailed three-dimensional density distribution should be obtainable by tomographic analysis of a series of such interferograms taken with the blade at different angles with respect to the object beam in the interferometer.

Three-dimensional flow-field density data should prove helpful in altering blade geometry to reduce the loud impulsive noise generated by transonic flow. The high-speed impulsive noise generated on the advancing-blade side of the rotor (where transonic flow is inevitable) is believed to radiate significantly more energy than the impulsive noise generated when the rotor blades interact with previously generated tip vortexes. In both cases, good data are essential for the theoretical prediction of the acoustic signature and for the verification of aerodynamic-transonic-flow numerical codes.

Holographic interferometry is nonintrusive. Furthermore, it is economical and suitable for large-scale experiments; there are no stringent optical requirements because the two object beams that produce the interference pattern use the same object-beam optics at different times, thus avoiding the generation of spurious fringe shifts that would otherwise be caused by differing path lengths.

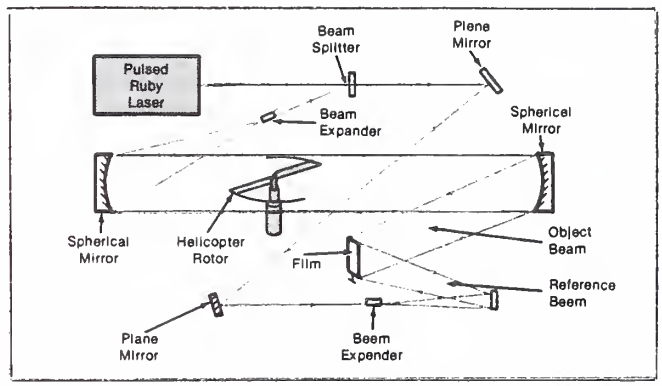

In the **Holographic Interferometry System**, two exposures are superimposed on the film to produce an interferogram. During the first exposure, the helicopter rotor blade is stationary. The second exposure is made with the blade rotating, at the instant the blade passes through the same position it occupied during the stationary exposure.

A holographic interferometry test setup is shown in the figure. Interferograms were produced using a pulsed ruby laser to "freeze" the rotor blade during the exposures. The object beam passed through a beam expander and was collimated into a beam 2 ft (0.6 m) in diameter by a spherical mirror. After passing the rotor, the object beam was directed to the film by a second mirror. The reference beam followed a separate path of similar length. After the two exposures were made (blade stationary and blade rotating), the film was developed. The interference pattern was reconstructed by illuminating the film with a continuous-wave He/Ne laser.

A variant of the technique can be used to provide a qualitative visualization of the three-dimensional flow field. A diffuser is inserted in the object beam just ahead of the rotor blade, and a two-exposure interferogram is recorded as before. The distribution of density change can be visualized by noting where the fringes are located in the three-dimensional real image created upon reconstruction.

This work was done by Yung H. Yu of **Ames Research Center**. *ARC-11474/TN*

FOR ADDITIONAL INFORMATION: *Contact: Director, Technology Transfer Division, P.O. Box 8757, BWI Airport, MD 21240; (301) 621-0100 Ext. 241*
REFER TO THE NUMBER LISTED AT THE END OF THIS ARTICLE

NASA Tech Brief
National Aeronautics and Space Administration
Langley Research Center, Hampton, Virginia

Liquid-Crystal Coats Help Make Flows Visible

Changes of color are rapid and reversible.

The visible indication of the transition of a boundary layer from laminar to turbulent flow plays an important role in aerodynamic tests in wind tunnels and in flight. The most popular methods for making boundary layers visible in such tests have included the sublimating-chemical technique and the oil-flow technique. However, each method has limitations that constrain its applicability. In a newly developed method, liquid-crystal coats are used to make visible such features of boundary-layer flows as transitions, separations, and the locations of shocks.

Typically, temperature and shear stress are the primary stimuli in response to which liquid-crystal coats selectively reflect discrete wavelengths (colors) of light. Because the fundamental chemical structure is unaffected by these changes, a liquid-crystal coat can respond repeatably to the same physical changes. Thus, the color changes can be reversible.

Liquid-crystal coats can respond very rapidly to changes in shear stresses or temperature distributions; characteristic response times as small as 0.2 second have been observed. The particular color observed depends on the viewing angle and on the local shear and temperature to which the liquid crystals are subjected. The vividness and brilliance of the reflected colors also depend on the amount and angle of incident light.

One flight evaluation of the liquid-crystal technique was conducted on a Lear Model 28/29 business jet airplane operated by NASA at its Langley Research Center in research on the reduction of viscous drag. The airplane provides, for research, an extensive combination of ranges of flight operating conditions, including mach numbers up to 0.805, maximum unit Reynolds numbers up to 2.65×10^6 ft^{-1} (8.69×10^6 m^{-1}), and altitudes up to 51,000 ft (15.6 km). The right winglet of the airplane was prepared for testing by coating it with a liquid-crystal mixture.

Correlations between transitions measured by hot films and by liquid crystals showed that the change in the color of the liquid-crystal coat corresponded to the first appearance of turbulent spots in the hot films. This response differs from that of sublimating chemicals, which show the end of the transition region.

The time-dependent response of a liquid-crystal coat was also evaluated. The transition on the winglet was changed by conducting sideslip oscillations with a period of about 2 cycles per second. The observed movement of the transition was in phase with the sideslip oscillation, indicating that the coat responded rapidly.

Another flight experiment involving liquid crystals was conducted with a Grumman OV-1B Mohawk airplane operated by NASA. In addition, a test of both liquid-crystal and sublimating-chemical indications of transitions was conducted in the Langley 14-by-22-ft (4.3- by-6.7-m) wind tunnel on a fuselage forebody. Comparison of the results showed good agreement between the two methods.

The use of liquid-crystal coats in the measurement of transitions provides data that can be very difficult to acquire by other visualization techniques. For flight applications, liquid crystals provide the capability for making transitions visible throughout almost the entire altitude and speed ranges of subsonic aircraft. The use of liquid crystals is not known to expose humans to any hazard of toxicity. Because liquid crystals are derived from the fatty acids of animals, they tend to be less hazardous than many other chemicals are. The liquid-crystal method is also applicable to the visible indication of supersonic flows and is suitable for general use in high- and low-speed wind-tunnel and water-tunnel testing.

This work was done by Bruce J. Holmes of **Langley Research Center** *and Clifford J. Obara of PRC-Kentron.*
LAR-14342/TN

FOR ADDITIONAL INFORMATION: *Contact: Director, Technology Transfer Division, P.O. Box 8757, BWI Airport, MD 21240; (301) 621-0100 Ext. 241*
REFER TO THE NUMBER LISTED AT THE END OF THIS ARTICLE

Environmental Science & Technology

0934 Sludge Dewatering by Freezing

0935 SUSV-Towed Snow Plow

0936 Radon Removal Techniques for Small Community Public Water Supplies

U.S. Army Corps of Engineers
Cold Regions Research & Engineering Laboratory
72 Lyme Road, Hanover, New Hampshire 03755-1290

Sludge Dewatering by Freezing

PROBLEM

Sludge produced by water and wastewater treatment plants is difficult and expensive to dewater. A dewatering process is necessary to reduce the volume and improve the handling characteristics of the sludge. Approximately 60% of the total cost of waste treatment is associated with sludge dewatering.

SOLUTION

CRREL has developed a new dewatering process called a sludge freezing bed. The bed works on the principle that natural freezing causes a separation of solid and liquid fractions. During thawing, the liquid fraction drains away leaving a dry, odorless material which is easily handled with mechanical equipment. The bed can be designed to work automatically so that operator time and attention is minimal.

RESULTS

Since the freezing bed makes use of natural freeze-thaw, its operating costs are significantly less than those of mechanical methods. Also, no chemicals are required. The skill level needed to operate a freezing bed is minimal.

STATE-OF-ART

There are two freezing beds in operation: one at Fort McCoy, Wisconsin, and the other at Fort Greely, Alaska. Both beds are designed to dewater anaerobically digested sludge. Laboratory tests indicate that these beds should remove 75% of the water. The remaining solids will be removed from the bed with a front end loader and landfilled. Results from the first year of operation will be available in June 1991.

FOR ADDITIONAL INFORMATION: Contact: C. James Martel, U.S. Army Cold Regions Research and Engineering Laboratory, 72 Lyme Road, Hanover, New Hampshire 03755-1290; (603)646-4464, FTS 561-4464.

U.S. Army Corps of Engineers
Cold Regions Research & Engineering Laboratory
72 Lyme Road, Hanover, New Hampshire 03755-1290

SUSV-Towed Snow Plow

PROBLEM/HISTORY

The U.S. Army's light forces have limited snow removal capabilities. Therefore, many military support vehicles have limited usefulness in operations during which a snow cover is present. Since many roads and trails will not have been kept open prior to hostilities, truck-mounted snow plows (if available) would be ineffective. In most instances, heavy tracked vehicles are required to move deep snow.

Light forces have been equipped with a large number of tracked, over-snow vehicles known as SUSVs (Small Unit Support Vehicles). Over-snow vehicles can be equipped with front- or rear-mounted plow blades, but to do so, the SUSV would require extensive design changes.

SOLUTION

CRREL engineers determined that a snow plow towed by the SUSV could enhance winter operations with minimal changes to the SUSV itself. From a series of 1/12-scale tests it was determined that a special linkage could be attached to the SUSV's pintle hook mounting bracket and thereby could control the attack angle of the plow. A 1/2-scale plow and 4-bar parallel linkage towing assembly were designed. This 1/2-scale plow, towed by a SUSV, has been tested in snow depths up to 30 inches with good results. It is estimated that the SUSV will have enough tractive reserve to pull the full-scale plow.

STATUS

A video tape describing the design and performance of the 1/2-scale plow is available from CRREL. The full-scale plow is being designed, and testing is scheduled for February 1992 in Alaska.

An Operational Needs Statement for the towed snow plow is being prepared by the 6th Infantry Division (Light) for the U.S. Army Engineer School.

FOR ADDITIONAL INFORMATION: Contact: Mr. Paul Richmond, U.S. Army Cold Regions Research and Engineering Laboratory, 72 Lyme Road, Hanover, New Hampshire 03755-1290; (603)646-4461, FTS 561-4461.

United States
Environmental Protection
Agency

Risk Reduction
Engineering Laboratory
Cincinnati, OH 45268

Research and Development

EPA

Project Summary

Radon Removal Techniques for Small Community Public Water Supplies

Introduction

As part of the 1986 amendments to the Safe Drinking Water Act, the U.S. Environmental Protection Agency (EPA) is to propose a rule for Maximum Contaminant Level Goals (MCLGs) and National Primary Drinking Water Regulations (NPDWR) including Maximum Contaminant Levels (MCLs) for radionuclides in drinking water. One of the radionuclides that will be regulated under the rule is radon-222 (radon). EPA is considering setting the MCL for radon in the range of 200 to 2,000 pCi/L. Data on the distribution of radon in groundwater supplies in the United States indicate that a large number of individual and public water supplies will be affected by an MCL in that range. In addition, many of these public water supplies will be ones serving small communities (< 76 m^3/day).

The rule will also contain recommendations with respect to Best Available Technologies (BATs) and analytical methods. Three conventional water treatment technologies (granular activated carbon (GAC), diffused bubble aeration, and packed tower aeration) have been used to remove radon from drinking water. The GAC process, which has been used to treat point-of-entry and small community water supplies, relies on the ability of radon to adsorb to the carbon. One unique aspect of this process is that the breakthrough/exhaustion profile typically seen when GAC is treating conservative (nondecaying) contaminants is not exhibited during radon removal.

The aeration methods are used because radon is a highly volatile gas with a relatively large Henry's constant (2.80 atm • m^3H_2O/m^3 air at 100°C) that can be easily transferred from water to air. Aeration methods have been used in individual, small community, and other public water supplies.

The primary purpose of this study was to evaluate the performance of full-scale GAC and diffused bubble and packed tower aeration systems when treating small community water supplies containing radon. In addition, several low technology alternatives and various modifications of the liquid scintillation counting technique used for analysis of radon in water were evaluated.

The specific objectives of the study were to:

- Evaluate full-scale GAC systems operating at two small communities in New Hampshire, by monitoring them for changes in radon removal, radiation emissions, and general water quality parameters (e.g., pH, iron, turbidity, microbial numbers);
- Conduct several specific monitoring events of the GAC systems to assess the effect on GAC performance of diurnal variations in water flowrate and raw water quality, high water flowrate, and backwashing;
- Core the GAC after several months of operation to determine if iron, manganese, microorganisms, radionuclides, or all of them were accumulating in the units;
- Evaluate full-scale diffused bubble and packed tower aeration systems operating in small communities in New Hampshire by monitoring them for radon removal, general water quality parameters, and off-gas emissions of radon;
- Operate the aeration systems over a range of volumetric air to water (A:W) ratios at two water flowrates to determine the effect of these parameters on radon removal;
- Evaluate three randomly packed plastic media in the tower aeration system with respect to radon removal efficiency;
- Evaluate the radon removal efficiency of several low technology modifications (e.g., free fall vs. bottom entry, spray nozzle entry, venturi entry, coarse bubble aeration) retrofitted to an existing small community atmospheric storage tank;
- Assess the effect of sampling techniques (e.g., free fall, hose connector, direct syringe collection, volatile organic analysis (VOA) bottle collection), storage time, scintillation cocktail, and extraction via shaking on the liquid scintillation analytical technique for analysis of radon in water.

Liquid Scintillation Technique

The effects of sampling technique (direct collection using a syringe versus filling a VOA bottle), storage (up to 21 days), and choice of scintillation cocktail (toluene- and mineral-oil-based cocktails and Opti-Fluor 0) on the liquid scintillation (LSC) analytical technique for radon in water were evaluated. Other experiments were conducted to determine the sources of variability in the method (field, preparation, instrument) and the validity of the extraction via shaking procedure currently defined by EPA.

Numerically, the direct syringe sampling technique always yielded the highest radon activities, whereas the VOA bottle filled with free falling water yielded the lowest. This is not surprising because less sample handling before injection into the scintillation vial and less agitation during sampling should result in less loss of radon. Though the VOA collection techniques involve extra handling of the sample, they can, however, produce results statistically similar to the syringe method, especially if a universal hose connector is used.

Conclusions and Recommendations

When designing a treatment system to remove radon from a small community water supply, good data on water flowrates and influent radon activities at the site are essential. These data are major inputs into the design models for the aeration and GAC systems. As observed in this study, for small community supplies, variations in flowrate and influent activity may be substantial and will, if underestimated, lead to inadequate system design and effluent radon activities that exceed the design goal. Variations in water quality at each site may require that pilot-scale testing be performed to determine the appropriate design and pre- or post-treatment requirements.

For GAC systems, the steady state adsorption-decay constant, a critical component of the design model, varied over time and was site specific. The GAC systems tested in this study had average effluent radon activities of 12,000 to 24,000 pCi/L. The GAC units accumulated iron, manganese and particulates (turbidity), and there were significant numbers of bacteria growing on the carbon. As a result, GAC systems may require periodic backwashing to prevent significant headless development. In some cases, pretreatment is recommended to decrease the backwashing frequency. Gamma/beta emissions measured at the surface of the GAC units were substantially greater than background measurements possibly requiring shielding to lower them to acceptable levels. The data indicated that retention of uranium-238 and -235, radium-226, and lead-210, which appear to be related to water quality (e.g., pH and alkalinity), may cause the GAC to be classified as a low level radioactive waste.

The diffused bubble aeration system tested at A:W ratios ≥ 5:1 yielded overall radon removal efficiencies from 90.0% to >99.6%. The radon removal efficiencies for the packed tower aeration system ranged from 92.5% to 99.8%, in spite of variations in water flowrate, influent radon activity, and packing type. Extrapolations of performance data obtained at one site with either aeration system should not, however, be made to systems with other configurations, process equipment, or low influent activities, or to those required to meet a more stringent MCL. Both aeration systems had off-gas radon activities that were 10^4 to 10^5 times higher than those of the ambient air, and their effect on the environment would need to be considered. As with all aeration systems, precipitation of iron and manganese can occur and result in operational problems. Therefore, raw water quality should be monitored to determine whether pretreatment is required.

Several recommendations can be made concerning the liquid scintillation analytical technique for radon in water. During sample collection, the universal hose connector should be used to fill VOA bottles. Maximum storage times for samples collected in VOA bottles should be established based on the MCL, practical quantification lever, radioactive decay, and leakage. Opti-Fluor 0 yielded the best results of the scintillation cocktails tested with respect to count rates, variability, and cost and is, therefore, recommended. The extraction procedure should not be used to calculate the efficiency factor; however, samples should be shaken, especially those with low activities, to ensure rapid transfer of radon to the scintillation cocktail.

The full report was submitted in fulfillment of Cooperative Agreement CR-812602 by the University of New Hampshire Environmental Research Group under the sponsorship of the U.S. Environmental Protection Agency.

N. E. Kinner, J.P. Malley, Jr., J. A. Clement, P. A. Quern, and G. S. Schell are with the University of New Hampshire Environmental Research Group, Durham, NH 03824.

***Kim R. Fox** is the EPA Project Officer (see below).*

The complete report, entitled "Radon Removal Techniques for Small Community Public Water Supplies," (Order No. PB 90-257 809/AS, Cost: $31.00, subject to change) will be available only from:

National Technical Information Service
5285 Port Royal Road
Springfield, VA 22161
Telephone: 703 487-4650

The EPA Project Officer can be contacted at:

Risk Reduction Engineering Laboratory
U.S. Environmental Protection Agency
Cincinnati, OH 45268

Manufacturing, Machinery & Tools

0937 Intelligent Machining Workstation

0938 Clean Ingot Manufacturing Technology for Superalloy Turbine Components

0939 Customized AutoCAD Develops into CRDA

0940 ADACS for Aircraft Engine Parts

0941 Diamond Turning of Stainless Steel

0942 Robot Controlled Test Bed

0943 MTI to Establish and Operate CALS Shared Resource Center

0944 Grease Inhibits Stress-Corrosion Cracking in Bearing Race—Operating life is extended at low cost.

0945 h-Parameter Analysis of Teleoperators—An electromechanical system is characterized by a mathematical model originally developed for electrical networks.

0946 Rapid Dry Etching of Photoresists Without Toxic Gases—A room-temperature process may not damage underlying semiconductor wafers. (Licensing Opportunity)

0947 Synchronizing Rotation of a Heavy Load—A simple setup of motors, pulleys, and belts provides both torque and synchronism.

Testing & Instrumentation

0948 Monitoring Welding Images and Data Simultaneously—Data on process conditions are superimposed in real time on images of the process.

Other Items of Interest

0949 Technique Developed for Fluoride Glass Windows

Technology Assessment
U.S. Air Force

Intelligent Machining Workstation

The primary goal of the Intelligent Machining Workstation (IMW) program, completed in September 1990, was to develop and demonstrate technologies to enable an automated, unmanned machining workstation that can rapidly create a good first part from a feature-based electronic part description. The technologies were jointly developed by Cincinnati Milacron Industrial Systems Group and the Robotics Institute of Carnegie Mellon University, with United Technologies Pratt & Whitney Aircraft in an advisory role.

The IMW planning system incorporates artificial intelligence technology into a set of knowledge-based software modules corresponding to areas of manufacturing engineering expertise. These modules include a feature-based Planner, a Holding Expert, a Part Modeler, a Work Element Manager, and a Human Interface. The major achievement of IMW is not only the implementation of the various expert modules, but the establishment and demonstration of an effective basic architecture to allow different expert manufacturing modules to communicate and make knowledgeable decisions for successful part fabrication.

The IMW has two modes of operation: planning and execution. During the planning phase the IMW utilizes a feature-based electronic part description as input and automates the generation of the operations plan and numerical control programs necessary to fabricate the part. The modules interact to develop the part work package. The Planner is a rule-based system which incorporates expert machinists' knowledge of feature interaction and part squaring. After examining the finished part and raw stock models, the Planner defines the sequence of part features to be cut and appropriate setup. The Holding Expert negotiates with the Planner to determine the exact fixturing for each part by considering part rigidity during the cut, location of part datums, and prevention of possible part obstruction by fixturing. The Cutting Expert interacts with Metcut's CUTTECH software to determine the machining parameters (tool selection, feed, speed, depth of cut, and so forth) necessary to produce each feature, and then generates the NC program to be executed on the machine tool. The Work Element Manager coordinates the interaction between the various expert modules. The Part Modeler serves as a solid modeling information database for the part in its initial, various intermediate, and final forms, as well as for the fixturing elements.

To allow the various experts to query and respond to one another, a generic manufacturing Feature Exchange Language was established. The software modules were developed on Sun and TI Explorer workstations.

In the IMW execution phase, the completed work package is used to provide necessary operator instructions and automatically drive the machine tool to fabricate the part. The machine tool currently being utilized is a Cincinnati Milacron three-axis vertical machining center.

IMW technology includes novel (non-cutting) tooling developed to extend the capabilities of the machine tool, which include a computer- controlled gripper and torque tool that allow autonomous fixture assembly by the machine tool. Other novel tools include support for on-machine vision and an adapter which allows the novel tools to be stored in the tool changer.

The IMW was developed in a series of three prototype systems differentiated by reduced manpower required and increased machining complexity, both in geometry and in material types. Automatic part operations planning and first-part correct manufacture were achieved for test parts in the early prototypes. Significant reductions were observed in the time and effort to produce part plans, develop NC instructions, and accomplish part proveout. The final prototype successfully performed all operations planning functions for a number of test parts. IMW can typically plan a part in 20-40 minutes as compared to days or weeks in many shops. The major accomplishments of IMW are:

- Feature based planning
- Autonomous planning enabling rapid generation of part plans
- Architecture and communication services for integrating intelligent manufacturing software modules
- Autonomous fixture assembly
- First part right

The primary benefit of the IMW program was the design and implementation of a prototype system to rapidly generate operations plans for parts, thus providing enormous time and cost savings over current methods.

IMW technology has significant potential in many small lot size, one of a kind, and/or quick turnaround environments, such as model shops, NC and planning departments, and repair/spare parts facilities. Further details are available in WRDC-TR-90-8031.

FOR ADDITIONAL INFORMATION: To discuss this effort further, contact: Project Engineer: Chuck Wagner, Air Force Manufacturing Technology Program, ATTN: AFWAL/WL/MTR, Wright Patterson AFB, OH 45433-6533; (513)255-8589. Refer to contract: F33615-86-C-5038.

Technology Assessment
U.S. Air Force

Clean Ingot Manufacturing Technology for Superalloy Turbine Components

The growing use of a retirement-for-cause engine disk management approach provides significant benefits associated with building a more life-cycle-cost effective engine disk; increasing its lifespan through improved manufacturing methods, even at a greater acquisition cost, can favorably affect the overall cost of the disk. Low cycle fatigue (LCF) capability relates directly to the cycles for crack initiation in engine disks, and nonmetallic oxide inclusions play a dominant role in governing the fatigue capability of high strength powder metallurgy superalloys. A large increase in disk life can be achieved by decreasing the size of inclusions. This effort was pursued under contract F33615-79-C-5006, "Manufacturing Technology for Improved Quality Remelt Stock for Powder Atomization", and this contract was established as a follow-on effort to quantify the effect on fatigue properties using such super-clean material.

The approach to accomplishing this effort was to produce clean powder from electron beam refined ingot stock with a nonmetallic inclusion content of less than 0.2 parts per million. Because of technical difficulties associated with the clean powder process, the process was modified to make disks instead by a fine grain ingot processing approach. Gas turbine engine disk shapes were then produced from this material, and mechanical property testing were conducted to quantify any improvements in fatigue life capabilities as a result of improved material cleanliness. The program was divided into five tasks: (1) electron beam refinement of IN100 starting material, (2) fine grain size ingot preparation, (3) processing of ingots into disk forgings, (4) mechanical property evaluation, and (5) cost analysis.

The program resulted in the successful processing of 20 disks in three configurations weighing from 18 to 85 pounds. Mechanical property testing showed that this material exhibited slightly lower tensile, increased stress-rupture, and approximately equal LCF capability compared to powder processed IN100. However, LCF cycles were not limited by oxide inclusions, but rather by either machining or unexpected Zr-S and Mo-B phase formation. This suggests that LCF improvements are still achievable with clean material if these other factors are controlled through alloy chemistry modifications and machining controls. Cost analysis showed that the processing approach followed in this program would cost about 50 percent more than powder processing, but save up to 20 percent in long-term or life cycle costs. Details regarding this effort are contained in AFWAL-TR-89-8007.

FOR ADDITIONAL INFORMATION: To discuss this effort further, contact: Project Engineer: Ken Kojola, Air Force Manufacturing Technology Program, ATTN: AFWAL/WL/MTPM, Wright Patterson AFB, OH 45433-6533; (513)255-5037. Refer to contract: F33615-83-C-5068.

Customized AutoCAD Develops into CRDA

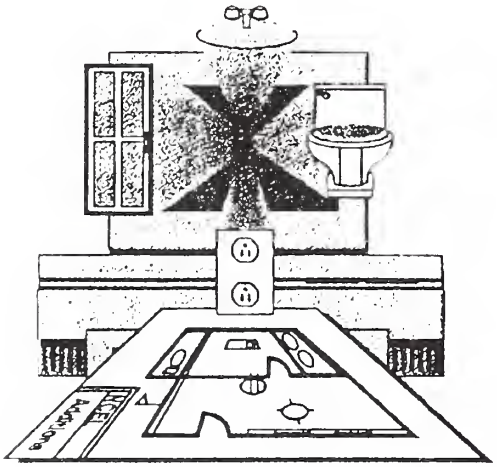

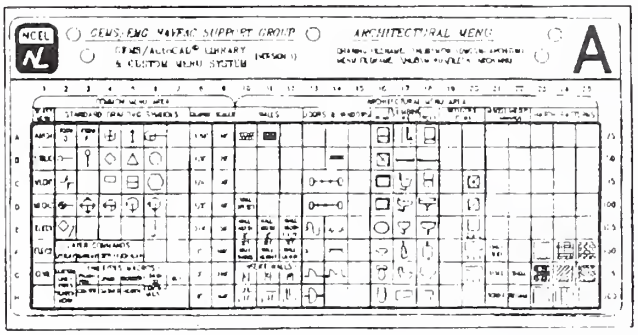

Figure 1. System and sample menus

The Naval Civil Engineering Laboratory (NCEL) Port Hueneme, California, under the sponsorship of the Naval Facilities Engineering Support Command (NAVFAC) has developed an architecture/engineering construction (AEC) microcomputer application software packaged based on five years of NAVFAC CADD experience called NCEL/AutoCAD Library and Custom Menu System (Figure 1). The software works in an integrated fashion inside AutoCAD. It allows facility designers to insert standard Navy symbols and details on their proper layers into facility drawings. By limiting choices to standard symbols, layers, and details, the software encourages standardization of architectural and engineering drawings.

This project has grown into a cooperative research and development agreement (CRDA), where the private company uses its own resources to develop and market the product and the Government agency contributes technical expertise and other nonmonetary support. The private firm benefits by obtaining exclusive rights to the technology it develops in the CRDA and by marketing new products with lower developmental costs.

For Additional Information:

Backup material on this effort is available from:

Navy Domestic Technology Fact Sheet Reader Reply Service Code E211
Naval Surface Weapons Center
Dahlgren, VA 22448-5000
(703) 663-8921

Refer to 160701/TN

Navy Manufacturing Technology

Automated Manufacturing Research Facility

National Institute of Standards & Technology
U.S. Department of Commerce, Gaithersburg, MD 20899

ADACS for Aircraft Engine Parts

Engineers at NIST, working with United Technologies Research Center (UTRC), are developing an automated system which produces precision chamfers on aircraft engine components fabricated from titanium and inconel. The chamfers, or beveled edges, must be placed on parts such as turbine engine blades and hubs to relieve potential areas of stress concentration and to ease assembly. Damage can be very expensive because of the extensive machining of the parts prior to the chamfering stage.

Engine manufacturers are automating the process to reduce the scrap rate. The automated system is called the Advanced Deburring and Chamfering System (ADACS). It is being developed in a cooperative effort between NIST and UTRC, and includes engine manufacturer Pratt and Whitney. To date, UTRC has developed process models which dictate the cutting force required to achieve a desired chamfer depth. The next phase of the project at NIST will combine UTRC's process expertise and NIST's experience in automation.

The ADACS consists of a six-axis electric robot fitted with an actuated chamfering tool. This tool is capable of high speed force control within a small work area. The approach is to use the conventional industrial robot as a coarse positioning device, while relying on the actuators and force sensors of the tool to provide control over cutting force and stiffness at the part edges. The tool also compensates for robot inaccuracies and other factors such as part misalignment and large tolerances. The system has maintained chamfers of 15 thousandths of an inch on titanium while traversing corners, in spite of part positioning errors on the order of tenths of inches.

The ADACS builds on work performed in NIST's Automated Manufacturing Research Facility over the past five years. Techniques were developed in the Cleaning and Deburring Workstation for generating robot trajectories off-line, using computer-aided design data. The NIST Real-time Control System (RCS) allows feedback from a variety of sensors to be easily integrated with the control of the robot, accommodating for robot inaccuracy which may result from off-line programming. Such techniques enable automatic generation of reliable robot programs in a matter of seconds or minutes, instead of the hours or days required for manual teaching.

FOR ADDITIONAL INFORMATION: To discuss this effort further, contact: Fred Proctor, Building 220, Room B127, AMRF Project, National Institute of Standards and Technology, Gaithersburg, MD 20899; Telephone (301)975-3425.

Navy Manufacturing Technology

Automated Manufacturing Research Facility

National Institute of Standards & Technology
U.S. Department of Commerce, Gaithersburg, MD 20899

Diamond Turning of Stainless Steel

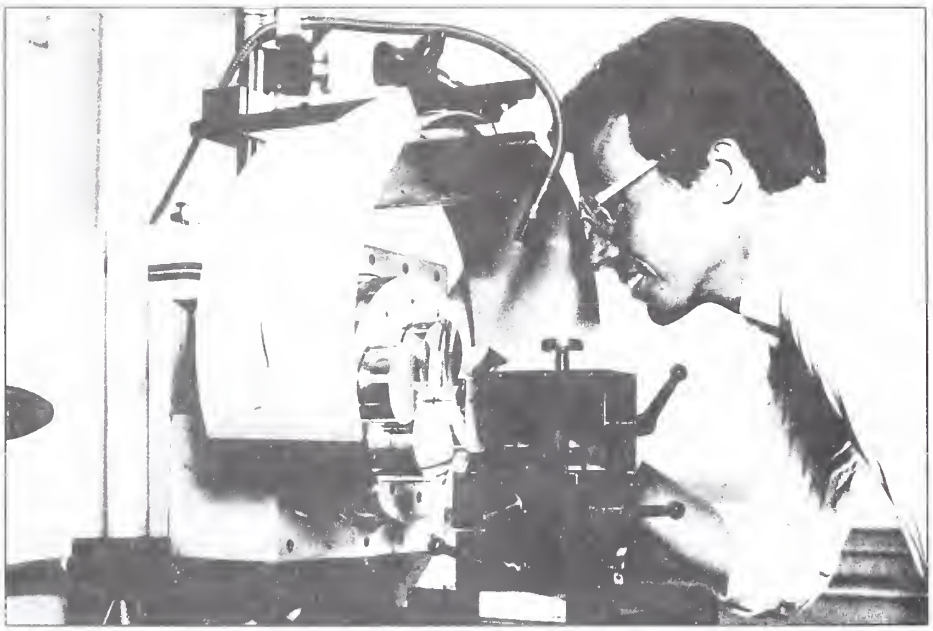

Machining Parabolae With a Diamond Tool

NIST researchers have successfully used diamond turning to machine very high quality surface finishes on stainless steel. This breakthrough is a step toward using the advantages of diamond turning in the production of such devices as military optics, scanners, computer memory disks, optical molds, and infrared imaging optics.

Single point diamond turning is used to achieve extremely accurate contoured surfaces that have optical quality surface finish. Previously, stainless steel could not be machined using diamond turning due to very high tool wear.

The recent tests performed jointly by NIST and Los Alamos National Laboratory showed that the prohibitive tool wear experienced in machining ferrous materials at room temperature could be almost eliminated by cooling the part and the tool using liquid nitrogen. This result has produced a practical way to machine stainless steel and also provides evidence of the cause of the tool wear, which is essential for understanding the diamond turning process and for improving it.

NIST is developing a facility for testing diamond turning techniques. The goals are to investigate properties of diamond turning and to develop a practical machining process for manufacturing of diamond turned products.

FOR ADDITIONAL INFORMATION: To discuss this effort further, contact: Chris Evans, Building 220, Room A107, AMRF Project, National Institute of Standards and Technology, Gaithersburg, MD 20899; Telephone (301)975-3484.

Robot Controlled Test Bed

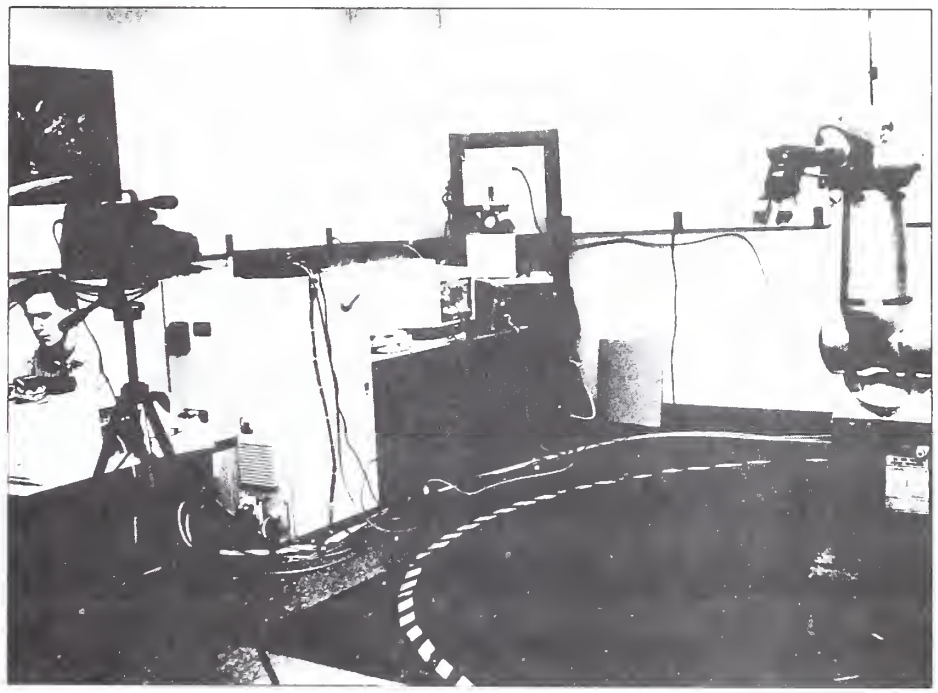

Robot Controlled Test Bed

NIST recently evaluated a set of robot control techniques to learn which produces the best performance for such fine manipulation tasks as assembly. The results will lead to improved performance of manufacturing robots.

The evaluation determined the behavior of different stiffness control algorithms in order to develop a better understanding of contact stability. Stiffness is an important property of an arm that determines its effectiveness in performing certain tasks. Many performance measurements were made including measuring the difference between actual and desired stiffness and determining the stability criteria when the robot came into contact with a wide range of environment stiffnesses.

Tests were conducted in NIST's Robot Control System Testbed which consists of a seven-degrees-of-freedom robot manipulator and a multiprocessor control system. In addition, real-time vision capability using the Pipelined Image Processing Engine (PIPE) is available. The control structure of the testbed is based on the NASA/NIST Standard Reference Model for Telerobot Control System Architecture (NASREM), which evolved from the principles of hierarchical control developed at the AMRF. The facility test NASREM's usefulness as well as various robot control ap-

proaches for NASA's Telerobotic Servicer Project.

Engineers use the testbed to compare different approaches to robot control. They run each algorithm on the robot and measure corresponding robot performance. The testbed facility is unique in the speed with which ideas can be tested. The NASREM standard defines interfaces which support all known algorithms. Programming and integrating a new algorithm into the system has relatively little system impact.

FOR ADDITIONAL INFORMATION: To discuss this effort further, contact: Dr. Ron Lumia, Building 220, Room B127, AMRF Project, National Institute of Standards and Technology, Gaithersburg, MD 20899; Telephone (301)975-3452.

National Center for Excellence in Metalworking Technology (NCEMT)

Navy Technology Fact Sheet

MTI to Establish and Operate CALS Shared Resource Center

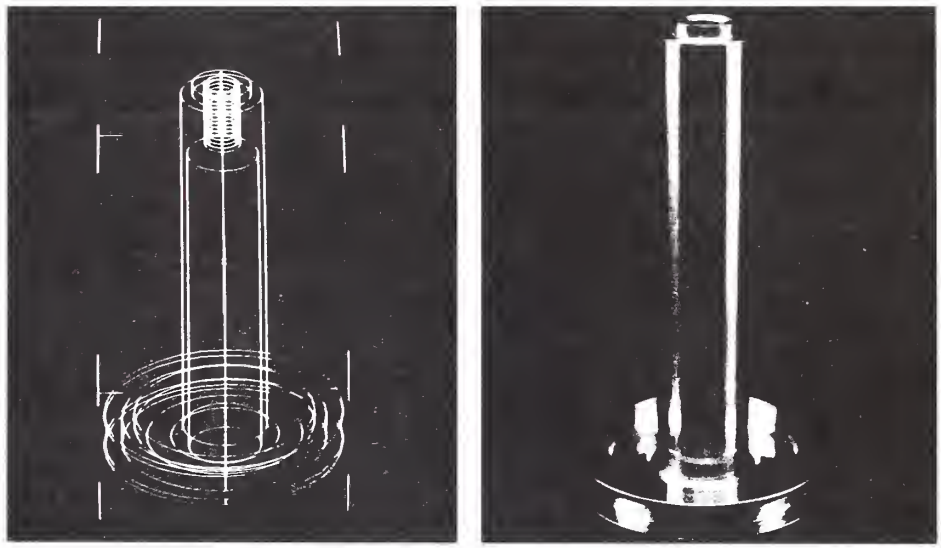

Computer Generated Representation Using CALS IGES and the Actual Part Produced

Metalworking Technology, Inc. (MTI) has been tasked to support the U.S. Navy and Air Force in the development and operation of the prototype Computer-Aided Acquistion and Logistics Support (CALS) Shared Resource Center (CSRC). CALS is the major initiative to establish an electronic means for storage, exchange and processing of the complex data associated with the design, manufacture, and procurement of military parts and systems. The goals of CALS include a reduction in part procurement cost through greater efficiency and enhanced procurement competitiveness.

The figure depicts a computerized simulation of a specialized piston. The image was generated from data represented by the CALS Initial Graphic Exchange Specification (IGES). The actual part produced from the IGES file and other CALS manufacturing process specifications is also shown.

A large percentage (up to 80%) of components in DOD weapons systems are produced by small to mid-size (less than 250 employees) manufacturers. The CSRC will assist these smaller manufacturers in becoming CALS compliant.

The CSRC goals include:

- Determining the extent and use of exisiting computer-based engineering product data by small to mid-size manufacturing organizations;
- Developing assistance and business outreach services to enable small to mid-size manufacturers to understand and participate in CALS;
- Establishing communications linkages between Navy and Air Force CALS activities and small businesses;
- Testing and supporting implementa-

tion of emerging standards.

To facilitate these goals, MTI will co-locate the CSRC at its facilities in Johnstown, Pennsylvania. An initial remote CSRC demonstration node will be located at the University of Scranton.

The CSRC will utilize state-of-the-art, off-the-shelf hardware and software in an open architecture environment. The CSRC will gather and disseminate product information on parts and components from the Air Logistics Centers and the Air Force Logistics Command. Data will also be collected from and transmitted to Navy logistic and parts centers, and the Navy Rapid Acquistion of Manufactured Parts program center.

FOR ADDITIONAL INFORMATION: To discuss this effort further, contact: David E. Chesebrough, CSRC Program Manager, National Center for Excellence in Metalworking Technology, 1450 Scalp Avenue, Johnstown, PA 15904; Telephone (814)269-2470.

NASA Tech Brief
National Aeronautics and Space Administration
Marshall Space Flight Center, Alabama

Grease Inhibits Stress-Corrosion Cracking in Bearing Race

Operating life is extended at low cost.

Coating with a suitable grease has been found to inhibit stress-corrosion cracking in the bore of the inner race of a ball-bearing assembly that operates in liquid oxygen. The grease apparently protects the bore and its corner radii from corrosion-initiating and -accelerating substances like moisture and contaminants, which can enter during assembly. Previously, stress-corrosion cracking in the bore has been prevented by either (1) maintaining the bore clean and extensively purging and drying it, all requiring 72 hours of assembly time, or (2) shot-peening and nickel-plating the bore, at a cost of $658 per bearing (1989 prices). The principal advantages of coating with the special grease are that unlike the previous methods, it is relatively inexpensive (about $5 per bearing) and involves very little extra assembly time.

The efficacy of the grease-coating method was demonstrated in a simple experiment. Three inner races of 440C stainless steel were prepared. One race was left uncoated, the bore and corner radii of the second race were coated with Braycote 640 AC-MS grease, and the bore and corner radii of the third race were coated with Krytox grease with a strontium nitrate additive. The races were installed on a molybdenum-coated mandrel (see figure) with an interference fit at a hoop stress of 45 kpsi (310 MPa) by initially shrinking the mandrel in liquid nitrogen, then sliding the races onto the mandrel while it was still cold.

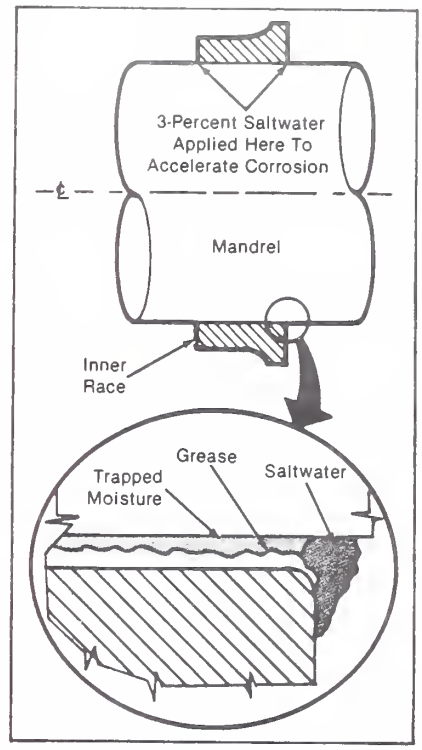

Inner Races of ball-bearing assemblies were tested for resistance to stress-corrosion cracking by shrink-fitting them onto a mandrel, applying saltwater, and exposing them to a humid environment.

During the brief interval between removal from the liquid-nitrogen bath and the installation of the races, moisture condensed from the atmosphere onto the mandrel. When the mandrel warmed up and expanded into contact with the bores of the races, the moisture was trapped between the bores and the mandrel. Any pitting (caused, for example, by corrosion initiated by the trapped moisture) near the corner radii would concentrate the already high hoop stress and might thereby cause the ring to fracture.

The shaft and races were placed in a humid environment and a 3-percent saltwater solution was applied to accelerate corrosion. The uncoated race failed in 7 hours. The greased races lasted more than a month and had not yet failed when the results of the experiment were recorded.

This work was done by Robert F. Beatty and Scott E. McVey of Rockwell International Corp. for **Marshall Space Flight Center.** *MFS-29664/TN*

FOR ADDITIONAL INFORMATION: *Contact: Director, Technology Transfer Division, P.O. Box 8757, BWI Airport, MD 21240; (301) 621-0100 Ext. 241*
REFER TO THE NUMBER LISTED AT THE END OF THIS ARTICLE

NASA Tech Brief
National Aeronautics and Space Administration
NASA's Jet Propulsion Laboratory, Pasadena, California

h-Parameter Analysis of Teleoperators

An electromechanical system is characterized by a mathematical model originally developed for electrical networks.

The hybrid two-port input/output mathematical model originally developed for the small-signal analysis of transistors, amplifiers, and electrical networks in general has been adapted to the analysis of a teleoperator that senses forces and velocities at the master and slave. The hybrid two-port model is well suited to characterization of the bidirectional flows of energy in terms of the relationships between input and output signals. The hybrid model (as distinguished from other two-port models) leads to an intuitive representation of the performance of the system and can be used to design the system according to the concept of bilateral impedance control.

The interface between the human operator and the master and the interface between the slave and the environment are the two ports through which the teleoperator exchanges energy between the human operator and the environment. In this exchange, the human operator exerts controlling forces on the environment through the teleoperator, while feedback from the slave back to the master increases the sense of realism with which the human operator senses the environment (which includes the manipulated object).

The two-port hybrid model is extended to the teleoperator by the analogy between effort (force) and voltage and the analogy between flow (velocity) and electrical current (see Figure 1). Thus, the parameters of the hybrid two-port model of a real or simulated teleoperator system can be obtained from its measured or computed input and output dynamical properties, in analogy with the input/output electrical properties and corresponding transimpedance and transadmittance parameters (h parameters) of a purely electrical two-port system.

The hybrid two-port model is linear: The h parameters are derived, in effect, from the second term of a Taylor-series expansion that describes the behavior of the system in the vicinity of the operating point. Thus, in the purely electrical case, the hybrid two-port model is used for small-signal analysis and is applied to a nonlinear electrical system by specifying the operating point in question (e.g., the dc biases on a transistor). Analogously, the hybrid two-port model can be applied to a nonlinear

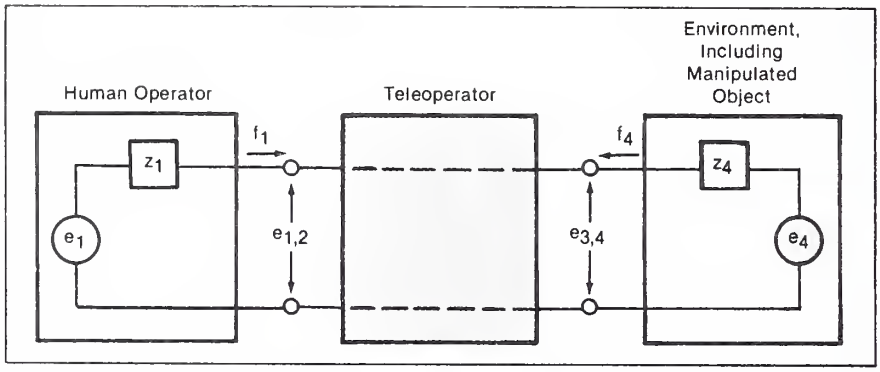

Figure 1. The **Teleoperator Acts as a Two-Port** input/output "black-box" device between the human operator and the environment

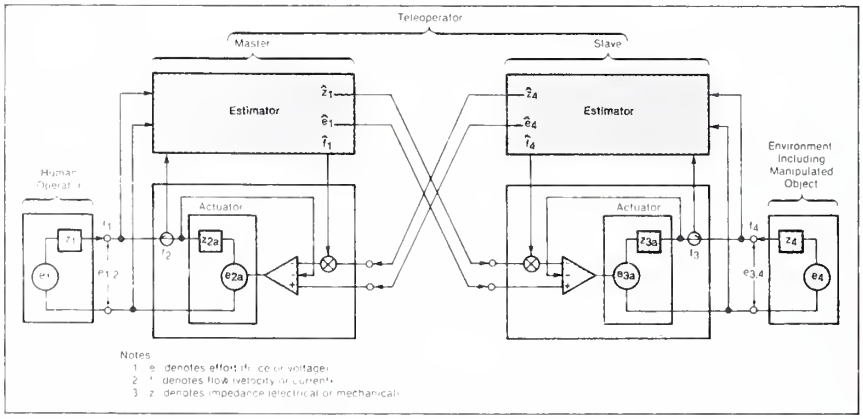

Figure 2. This **Teleoperator Incorporates Bilateral Impedance Control** for improved performance in the presence of delays in propagation of signals through the teleoperator.

teleoperator by specifying the operating point in terms of the applicable position and velocity vectors.

Figure 2 illustrates the incorporation of the hybrid two-port model into a mathematical model of bilateral impedance control. Existing systems like those of Figure 1 cannot operate well with even small delays because information on impedances is transmitted piecemeal as efforts and flows are iterated around the complete control loop. In bilateral impedance control, a local servoloop enforces a commanded effort and impedance. The information communicated across the delay can be appropriately filtered to stabilize the system. In the steady state, this enables the operator to perceive the characteristics of the environment accurately and presents the environment with a suitable impedance selected by the operator.

Bilateral impedance control depends on estimators that are capable of identifying the impedance of the environment and of the human operator. In general, such estimation is very difficult because of problems posed by numerical conditioning and noise. Although ideal responses may be difficult to achieve, assumptions about the environment can extend the usefulness of this approach. For example, the estimators can be assisted by an intelligent system with a reduced set of impedance vectors ($\hat{Z}_j$). The task of each estimator is then to classify the effort- and flow-sensor readings into one of the $\hat{Z}_j$.

This work was done by Blake Hannaford of Caltech for **NASA's Jet Propulsion Laboratory.** *NPO-17527/TN*

NASA Tech Brief
National Aeronautics and Space Administration
Ames Research Center, Moffett Field, California

Licensing Opportunity

Rapid Dry Etching of Photoresists Without Toxic Gases

A room-temperature process may not damage underlying semiconductor wafers.

An experimental dry etching technique may have the potential to strip photoresists from semiconductor wafers without damaging the semiconductor materials. The technique strips quickly at room temperature; it is not necessary to heat the substrates and thereby cause unwanted diffusion of dopants in the semiconductors. No hazardous or toxic chemicals are used.

The technique makes use of the afterglow that exists downstream from plasma generated by a radio-frequency electric field. The constituents of the afterglow react with a sacrificial polymer to make reactive gases that quickly etch-away the photoresist. The use of the afterglow instead of the plasma itself avoids exposure of the semiconductor wafer to most of the high-energy ions, electrons, photons, and electric fields that are likely to damage devices — especially integrated circuits — in the wafer.

A plasma reactor with external electrodes generates reactive species from glowing oxygen gas (see figure). The wafer with photoresist is positioned on a pedestal at least 16 cm downstream from the reactor and around a 90° bend in the gas stream.

A sheet of polyethylene is placed next to the wafer on the pedestal. The oxygen species in the afterglow act on the polyethylene so that it outgasses substances that attack the photoresist on the wafer, converting the photoresist to harmless vapors that flow away with the oxygen stream. Such other polymers as polyoctenamer are also effective. The main criterion is that the sacrificial polymer have a low vapor pressure — less than 0.001 torr ($\lesssim$0.1 Pa) — and that it react readily with the afterglow species.

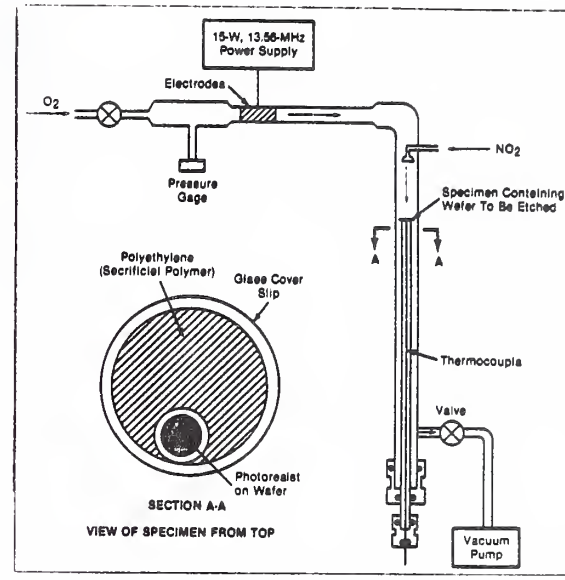

The **Water is Separated From the Radio-Frequency Plasma** by distance and a bend. In one of the many possible configurations of the wafer and the sacrificial polymer, the wafer is almost entirely surrounded by the polymer.

In a demonstration, a 7.5-μm-thick layer of Shipley Microdeposit S1400-27, a commonly used photoresist, was deposited on a glass cover slip and hard-baked according to the manufacturer's directions. When it was exposed to the afterglow with the sacrificial polymer, it was etched away 35 times faster than was a similar specimen without the sacrificial polymer.

This work was done by Narcinda R. Lerner and Theodore Wydeven of **Ames Research Center.**

This invention is owned by NASA, and a patent application has been filed. Inquiries concerning nonexclusive or exclusive license for its commercial development should be addressed to the Patent Counsel, Ames Research Center. Refer to ARC-11873/TN.

Ames Research Ctr.
Technology Utilization Officer: Laurance Milov
Mail Code 223-3
Moffett Field, CA 94035
(415) 694-4044
Patent Counsel:
Darrell G. Brekke
Mail Code 200-11
Moffett Field, CA 94035
(415) 694-5104

FOR ADDITIONAL INFORMATION: *Contact: Director, Technology Transfer Division, P.O. Box 8757, BWI Airport, MD 21240; (301) 621-0100 Ext. 241*
REFER TO THE NUMBER LISTED AT THE END OF THIS ARTICLE

NASA Tech Brief
National Aeronautics and Space Administration
Goddard Space Flight Center, Greenbelt, Maryland

Synchronizing Rotation of a Heavy Load

A simple setup of motors, pulleys, and belts provides both torque and synchronism.

A drive system rotates a large-inertia load at constant low speed. The system was developed to rotate a large instrument — a differential microwave radiometer that measures cosmic background radiation — at 120 rpm in synchronism with 60-Hz alternating-current power.

Synchronous stepping motors were originally selected for driving the instrument. These motors, however, were found to be incapable of starting or maintaining the desired synchronous rotation. The solution was to add an induction motor and a belt-and-pulley transmission, which effectively connects the outputs of the induction and synchronous motors in parallel (see figure). The induction motor provides the starting and maintaining torque. The diameters of the pulleys are chosen so that at the shaft on which the instrument rotates, the rotation that would be caused by the induction motor acting alone slightly leads the rotation that would be caused by the synchronous motor acting alone. The synchronous motor thus becomes an additional load with a fixed rate of rotation and forces the induction motor into synchronism with the ac power.

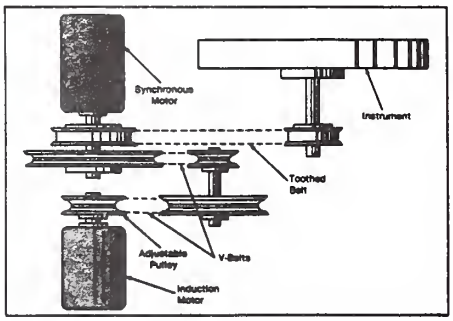

The **Induction Motor Drives** two loads: a rotating instrument and a slightly lagging synchronous motor. The induction motor provides ample torque to start and maintain rotation, and the synchronous motor ensures that the rotation is synchronized with the ac power supply.

This work was done by Roger Ratliff of **Goddard Space Flight Center.**
GSC-13325/TN

FOR ADDITIONAL INFORMATION: *Contact: Director, Technology Transfer Division, P.O. Box 8757, BWI Airport, MD 21240; (301) 621-0100 Ext. 241*
REFER TO THE NUMBER LISTED AT THE END OF THIS ARTICLE

NASA Tech Brief
National Aeronautics and Space Administration
Marshall Space Flight Center, Alabama

Monitoring Welding Images and Data Simultaneously

Data on process conditions are superimposed in real time on images of the process.

A video/computer subsystem of a welding system produces an overlay, on a video image, containing numerical data on the parameters of the welding operation being viewed. The system was developed to assist a welding-machine operator in determining the width of the back bead of the weld.

The computer gathers data from sensors while a video camera observes the weld in progress. The computer sends the data to a vision processor in the computer, which superimposes the data on the image from the camera. The operator thus can watch the weld bead simultaneously with the instantaneous values of such data as elapsed time, welding current, and processed sensor measurements of the weld area, such as weld back-bead width and depth of penetration, pool temperature, or top bead dimensions.

The video image and superimposed data can be recorded on magnetic video tape. The welding operation can later be reviewed in slow motion or even frame by frame. The pertinent weld data will always be instantly available to the viewer and correlated in time with the image of the weld.

This work was done by Ray C. Delcher and Matthew A. Smith of Rockwell International Corp. for **Marshall Space Flight Center.** *MFS-29772/TN*

FOR ADDITIONAL INFORMATION: *Contact: Director, Technology Transfer Division, P.O. Box 8757, BWI Airport, MD 21240; (301) 621-0100 Ext. 241*
REFER TO THE NUMBER LISTED AT THE END OF THIS ARTICLE

Materials

0949 Technique Developed for Fluoride Glass Windows

0950 Alternative AlxGa1-xAs/GaAs Transistors for Neural Networks—Current gain is increased through reduction of bulk leakage and surface-recombination currents.

0951 GaAsP Photodiodes as X-Ray Detectors—GaAsP cells cost less than Si cells do and are less damaged by radiation.

0952 High-Gain AlxGa1-xAs/GaAs Transistors for Neural networks—Darlington pairs exhibit current gains of 4,000. (Licensing Opportunity)

0953 High-Power AlGaAs Quantum-Well Lasers on Si Substrates—Improved devices are made by migration-enhanced molecular-beam epitaxy and metalorganic vapor-phase epitaxy.

0954 Stiff, Strong Splice for a Composite Sandwich Structure—Layers of alternating fiber orientation are interposed between thin ears in an adhesive joint. (Licensing Opportunity)

Testing & Instrumentation

0955 Defect Area Determines Organic Coating

0956 Device Developed to Inspect Materials

Other Items of Interest

0941 Diamond Turning of Stainless Steel

NAVY
Domestic Technology Transfer Fact Sheet

Technique Developed for Fluoride Glass Windows

The Naval Research Laboratory (NRL), Washington, D.C., reports the development of a technique for the preparation of 20-kilogram heavy metal fluoride (HMF) glass windows, the largest fluoride glass windows that have been made to date. The 20-kg windows are greater than one-inch thick and nearly 18 inches in diameter. They are produced under contract to the Owens-Corning Fiberglass Company and are reported large enough to be used for ground-based and shipboard high energy laser (HEL) systems.

Although HMF glasses offer a number of advantages over other materials, until, now, they could not be produced in large enough sizes to be of practical use as an HEL optical component. However, the new windows are large enough and can compete with, and surpass some of the current HEL optical components.

The new preparation techniques were combined with traditional optical glass-forming techniques to produce these windows. Small batches of glass were premelted and used as cullet. The cullet was then remelted in a large platinum crucible, and the molten glass was cast from this crucible into a brass mold preheated to an appropriate temperature to prevent cracking and crystallization of the window.

HMF glasses are desirable for HEL optical components because they have very low optical loss at longer wavelengths. They have a broad transmission range, and they offer the possibility of producing windows with zero optical path distortion.

For Additional Information:

Backup material on this effort is available from:

Navy Domestic Technology Fact Sheet Reader Reply Service
Code E211
Naval Surface Weapons Center
Dahlgren, VA 22448-5000
(703) 663-8921

Refer to 160704/TN

NASA Tech Brief
National Aeronautics and Space Administration
NASA's Jet Propulsion Laboratory, Pasadena, California

Alternative $Al_xGa_{1-x}As$/GaAs Transistors for Neural Networks

Current gain is increased through reduction of bulk leakage and surface-recombination currents.

Further development efforts have yielded an alternative version of the transistors described in the preceding article, "High-Gain $Al_xGa_{1-x}As$/GaAs Transistors for Neural Networks" (NPO-18101). These efforts have focused on determining the effects of various aspects of the design and of the fabrication processes upon leakage currents and, consequently, on current gains.

It is difficult to obtain high and reproducible current gains in double-heterojunction bipolar transistors with bases containing diffused zinc like those of the preceding article largely because such transistors have leakage currents much greater than those of the more-conventional etched-base double-heterojunction bipolar transistors. The leakage currents are mainly caused by recombinations of charge carriers in the depletion regions, in the bulk regions, and on the surfaces. Furthermore, the diffusion of the Zn dopant out of the base region at the high fabrication temperatures can destroy the integrity of the emitter-base heterojunction.

The figure shows the alternative transistor configuration. Research on the aforementioned and other factors that affect current gains led to the conclusion that the current gain of such a transistor could be maximized by (1) reducing the leakage currents that flow laterally through the homojunction between the zinc-diffused extrinsic $Al_{0.3}Ga_{0.7}As$ base layer and the $Al_{0.3}Ga_{0.7}As$ emitter layer, (2) reducing the thermal degradation, during fabrication, of minority-carrier lifetime in the base, and (3) optimal control of the diffusion of Zn as a function of temperature and time during fabrication.

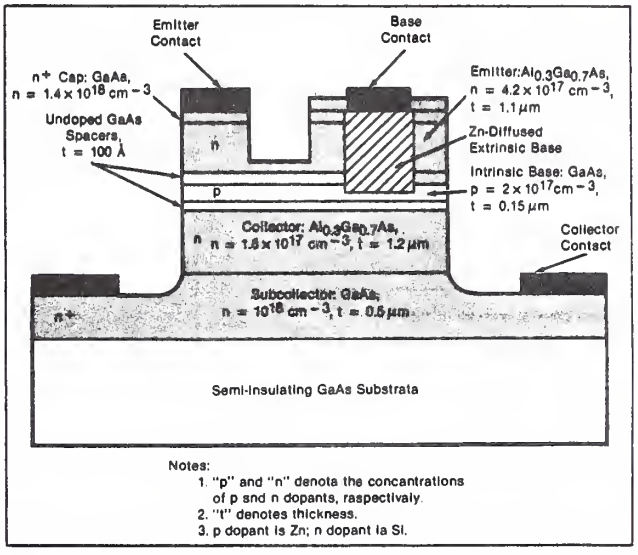
Emitter Contact
Base Contact
n+ Cap: GaAs, n = 1.4 x 10^18 cm^-3
Undoped GaAs Spacers, t = 100 Å
Emitter: Al0.3Ga0.7As, n = 4.2 x 10^17 cm^-3, t = 1.1 μm
Zn-Diffused Extrinsic Base
Intrinsic Base: GaAs, p = 2 x 10^17 cm^-3, t = 0.15 μm
n
p
Collector: Al0.3Ga0.7As, n = 1.8 x 10^17 cm^-3, t = 1.2 μm
Collector Contact
Subcollector: GaAs, n = 10^18 cm^-3, t = 0.5 μm
n+
Semi-Insulating GaAs Substrate
Notes:
1. "p" and "n" denote the concantrations of p snd n dopants, raspectivaly.
2. "t" denotes thickness.
3. p dopant is Zn; n dopant la Si.

This **Zinc-Diffused-Extrinsic-Base Double-Heterojunction Bipolar Transistor** differs from the one described in the preceding article in the design and fabrication of the connection between the external metal contact and the intrinsic base layer.

Specifically, the lateral leakage currents can be suppressed by etching an isolating channel between the emitter and extrinsic base regions. The highest current gain is obtained when the channel is etched to a depth that leaves a depleted $Al_{0.3}Ga_{0.7}As$ emitter layer about 1,000 Å thick covering the intrinsic base layer. The reason is that at this optimal etching depth, the surface-depletion layer and the intrinsic base-emitter-junction-depletion layer can punch through and the leakage currents are effectively blocked from the emitter periphery. This layer acts as a passivation layer and reduces the surface-recombination currents aw well. The depth of diffusion of zinc to form the extrinsic base layer is controlled accurately so that it reaches the base layer and so that the diffusion process causes minimal degradation of the minority-carrier lifetime in the intrinsic base layer.

Specimens of the transistors exhibited dc common-emitter current gains as high as 200. With further improvements in design and processing, it may be possible to obtain gains comparable to those of the etched-base transistors. A monolithically integrated Darlington pair of such transistors exhibited an overall current gain of 6,000.

This work was done by Jae-Hoon Kim and Steven H. Lin of Caltech for **NASA's Jet Propulsion Laboratory**.
NPO-18177/TN

FOR ADDITIONAL INFORMATION: *Contact: Director, Technology Transfer Division, P.O. Box 8757, BWI Airport, MD 21240; (301) 621-0100 Ext. 241*
REFER TO THE NUMBER LISTED AT THE END OF THIS ARTICLE

NASA Tech Brief
National Aeronautics and Space Administration
NASA's Jet Propulsion Laboratory, Pasadena, California

GaAsP Photodiodes as X-Ray Detectors

GaAsP cells cost less than Si cells do and are less damaged by radiation.

Tests show that commercial G1126-02 GaAsP photodiodes designed as ultraviolet detectors can be modified easily for use as x-ray detectors. At present, x-ray and other highly energetic radiation are usually measured with specially fabricated silicon cells. The modified GaAsP photodiodes cost about one third as much as the silicon cells and are more resistant to damage by radiation.

The GaAsP photodiodes have quartz windows. When used to measure ultraviolet fluxes, the windows or other apertures in the optical paths are covered with optical filters. To modify one of these photodiodes for the x-ray application, one removes the quartz window and replaces it with an aluminum foil, which blocks ultraviolet and visible radiation.

To verify the concept, GaAsP cells were tested with quartz windows, without window covering, and with windows of aluminum foil 1 mil (0.025 mm) thick. The figure presents the results of one of the tests, showing that the tested photodiode does indeed function as a detector of photons with energies from 20 to 100 keV.

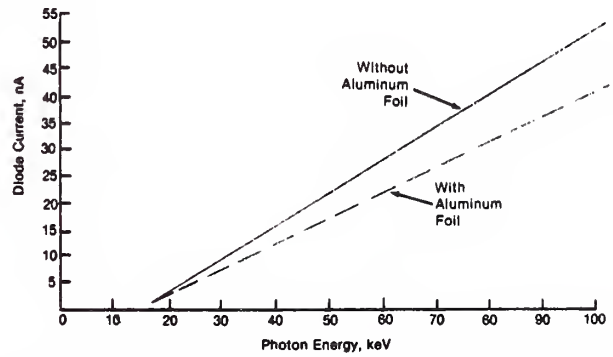

The **Approximate Relative Spectral Responsivity** of a GaAsP photodiode with and without an aluminum-foil window indicates that the aluminum foil can be used to block visible and ultraviolet light and that the photodiode can detect x rays that penetrate the foil.

This work was done by Eric G. Laue of Caltech for **NASA's Jet Propulsion Laboratory.** *NPO-17849/TN*

FOR ADDITIONAL INFORMATION: *Contact: Director, Technology Transfer Division, P.O. Box 8757, BWI Airport, MD 21240; (301) 621-0100 Ext. 241*
REFER TO THE NUMBER LISTED AT THE END OF THIS ARTICLE

NASA Tech Brief
National Aeronautics and Space Administration
NASA's Jet Propulsion Laboratory, Pasadena, California

Licensing Opportunity

High-Gain $Al_xGa_{1-x}As$/GaAs Transistors for Neural Networks

Darlington pairs exhibit current gains of 4,000.

High-gain $Al_xGa_{1-x}As$/GaAs npn double heterojunction bipolar transistors have been developed for use as phototransistors in optoelectronic integrated circuits, especially in artificial neural networks. In the contemplated optoelectronic implementation of a neural network, a two-dimensional array of photodetectors, saturating amplifiers, and light sources would be integrated on a monolithic circuit chip. Each light source would represent the output of a neuron; the light would be diffracted to other neurons by holographic optical elements. When the total optical input to a neuron was below a threshold level, the output of the neuron would be zero. When the total input exceeded that level, the output of the neuron would rise to a saturation value. $Al_xGa_{1-x}As$/GaAs double-heterojunction bipolar transistors would perform both the photodetection and saturating-amplification functions of the neurons. These transistors are good candidates for such an application because they are structurally compatible with laser diodes and light-emitting diodes, can detect light, and can provide the high current gain needed to compensate for losses in the holographic optical elements.

The developed transistors (see figure) were grown epitaxially by metal-organic chemical-vapor deposition on semi-insulating substrates of (100)-oriented GaAs doped with Cr. The GaAs and $Al_xGa_{1-x}As$ layers were grown from $Ga(CH_3)_3$, $Al(CH_3)_3$, and AsH_3 gases in H_2 carrier gas. The p and n dopants were Zn and Si, respectively. During the growth of the layers, the temperatures of the substrates were maintained at about 730°C.

To obtain large current gain, it was necessary to suppress diffusion of Zn out of the base layer during the deposition process. A reduction in the deposition temperature would have had this effect but would also have resulted in a greater number of undesired nonradiative recombination centers in the light sources that would eventually be integrated with the transistors. The nonradiative recombination centers will significantly degrade performance of the light sources. Therefore, to reduce the out-diffusion of Zn, the concentration of Zn was reduced below what would otherwise be considered normal for transistors of this type. In general, a reduction in the base doping causes an increase in the base resistance and a consequent increase in the switching time of the transistors. However, in a neural network, even a relatively long switching time of 1 μs is acceptable.

In tests of electrical characteristics, a transistor of the new type exhibited a common-emitter current gain of 500. A wire-connected pair of such transistors in the Darlington configuration exhibited an overall current gain of 4,000, which more than satisfies the estimated requirement of 2,500 for an optoelectronic neural network. An experimental monolithic 10×10 array of optoelectronic neurons was built, and the fully functional operation of the neuron arrays was successfully demonstrated.

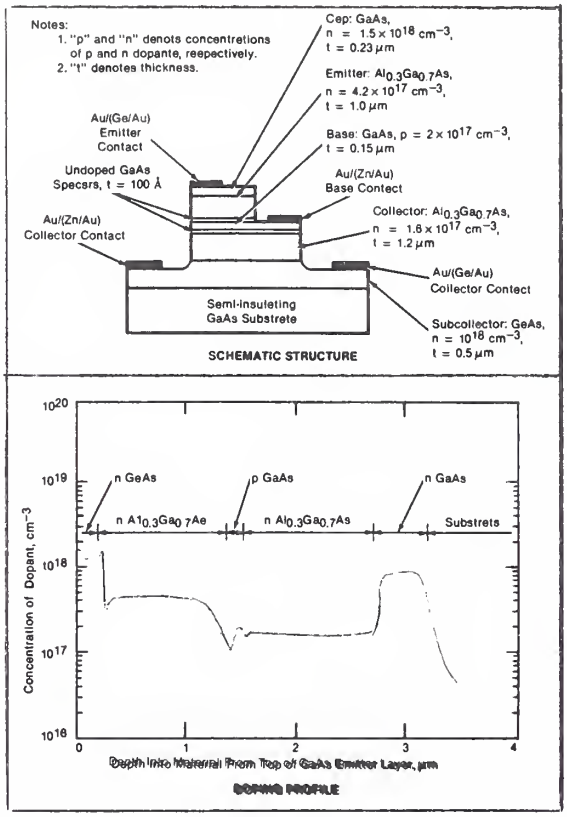
Notes:
1. "p" and "n" denots concentretions of p and n dopante, reepectively.
2. "t" denotes thickness.
Cep: GaAs, n = 1.5 × 10^18 cm^-3, t = 0.23 μm
Emitter: Al0.3Ga0.7As, n = 4.2 × 10^17 cm^-3, t = 1.0 μm
Au/(Ge/Au) Emitter Contact
Base: GaAs, p = 2 × 10^17 cm^-3, t = 0.15 μm
Undoped GaAs Specsrs, t = 100 Å
Au/(Zn/Au) Base Contact
Au/(Zn/Au) Collector Contact
Collector: Al0.3Ga0.7As, n = 1.6 × 10^17 cm^-3, t = 1.2 μm
Au/(Ge/Au) Collector Contect
Semi-Insuleting GaAs Substrete
Subcollector: GeAs, n = 10^18 cm^-3, t = 0.5 μm
SCHEMATIC STRUCTURE
10^20
10^19
10^18
10^17
10^16
n GeAs
p GaAs
n GaAs
n Al0.3Ga0.7Ae
n Al0.3Ga0.7As
Substrets
Concentration of Dopant, cm^-3
0
1
2
3
4
Depth Into Material From Top of GaAs Emitter Layer, μm
DOPING PROFILE

This **$Al_xGa_{1-x}As$/GaAs npn Double-Heterojunction Bipolar Transistor** was grown epitaxially by metal-organic chemical-vapor deposition. The concentration of dopant was measured by an electrochemical profiler.

This work was done by Jae-Hoon Kim and Steven H. Lin of Caltech for **NASA's Jet Propulsion Laboratory.**

This invention is owned by NASA, and a patent application has been filed. Inquiries concerning nonexclusive or exclusive license for its commercial development should be addressed to the Patent Counsel, NASA Resident Office-JPL. Refer to NPO-18101/TN.

Jet Propulsion Lab.
NASA Resident Office
Technology Utilization Officer Gordon S. Chapman
Mail Stop 180-801
4800 Oak Grove Drive
Pasadena, CA 91109
(818) 354-4849
Patent Counsel Paul F. McCaul
Mail Code 180-801
4800 Oak Grove Drive
Pasadena, CA 91109
(818) 354-2734
Technology Utilization Mgr. for JPL Norman L. Chalfin
Mail Stop 156-211
4800 Oak Grove Drive
Pasadena, CA 91109
(818) 354-2240

FOR ADDITIONAL INFORMATION: *Contact: Director, Technology Transfer Division, P.O. Box 8757, BWI Airport, MD 21240; (301) 621-0100 Ext. 241*
REFER TO THE NUMBER LISTED AT THE END OF THIS ARTICLE

NASA Tech Brief
National Aeronautics and Space Administration
NASA's Jet Propulsion Laboratory, Pasadena, California

High-Power AlGaAs Quantum-Well Lasers on Si Substrates

Improved devices are made by migration-enhanced molecular-beam epitaxy and metalorganic vapor-phase epitaxy.

$Al_xGa_{1-x}As$ lasers of the graded-index-of-refraction, separate-confinement-heterostructure, single-quantum-well type have been fabricated on silicon substrates by migration-enhanced molecular-beam epitaxy followed by metalorganic vapor-phase epitaxy. These lasers are intermediate products of a continuing effort to develop low-threshold-current, high-efficiency lasers for parallel optical interconnections between large-scale optoelectronic integrated circuits.

Figure 1 illustrates the composition-vs.-depth profile of one of these lasers. The initial (leftmost in this figure) layer of GaAs doped with silicon (n dopant) was grown by migration-enhanced molecular-beam epitaxy on an n-doped silicon (100) substrate tilted 4° toward the [110] direction. In this particular version of migration-enhanced molecular-beam epitaxy, two sublayers of the initial GaAs layer were deposited in the following sequence:

1. The first 150 monolayers of GaAs were grown by migration-enhanced molecular-beam epitaxy, in which Ga and As beams were supplied alternately and the substrate was heated to $\lesssim 400$ °C — less than the conventional molecular-beam-epitaxy temperature of $\gtrsim 580$ °C — to reduce the density of defects.
2. The second sublayer, 1.5 to 2.0 μm thick, was grown by molecular-beam epitaxy that was conventional in that Ga and As beams were supplied simultaneously but unconventional in that the temperature was kept $\lesssim 400$ °C.

The $Al_xGa_{1-x}As$ layers of the graded-index-of-refraction, separate-confinement-heterostructure quantum well were deposited by metalorganic vapor-phase epitaxy at a temperature of 750 °C and a pressure of 76 torr (10 kPa). The sources of gallium, aluminum, and arsenic were trimethylgallium, trimethylaluminum, and arsine, respectively; the sources of the p dopant (zinc) and the n dopant (silicon) were diethylzinc and silane in hydrogen, respectively. The heterostructures thus deposited were fabricated into lasers by cleaning, polishing, deposition of metal contacts, and cleavage along the [011] direction to form the laser facets.

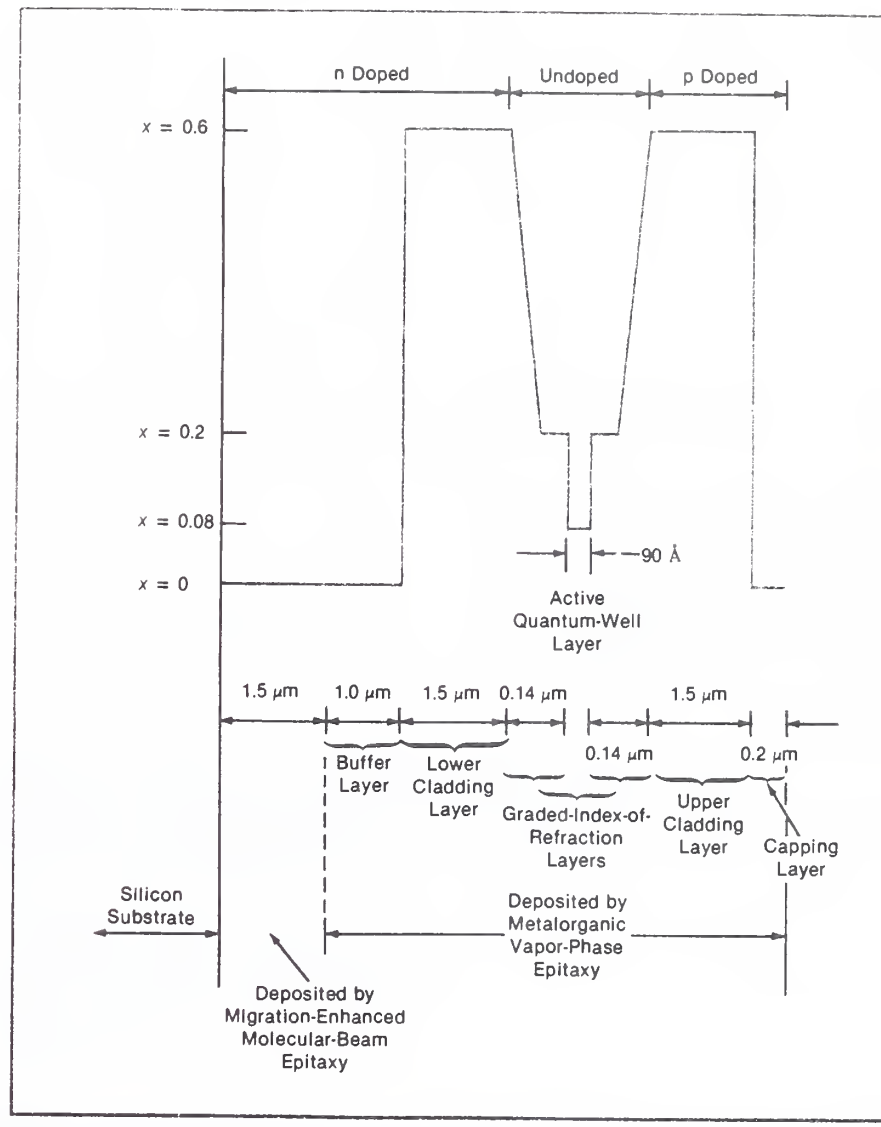

Figure 1. The **Atomic Fraction, *x*, of Aluminum** in $Al_xGa_{1-x}As$ is plotted as a function of distance (decreasing depth) from the surface of the Si substrate.

The lasers were tested and found to have excellent current-vs.-voltage characteristics that included sharp forward turn-on at 1.1 V and reverse breakdown at 8 V. Figure 2A shows the output power as a function of injection current of a laser with a cavity length of 500 μm and a stripe differential width of 110 μm, without coating on the facets, at room temperature. This plot indicates a differential quantum efficiency of 40 percent. It also indicates a 300-mA threshold current, which corresponds to a threshold current density of 550 A/cm^2 — considerably better than the 1- to 2-kA/cm^2 threshold-current density of prior $Al_xGa_{1-x}As$ lasers on Si substrates. In addition, the peak output power of more than 400 mW per facet may be the highest peak power observed to date on low-threshold-current lasers on Si

substrates. The laser shows stable operation to more than 400 mW per facet at $6I_{th}$. The full width at half maximum of the farfield pattern in Figure 2B varies from 3° to 6° over the entire pumping range.

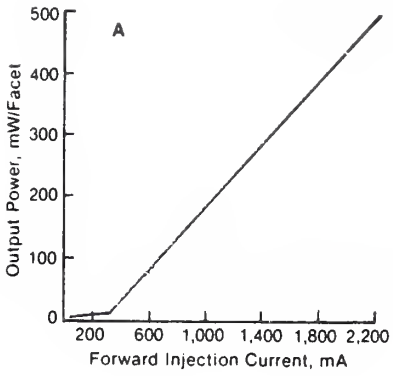

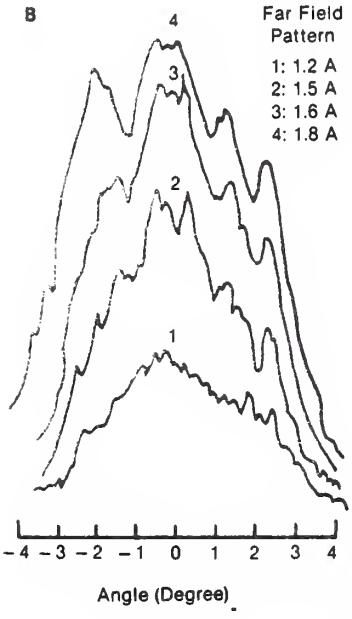

Figure 2a. The **Output vs. Injection Current** of a laser of the type described in the text indicates a differential quantum efficiency of 40 percent and a threshold current of 300 mA. Figure 2b. The Far-Field Patterns of a laser are plotted as a function of angle at different pumping levels.

This work was done by Jae-Hoon Kim, Robert J. Lang, Gouri Radhakrishnan, and Joseph Katz of Caltech for **NASA's Jet Propulsion Laboratory.**
NPO-17988/TN

FOR ADDITIONAL INFORMATION: *Contact: Director, Technology Transfer Division, P.O. Box 8757, BWI Airport, MD 21240; (301) 621-0100 Ext. 241*
REFER TO THE NUMBER LISTED AT THE END OF THIS ARTICLE

NASA Tech Brief
National Aeronautics and Space Administration
Ames Research Center, Moffett Field, California

Licensing Opportunity

Stiff, Strong Splice for a Composite Sandwich Structure

Layers of alternating fiber orientation are interposed between thin ears in an adhesive joint.

A new type of splice for a composite sandwich structure reduces the peak shear stress in the structure. The splice, which was developed for a structural joint in the spar of a helicopter rotor blade, also increases the precision of control over the thickness of the adhesive at the joint.

The spar consists of two pieces — a leading-edge half and a trailing-edge half, both having C-shaped cross sections. The new splice (see figure) bonds the halves together to form a structural spar that can carry high torsional shear; high bending moments from aerodynamic loads; and additional loads from flap shear, chord shear, and related bending moments. The joint is easy to make, requires no additional pieces, and adds little weight. The bending stiffness across the joint remains high so that deflections of the airfoil surface under aerodynamic loads are minimized. The new joint supplants single- and double-overlap joints. The single-overlap joint suffers from low bending stiffness and high peak shear and tension stresses. The double-overlap joint is superior to the single-overlap version but is difficult to make.

The new joint includes a pair of ears bonded with a graphite filler laminate. The thin ears can conform to the curvature of the thicker graphite laminate between them, yielding a spatially gradual and therefore more uniform distribution of tension stress across the bond lines and consequently smaller tension peaks. The cross-sectional area that provides bending stiffness is reduced by only the thickness of an ear.

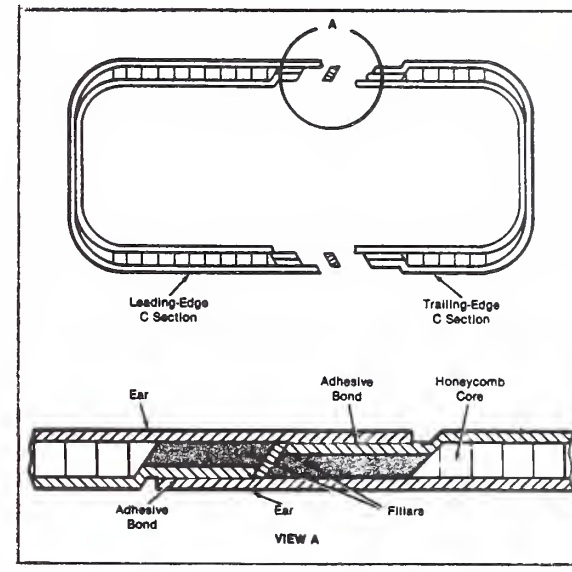

Thin Ears Join Sections of the spar of a helicopter rotor. A thick graphite filter laminate is sandwiched between the thin laminate ears by an adhesive.

The ears are relatively stiff laminates of 90° and 45° fiber orientations, while the filler laminate with its ±45° fiber orientations is relatively compliant. The combination of stiff ears and compliant filler contributes further to the spatially and temporally gradual transfer of loads to reduce the peak shear stresses.

This work was done by Mark R. Osterloh, Karen E. Sliwinski, and Ronald R. Anderson of Rockwell International Corp. for **Marshall Space Flight Center.**

Inquiries concerning rights for the commercial use of this invention should be addressed to the Patent Counsel, Marshall Space Flight Center. Refer to MFS-29725/TN.

George C. Marshall Space Flight Center
Technology Utilization Officer Ismail Akbay
Code AT01
Marshall Space Flight Center,
AL 35812
(205) 544-2223
Patent Counsel Leon D. Wofford, Jr.
Mail Code CC01
Marshall Space Flight Center,
AL 35812
(205) 544-0024

FOR ADDITIONAL INFORMATION: *Contact: Director, Technology Transfer Division, P.O. Box 8757, BWI Airport, MD 21240; (301) 621-0100 Ext. 241*
REFER TO THE NUMBER LISTED AT THE END OF THIS ARTICLE

Defect Area Determines Organic Coating

Coating breakdown is a major maintenance cost on ships. It is therefore desirable to have a rapid technique for predicting or evaluating coating performance nondestructively.

The breakpoint frequency method, which allows determination of the electrochemically active area of a coated metal in seawater was refined and used by the David Taylor Research Center (DTRC) scientists at Bethesda, Maryland. A computer model is used to explain the basis of the breakpoint method, and the model is compared to impedance and visual data from epoxy-coated steel panels in ASTM artificial seawater with and without an intentional defect of known area.

The breakpoint frequency method was extremely useful in determining the electrochemically active area of coated steel in seawater. The equivalent circuit model used in this analysis was capable of fitting actual data on coated steel panels with and without an intentional defect. A correlation was obtained between the breakpoint frequency and the visually estimated electrochemically active area on epoxy coatings of a variety of thicknesses. This method offers a simple alternative to determination of defect areas via the use of the pseudocapacitance from difficult-to-analyze, low frequency impedance data. This approach also can detect the beginnings of coating breakdown long before visual indications are present.

For Additional Information:

Backup material on this effort is available from:

Navy Domestic Technology Fact Sheet Reader Reply Service
Code E211
Naval Surface Weapons Center
Dahlgren, VA 22448-5000
(703) 663-8921

Refer to 160604/TN

NAVY
Domestic Technology Transfer Fact Sheet

Device Developed to Inspect Materials

The Naval Surface Warfare Center (NAVSWC), Silver Spring, Maryland, has developed a device for inspection of materials by eddy current methods. The device comprises an encircling coil transmitter, and a receiver. When applied to filament-wound, carbon fiber-reinforced composites, the transmitter induces eddy current flow in the circumferentially wound fibers. The receiver detects localized variations in this current flow, which may be due to fiber breakage or to variations in fiber density. The receiver may be a U-shaped eddy current probe, or possibly a Hall probe, or a SQUID. The device can be used for the inspection of any component that has conductivity in the circumferential direction; conduction paths need not be limited to this direction.

For Additional Information:

Backup material on this effort is available from:

Navy Domestic Technology Fact Sheet Reader Reply Service
Code E211
Naval Surface Weapons Center
Dahlgren, VA 22448-5000
(703) 663-8921

Refer to 160705/TN

Medicine & Biology

0957 National Cell Culture Center

0958 Accelerating Protons to Treat Cancer

0959 Compact Apparatus for Growth of Protein Crystals—Growth can be initiated and terminated automatically. (Licensing Opportunity)

0960 Research Animal Holding Facility Prevents Space Lab Contamination—A healthy environment for both rodents and human researchers is maintained.

0961 Software for Design of Life-Support Systems—A special-purpose computer program combines conventional mathematical models with an expert software system.

Testing & Instrumentation

0962 Detection of Enzymes Using Agar Gel

0963 Pocket Optometer Developed for Biofeedback Training

NIH
Research & Technology
Federal laboratory resource
U.S. Department of Health and Human Services Public Health Service National Institutes of Health

National Cell Culture Center

The National Cell Culture Center (NCCC) offers large-scale production of animal cells at a reduced cost for use by biomedical researchers. The center, supported by the Biological Models and Materials Research Program of the National Center for Research Resources, is operated as an independent unit within its parent company, Endotronics, Inc., in Minneapolis, Minnesota. NCCC is a resource facility established in October 1990 to alleviate the shortage of affordable facilities and expertise for the production of cells and cell products in very large quantitites, according to Dr. Mark D. Hirschel, principal investigator and program director.

"There is a strong need for a center that can supply cells and cell products in large amounts. No one else is doing it on a nationwide scale. Lots of universities have their own laboratories to produce small amounts of, for example, monoclonal antibodies. But those facilities are not suited for large-scale production—in the gram range, as opposed to the microgram range," he says.

"While doing preliminary research many investigators discover an enzyme or a growth factor that would be of great value to the project, if they could get more of it. But they cannot generate enough of the material themselves, and without an outside source of material they cannot make the leap from preliminary research to a full-scale project," Dr. Hirschel says.

Commercial sources for cells and cell products exist in some parts of the country, according to Dr. Hirschel, but the expense has been far too great for most researchers to use them. Moreover, relying on various local commercial sources rather than on a single, centralized production facility has meant that the material is not always produced under the same well-defined, carefully controlled conditions.

Courtesy of the National Cell Culture Center

New cell cultures are started in small culture flasks and gradually expanded, reaching final volumes of up to 100 liters. Research associate Scott Waniger is shown expanding a culture of cells into a 10-liter flask.

Dr. Hirschel estimates that the cost of cells and cell products from the National Cell Culture Center is approximately half that charged by commercial sources, and strict quality control of all bioproducts is maintained.

The NCCC services include production of monoclonal antibodies; non-hybridoma cell products such as recombinant proteins, growth factors, tumor antigens, hormones, and enzymes; mammalian tumor or lymphoid cells; and specialized cells such as tumor-infiltrating lymphocytes (TIL) and lymphokine-activated killer (LAK) cells.

The center is dedicated to providing these materials and access to state-of-the-art cell culture instrumentation and techniques to small research groups as well as to larger collaborative organizations. "We offer a full range of production facilities from cell growth in small flasks to large automated bioreactors," Dr. Hirschel notes.

The kinds of research projects that can utilize the NCCC's services are "just all over the map," he says. For example, investigators working on characterizing the structure or functional regulation of a particular protein need large amounts to conduct their research. Other investigators studying a particular enzyme involved in allergic and inflammatory disease processes may need large quantities of cells to purify and clone the enzyme. A third project may require the NCCC's services to aid in delineating the molecular structure of a cell receptor involved in tumorigenicity and cell differentiation.

To date, Dr. Hirschel and his staff of three at the NCCC have collaborated on more than 20 such projects. "Now the operation is up and running," he says. "We have completed

several contracts successfully. Our goal is to handle at least 50 different contracts per year, and we should be able to do that easily." He emphasizes that each project is different, and that the requirements for cells or cell products can vary a great deal. "One project may need 1 kg of cells each month for the next 12 months. Another may only require one-tenth of that every other month," he says.

In addition to supplying researchers with cell culture material, the NCCC staff "provides guidance on anything associated with large-scale cell production, if investigators want to set up their own facility. We're here as a resource," Dr. Hirschel says, adding that the parent company, Endotronics, can provide researchers with the equipment they may need to start large-scale manufacture of biologicals.

In the future he and his associates hope to offer users other services as well. They plan to preserve researchers' cell lines at the center as a backup in case something happens to the material at a user's own facility. They also want to provide users with information such as the optimal growth conditions for particular types of cells. "We have the expertise for this now, and we do it for ourselves all the time; we'll probably be doing this service for users in the near future," Dr. Hirschel says.

Another objective of the NCCC staff is to establish the most effective production technique for various cells and cell products. This information will be passed on to users, so that those who decide to expand their projects after doing preliminary work can rely on the NCCC to help them identify the best way to produce large quantities of the necessary material.

A unique hollow fiber bioreactor system developed by Endotronics is especially useful for culturing cells that secrete monoclonal antibodies and other secreted proteins. These bioreactors are used in both small- and large-scale applications. The center's typical hollow fiber bioreactor is essentially a cartridge 10 inches long and 2 inches in diameter. It contains approximately 9,000 porous fibers, each 220 micrometers in diameter, composed of polypropylene, cellulose acetate, or polysulfone. The cells are maintained in the spaces surrounding these fibers. The culture medium flows through the fibers, and nutrients such as glucose and amino acids diffuse across the fiber membrane to nourish the cells. Metabolic waste products flow from the cells into the fibers and are removed from the culture. "So there is constant perfusion within the culture, very much like the physiological conditions within the body," Dr. Hirschel notes.

This setup, which creates very small diffusion distances between cells and fresh culture medium, allows cells to grow at a very high density and allows continuous harvesting of cell products. Thus "murine hybridoma cells routinely reach densities of 108 cells per mL while secreting milligram quantities of monoclonal antibody per day for several weeks," he says. This cell density is 100 to 500 times higher than the density obtainable with more conventional culture methods, Dr. Hirschel adds.

Previously, a major disadvantage of growing such dense cultures was that a slight shift in pH balance or oxygen content could rapidly destroy the entire culture. However, the hollow fiber system is automated, with continuous computer- or microprocessor-controlled monitoring of such factors. The instrument can therefore correct for minor shifts immediately and maintain an optimal culture environment.

The bioreactor is available as a small benchtop pilot-scale production instrument. A small-scale culture produced in the pilot instrument can accurately predict the full-scale production capacity before significant resources are committed to the full-scale project, adds Dr. Hirschel.

Investigators who are interested in using the NCCC's services should complete an application that includes a description of the research project for which the material is needed. "That's the key portion of the application, which is evaluated for scientific merit by a scientific advisory committee. The applications are prioritized on this basis," Dr. Hirschel says, adding that research groups working on both small and large projects are eligible to apply.

Once an investigator's application is accepted, the user can submit the appropriate cell line if the center does not already have it. New cell lines are quarantined for 1 month to determine if they are contaminated with mycoplasma, a ubiquitous bacterial contaminant that "can be absolutely devastating to the research" and can jeopardize all cell cultures in the laboratory if it is not detected and eliminated immediately. After the quarantine period the cell culture goes into production, a process that can take from 1 week to several months to complete, depending on what the user needs.

For more information on the National Cell Culture Center, contact:
Dr. Mark D. Hirschel
Program Director
National Cell Culture Center
Endotronics, Inc.
8500 Evergreen Boulevard
Minneapolis, MN 55433
Telephone: (800) 325-1112;
(612) 786-0302

Department of Defense Fact Sheet

Strategic Defense Initiative Organization

Accelerating Protons to Treat Cancer

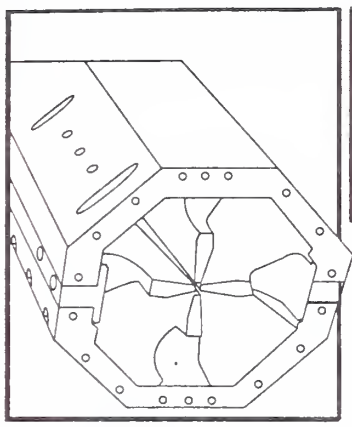

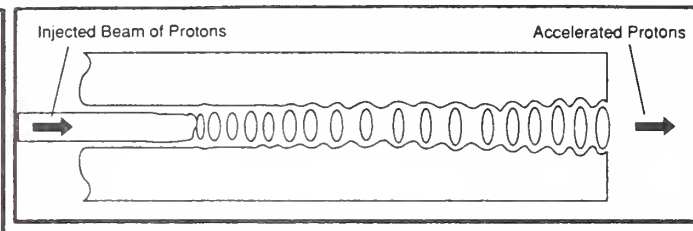

The quadrupole consists of four vanes that protrude from the cavity walls in the shape of a plus (+) sign. Radio-frequency power is applied to the quadrupole, which produces oscillating fields between the tips of the electrodes that bunch and accelerate a beam of protons.

Figure 2

The Radio Frequency Quadrupole (RFQ) Linear Accelerator (Linac) is the first stage of a high-energy proton accelerator that is attacking cancer - America's No. 1 killer. The proton accelerator was originally developed at Los Alamos National Laboratory with SDI funding, and a version of it is now operating at Loma Linda University Medical Center. The Loma Linda RFQ Linac was commercialized by AccSys Inc., (Pleasanton, Cal. one of the SDI/Los Alamos team members.

The RFQ Linac enables a reduction in size of an accelerator from a device 3 stories high to one only 3 feet high. At the same time, it significantly cuts the cost.

Employing protons to treat cancer tends to be safer for the patient than conventional radiation. Conventional radiation may kill the cancer cells, but it also damages adjacent healthy tissue. In fact, in some deep tumors, more intervening healthy tissue is radiated than the tumor itself. Because of this, the therapist may apply less than the optical dose of radiation to the tumor to prevent excessive damage to surrounding tissue. This conservative approach may allow the tumor to continue to grow (see Figure 2).

Proton beams, fortunately, scatter very little energy, depositing nearly all their energy at the target, with much less damage to adjacent healthy tissue. Hence, protons can be applied in higher doses, more thoroughly destroying the tumor. Since protons are charged particles, one can more precisely control their path with electric fields than neutrons, whose motion tends to be more scattered.

The Loma Linda facility can treat up to four patients simultaneously. The facility is expected to treat thousands of patients each year who suffer from a range of tumors - from those in the digestive system to those in the eye and brain.

The RFQ Linac could also serve in non-destructive testing, sub-atomic particle research, performing oil well logging, and mineral analysis. It could potentially analyze or treat nuclear waste.

FOR ADDITIONAL INFORMATION: Contact: Technology Applications Office, Strategic Defense Initiatives Organization, OSD/SDIO/TNI, The Pentagon, Washington, DC 20301-7100; (703) 693-1563.

NASA Tech Brief
National Aeronautics and Space Administration
Marshall Space Flight Center, Alabama

Licensing Opportunity

Compact Apparatus for Growth of Protein Crystals

Growth can be initiated and terminated automatically.

A compact apparatus proposed specifically for the growth of protein crystals in microgravity could also be used in terrestrial laboratories in which it is desired to initiate and terminate growth at prescribed times automatically. The apparatus would have few moving parts. It would also contain no syringes, which are difficult to clean, load, and unload and which can introduce contaminant silicone grease into the crystallization solution. After the growth of the crystals was terminated, the specimens could be retrieved and transported simply.

The apparatus (see figure) would be a 12- by 8- by 2-cm transparent, polycarbonate tray assembly that would contain 24 crystal-growth chambers, each 15 mm in diameter and 16 mm deep. Centered within each chamber would be a movable pedestal (piston), a guide sleeve, and an O-ring seal. At the tip of each pedestal (piston), there would be a depression, 3 mm deep and 5 mm in diameter, that would serve as a crystal-growth compartment. Each such depression could contain up to 0.1 mL of the protein/precipitant mixture.

The sleeves and O-rings would allow the pedestals to move vertically approximately 3 mm while maintaining the seals among the chambers. The 4-mm annulus formed by the walls of the chambers and the pedestal would serve as the reservoir for the precipitant solution. A doughnut-shaped wick of high-molecular-weight polyethylene or other porous material would fit into the annulus to contain the precipitant solution and to provide adequate surface area for the vapor-equilibration crystal-growth process to occur.

Under normal conditions, a protein/precipitant solution would be placed in the crystal-growth compartment in each pedestal while the precipitant solution was added to the annulus containing the porous wick. The solutions in the tray assembly would then rapidly be frozen to a temperature of −150 °C or lower and remain frozen until the experiment was activated. Upon activation, the solutions would be allowed to thaw — initiating the growth process — and then maintained at a constant temperature.

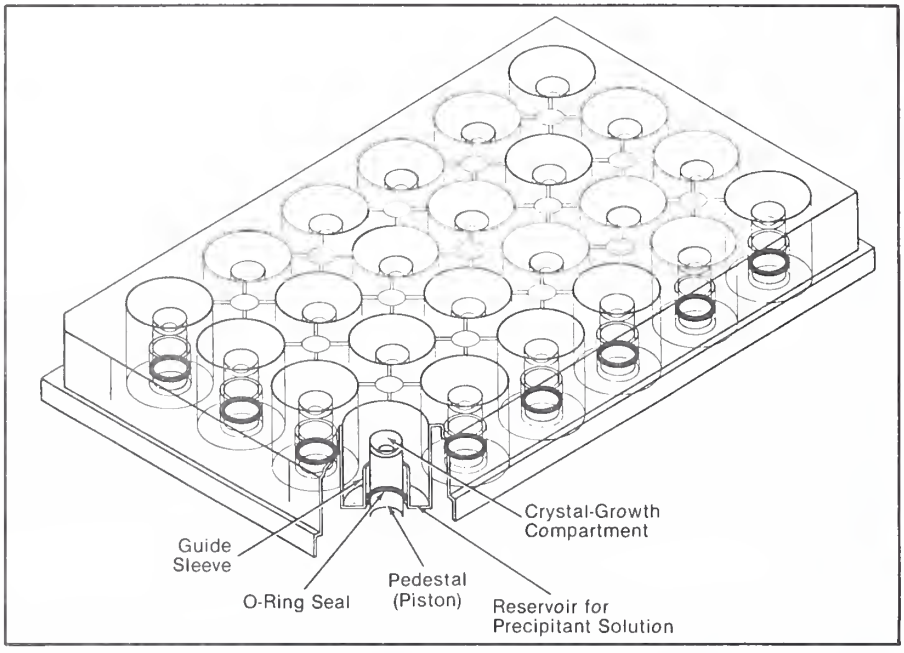

This **Compact Vapor-Diffusion Apparatus** for the growth of protein crystals would enable experimenters to initiate and terminate growth by remote or automatic control at prescribed times.

To terminate growth, a ganging mechanism under the tray would simultaneously seal the 24 crystal-growth compartments by pushing the pedestals in them up against a 12- by 8-cm strip of polypropylene tape supported under a 12- by 8- by 2-cm polycarbonate tray cover. The cover would provide additional containment for the experiment and reinforce the tape. The specimen in each chamber could be removed by simply cutting through the tape seal over the desired chamber and removing the crystals, leaving the other experiments undisturbed.

In cases in which freezing would negatively affect crystallization, the tray cover could be modified to provide an O-ring seal for each crystal-growth compartment. In this configuration, growth would be initiated when the ganging mechanism moved the pedestals away from the cover, thus allowing communication between the crystal-growth compartments and the precipitants. Growth would be terminated by using the ganging mechanism to move the pedestals back into the original sealed position. In a variant of this concept, tape would be used to seal the crystal-growth compartments both before activation and at the time of termination of growth.

This work was done by Daniel C. Carter and Teresa Y. Miller of **Marshall Space Flight Center.**

Inquiries concerning rights for the commercial use of this invention should be addressed to the Patent Counsel, Marshall Space FLight Center. Refer to MFS-28507/TN.

George C. Marshall Space Flight Center
Technology Utilization Officer Ismail Akbay
Code AT01
Marshall Space Flight Center,
AL 35812
(205) 544-2223
Patent Counsel
Leon D. Wofford, Jr.
Mail Code CC01
Marshall Space Flight Center,
AL 35812
(205) 544-0024

NASA Tech Brief
National Aeronautics and Space Administration
Ames Research Center, Moffett Field, California

Research Animal Holding Facility Prevents Space Lab Contamination

A healthy environment for both rodents and human researchers is maintained.

A research animal holding facility (RAHF) and rodent cage prevent solid particles (feces, food bits, hair), micro-organisms, ammonia, and odors from escaping into the outside environment during spaceflight. The cage (see figure) houses two rodents in separate compartments. When installed in a cage module, the cage mates with gaskets that form a barrier for internal gases and particles. In addition, the cage is maintained at a pressure slightly below ambient to prevent gases and particles from flowing outward.

A removable waste tray at the base of the cage contains a layer of porous polyester padding treated with phosphoric acid to inhibit the production of ammonia during the decomposition of rodent urine. A layer of charcoal-impregnated fibers is placed under the polyester pad to control odors. Under that is a thin, electrically charged woven-fiber pad supported by a fine screen and bottom stainless-steel grill. Urine and feces are dried by the flow of air through the tray to inhibit decomposition.

The tray can easily be removed and replaced with a clean one. An astronaut inserts a cover into the cage module to seal the tray, removes the tray, places it in a bag for later analysis and disposal, and inserts a new tray. To prevent food particles from escaping, the astronaut follows a similar procedure for removing and replacing a feeding tray.

During the removal or insertion of a cage or tray, an auxiliary high-flow centrifugal blower is turned on to generate a vigorous suction in the open module in addition to the small operating suction maintained in the module by the environmental control system. The additional inward flow helps to keep particles and gases inside until the tray or cage is returned to the module.

The cage is 1 of 12 in a cage module. An environmental control system behind the cage module circulates air through the cages, controls the temperature and humidity, exhausts filtered air to the outside environment through a charcoal bed and bacterial filter, and accepts fresh air from the outside.

The RAHF system passed a 12-day ground-based biocompatibility test. No particles larger than 150 μm and no micro-organisms in the laboratory environment outside the holding facility could be traced to the holding facility. No odors were detected by a panel of qualified subjects. No ammonia was detected, and carbon dioxide buildup was less than 0.35 percent.

This work was done by P.D. Savage, Jr., G.C. Jahns, B.P. Dalton, R.P. Hogan, and A.E. Wray of **Ames Research Center.**
ARC-12599/TN

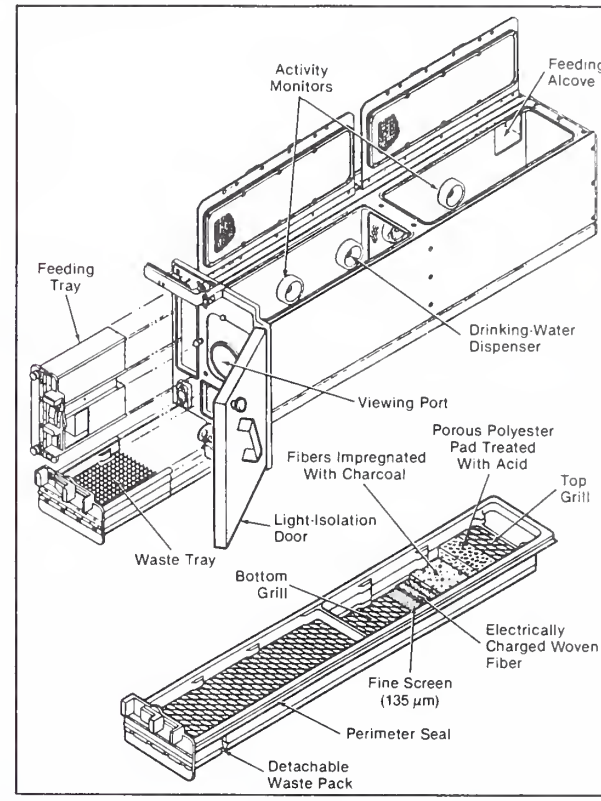

The **Rodent Cage Contains Compartments** for two animals. For each, it provides a drinking-water dispenser, a feeding alcove, and an activity-monitoring port. The feeding and waste trays are removable. The layered structure of the waste tray inhibits the generation of ammonia and the decomposition of urine and feces.

FOR ADDITIONAL INFORMATION: *Contact: Director, Technology Transfer Division, P.O. Box 8757, BWI Airport, MD 21240; (301) 621-0100 Ext. 241*
REFER TO THE NUMBER LISTED AT THE END OF THIS ARTICLE

NASA Tech Brief
National Aeronautics and Space Administration
Ames Research Center, Moffett Field, California

Software for Design of Life-Support Systems

A special-purpose computer program combines conventional mathematical models with an expert software system.

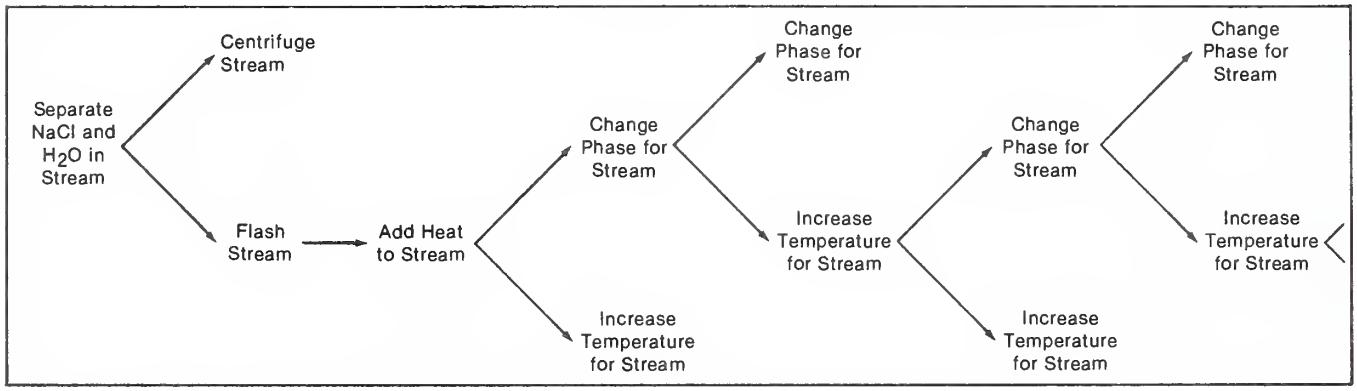

DAWN Constructs a Task Tree as it leads a user through a simulated process, offers alternatives (centrifuge stream or flash stream, for example), and indicates where an alternative is not feasible (e.g., an increase in the temperature of the stream is impossible at the first addition of heat because the water is ice at this stage and must first be melted).

The Design Assistant Workstation (DAWN) computer program is the prototype of an expert software system for the analysis and design of regenerative, physical/chemical life-support systems that will revitalize air, reclaim water, produce food, and treat waste. DAWN incorporates both conventional software for quantitative mathematical modeling of physical, chemical, and biological processes and an expert system that offers the user its stored knowledge about materials and processes. DAWN enables a user to jump from one design level to another — for example, from a detailed evaluation of reaction kinetics to an overall concept of the process to an overall energy balance.

The user can call on the conventional software for help in solving clearly defined problems for which ample data are available. Then the user can ask the expert system for qualitative, common-sense reasoning and rules of thumb in developing new concepts for which few empirical data are available.

For example, if a designer wished to consider the separation of water from salt, DAWN would propose two alternatives: centrifuging or flashing (see figure). Suppose that the designer decides to consider flashing. DAWN then leads the designer through an evaluation. It informs the designer that flashing is a viable alternative if the boiling points of the components are far away from each other. It finds that heat must be added to the stream to effect flash separation and that the first effect of the addition of heat would be a change of phase (it would not be a change of temperature; DAWN "knows" that in this case the water must first change from a solid to a liquid). DAWN continues to simulate the effect of the addition of heat and defines each change of state until the goal of separation is reached. The user can ask to see the characteristics of the mixture at any state.

This example illustrates how DAWN accepts a goal (separation), breaks it down into possible subgoals (flash, centrifuge), and simulates the effects (a sequence of states) of the process associated with the chosen subgoal (in this case, the addition of heat associated with flashing). The user can control the path of the design and simulation. For example, the path can be varied by addition of subgoals or by beginning with a higher-level goal like an incineration process or a lower-level goal like a change of phase of water.

At the process level, DAWN has a "smart front end," wherein the user defines a process in some detail, and a "smart back end," wherein the user compares the results of a quantitative simulation (based on conventional software models) with the predictions made by the smart front end. The smart back end helps the user make rough calculations, suggests basic assumptions, offers some quantitative reference data, and explains equations.

This work was done by Mary R. Rudokas and Elizabeth R. Cantwell of **Ames Research Center** *and Peter I. Robinson and Timothy W. Shenk of RECOM.* *ARC-12665/TN*

FOR ADDITIONAL INFORMATION: *Contact: Director, Technology Transfer Division, P.O. Box 8757, BWI Airport, MD 21240; (301) 621-0100 Ext. 241*
REFER TO THE NUMBER LISTED AT THE END OF THIS ARTICLE

NAVY
Domestic Technology Transfer Fact Sheet

Detection of Enzymes Using Agar Gel

The Naval Dental Research Institute (NDRI), Great Lakes, Illinois, evaluated a simple quantitative BAPNA-in-agar assay that can be employed for measuring trypsin-like activities of oral micro-organisms or applied clinically for tests of human plaque samples. Information from the clinical tests could help to identify patients undergoing changes in disease status or could be useful in monitoring the success of therapeutic measures.

Exploratory tests with the subgingival plaque samples indicated that the BAPNA-in-agar system can serve as a rapid, simple method for detecting microbial trypsin-like activity.

For Additional Information:

Backup material on this effort is available from:

Navy Domestic Technology Fact Sheet Reader Reply Service
Code E211
Naval Surface Weapons Center
Dahlgren, VA 22448-5000
(703) 663-8921

Refer to 160504/TN

NAVY
Domestic Technology Transfer Fact Sheet

Pocket Optometer Developed for Biofeedback Training

The Naval Aerospace Medical Research Laboratory (NAMRL), Pensacola, Florida, has developed a Scheiner-principle optometer for self-evaluation of accommodative state and biofeedback training. The specific advantages of the new invention over earlier optometers are: simplicity of design, hand held, portable implementation, lightweight, small size, and low manufacturing cost. The use of a monochromatic light source eliminates the effects of chromatic aberrations in the subject's eye, and effectiveness as a training aid.

Four prototypes of the optometer have been built and were used to implement biofeedback training to correct night myopia in 12 Navy aviation candidates. All subjects were emmetropic in full light. Training was limited in duration due to the transient nature of subject availability but was reasonably successful in 10 out of the 12 cases.

For Additional Information:

Backup material on this effort is available from:

Navy Domestic Technology Fact Sheet Reader Reply Service
Code E211
Naval Surface Weapons Center
Dahlgren, VA 22448-5000
(703) 663-8921

Refer to 160603/TN

Natural Resources Technology & Engineering

0964 Geographical Variations in Measured Lightning Fields—Features of local terrain affect electric fields.

NASA Tech Brief
National Aeronautics and
Space Administration

Geographical Variations in Measured Lightning Fields

Features of local terrain affect electric fields.

A brief report describes a continuing program of measurements to determine variations, caused by the local terrain, in the vertical electric fields radiated by distant lightning. The lightning electromagnetic field can be increased or decreased with respect to a nominal value, depending on the slope of the local terrain, the extent of local vegetation, and the distances, sizes, and shapes of nearby structures.

The study involves comparisons of measurements of the same lightning strokes taken at different sites. Each site is equipped with, among other things, a flat-plate antenna — essentially, a large parallel-plate capacitor that responds to frequencies up to a few MHz. The antenna at each site is mounted on the ground because in that position its gain is well defined and is simply proportional to its area.

To obtain meaningful comparisons, it is necessary to take measurements for which the nominal vertical electric fields are equal at the sites being compared. The simplest way to assure this condition is to consider data from only those lightning strokes that occur at distances from the sites much greater than the distances between the sites. The distances and/or locations of the lightning strokes can be determined by an existing lightning-locating network. Alternatively, if the lightning is not detected by the network, then the distances to the nearest clouds capable of producing lightning can be assumed to be the applicable distances and can determined by radar and/or satellite remote sensing.

This work was done by Launa Maier of **Kennedy Space Center.** *To obtain a copy of the report, "Measurement of Electromagnetic Enhancement Due to Site Nonuniformities."* *KSC-11449/TN*

FOR ADDITIONAL INFORMATION: *Contact: Director, Technology Transfer Division, P.O. Box 8757, BWI Airport, MD 21240; (301) 621-0100 Ext. 241*
REFER TO THE NUMBER LISTED AT THE END OF THIS ARTICLE

Physical Sciences

Testing & Instrumentation

0965 Magnetic Effects Measured

0966 Self-Heterodyne Laser-Spectrum Analyzer—Spectral widths of as little as 100 kHz can be measured.

0967 Modification of Catadioptric Telescope for Laser Velocimetry—A commercially available unit can be made to work well.

0968 Scanning X-Ray or Extreme-Ultraviolet Monochromator—The angle of incidence would be varied to change the wavelength of Bragg reflection.

0969 Three-Dimensional Acousto-Optical Spectrum Analyzer—Integration in the third dimension (time) yields superfine resolution.

Other Items of Interest

0925 Mathematical Model for Deposition of Soot—This model is expected to be more generally applicable than prior experimental correlations have been. (Licensing Opportunity)

NAVY
Domestic Technology Transfer Fact Sheet

Magnetic Effects Measured

The Naval Surface Warfare Center (NAVSWC), Silver Spring, Maryland, has developed a process to measure magnetic effects due to eddy currents induced in relatively large objects. A reference sensor is located to measure applied field only. Then an estimate of applied field at the locus of a plurality of measurement sensors is constructed and stored. Next, a conductive object is placed in the vicinity of the measurement sensors, in the applied field, and measurements are made of the applied field and eddy current effects. Finally, the stored estimate is used to compensate the applied field so that eddy current effects can be observed.

For Additional Information:

Backup material on this effort is available from:

Navy Domestic Technology Fact Sheet Reader Reply Service
Code E211
Naval Surface Weapons Center
Dahlgren, VA 22448-5000
(703) 663-8921

Refer to 160605/TN

NASA Tech Brief
National Aeronautics and Space Administration
Goddard Space Flight Center, Greenbelt, Maryland

Self-Heterodyne Laser-Spectrum Analyzer

Spectral widths of as little as 100 kHz can be measured.

An apparatus measures the spectral widths of the light emitted by GaAs or other narrow-linewidth diode lasers at wavelengths between 800 and 900 nm. Operating on a quasi-homodyne or self-heterodyne principle, the apparatus provides relatively high spectral resolution: it can measure spectral widths of the order of 100 kHz. In comparison, the best resolution obtainable from a Fabry–Perot etalon at wavelengths from 800 to 900 nm is about 12 MHz.

In the apparatus (see figure), the light from the diode laser under test is sent along two arms of an interferometer. An acousto-optical modulator in one arm shifts the frequency of the light in that arm by 200 MHz. The other arm is a delay line that consists of a single-mode optical fiber 1.2 km long. The outputs of the two arms are summed in an avalanche photodiode.

The output of the photodiode is viewed on a spectrum analyzer. The spectrum includes a spike at the 200-MHz beat note and a Lorentzian distribution (a measure of incoherence) around the spike. The half width at half maximum of the Lorentzian component is considered to be the spectral width of the laser light. The fine spectral resolution of this apparatus can provide data relevant to the use of AlGaAs diode lasers in such applications as coherent optical communication through free space and injection seeding of solid-state lasers. The data can also be used to explore the connection between the lifetimes and spectral widths of diode lasers.

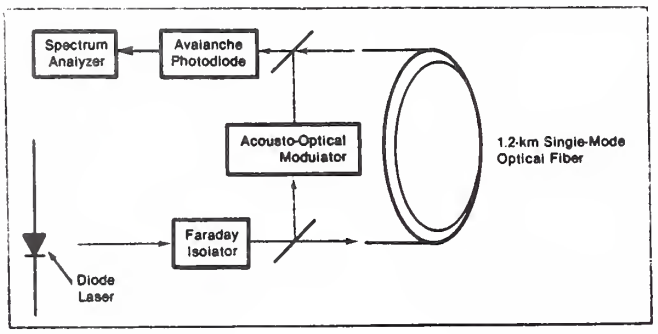

The **Heterodyne Laser-Diode Spectrometer** resolves the spectrum of a laser diode to as little as 100 kHz.

This work was done by Babak Saif and Bernard D. Seery of **Goddard Space Flight Center.** *GSC-13397/TN*

FOR ADDITIONAL INFORMATION: *Contact: Director, Technology Transfer Division, P.O. Box 8757, BWI Airport, MD 21240; (301) 621-0100 Ext. 241*
REFER TO THE NUMBER LISTED AT THE END OF THIS ARTICLE

NASA Tech Brief
National Aeronautics and Space Administration
Ames Research Center, Moffett Field, California

Modification of Catadioptric Telescope for Laser Velocimetry

A commercially available unit can be made to work well.

Computations and an experiment have shown that a Schmidt–Cassegrain catadioptric (including both reflective and refractive optics) telescope can be modified for use in dual-beam laser Doppler velocimetry. The issues involved in the modification are not trivial, because the imaging tasks in the two applications are different. The telescope in a laser Doppler velocimeter must focus two Gaussian-profile laser beams at an intersection that defines the probe volume and collect the light backscattered from the probe volume for final focusing into a photodetector. The distance from the telescope to the probe volume is typically of the order of ten times the focal length. On the other hand, a typical commercial telescope is designed for viewing objects at a distance between 50 times the focal length and infinity and is not optimized for the simultaneous beam-focusing and backscatter-collecting functions.

The modification process for a given telescope is subject to the following issues:

1. Can good performance be obtained by simply repositioning the optical components of the catadioptric telescope?
2. What are the required modifications as a function of the f-ratio? (The f-ratio is the distance between the probe volume and the corrector plate of the telescope, divided by the diameter of that corrector plate.)
3. What is the aberration limit of the modified telescope as a function of the f-ratio?
4. What is the resulting collection solid angle as a function of f-ratio?
5. How well do the modified catadioptric optics perform in comparison to a lens of similar design?

The analytical approach taken to obtain answers to these questions emphasized the use of a simple ray-tracing computer program to analyze modified optical configurations. The ray-tracing software also incorporated a Gauss–Newton optimization algorithm, which systematically varied tagged parameters until successive iterations provided less than a 10^{-6} improvement in a target value, typically a point-focus specification. This feature was quite useful in the optimization of the collector system. The root-mean-square blur of ray bundles originating at the axis vertex in the object plane and converging to a best focus in the image plane was used as an indication of the imaging performance of the optical system. Both point-focus and confocal backscatter zoom configurations were considered. Finally, a paraxial Gaussian beam-propagation calculation was made to evaluate the beam-focusing function.

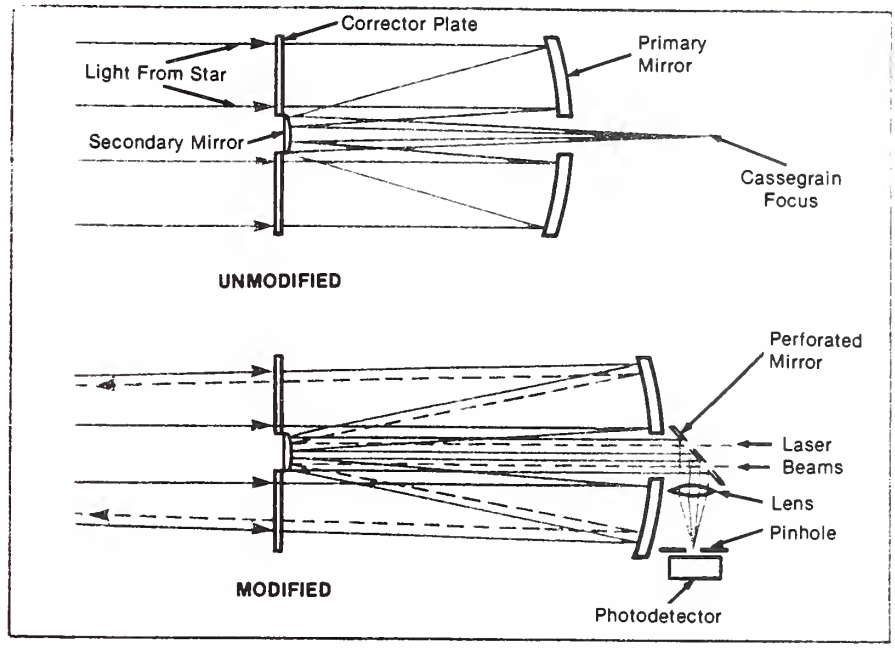

A **Schmidt-Cassegrain Astronomical Telescope** can be optimized by repositioning of its components to focus two laser beams on a nearby probe volume and confocally collect light backscattered from the probe volume.

This analytical procedure was first applied to a generic, aperture-normalized Schmidt–Cassegrain telescope that was based on an average of the specifications of several commercial units. The results of the computation showed that very good performance could be obtained for f-ratios as low as 4.0. Two relatively simple alternative modification procedures were found to maintain diffraction-limited imaging performance:

1. The three active elements (primary mirror, secondary mirror, and corrector plate) may be independently repositioned (see figure). This requires a lengthening of the telescope tube and modification of the secondary mirror mount.
2. The primary mirror may be relocated, and the secondary mirror may be replaced. This again requires a lengthening of the tube and replacement of the secondary mirror with a stock convex mirror or with a reflectively coated lens of the correct curvature.

The predicted performance of these modified telescope systems was compared with the predicted performance of large-aperture commercial lenses. The probe-volume imaging capability of the modified telescopes was found to be superior to that of the lenses for both monochromatic and dichromatic operation. Because of the central obstruction of the secondary mirror and the separation of the primary mirror from the corrector plate, the collection solid angle of the modified telescopes was considerably less than that of a lens of equivalent aperture, particularly at low f-ratio. However, the excellent imaging capabilities and large apertures of the modified telescopes offset this limitation.

The modified telescope (see figure) was also predicted to focus laser beams quite well. The negative-secondary-mirror/positive-primary-mirror combination provided a very small (high-energy-density) beam waist near the probe volume. The beam-waist and beam-intersection points were

predicted not to coincide (as is generally the case in dual-beam laser velocimetry). However, this deficiency may be treated with additional optics upbeam of the beam splitter to adjust the beam-waist location.

These promising predictions were tested in a laboratory. A 200-mm-aperture telescope was purchased and modified to the predicted optimum configuration for both point collection and dual-beam focusing. Measurements of the imaging resolution and of the diameter and location of the beam waist agreed well with the predictions.

This work was done by Stephen E. Dunagan of **Ames Research Center**. *For further information, Circle 128 on the TSP Request Card.*

This invention is owned by NASA, and a patent application has been filed. Inquiries concerning nonexclusive or exclusive license for its commercial development should be addressed to the Patent Counsel, Ames Research Center [see page 14]. Refer to ARC-12610/TN

FOR ADDITIONAL INFORMATION: *Contact: Director, Technology Transfer Division, P.O. Box 8757, BWI Airport, MD 21240; (301) 621-0100 Ext. 241*

REFER TO THE NUMBER LISTED AT THE END OF THIS ARTICLE

NASA Tech Brief
National Aeronautics and Space Administration
Marshall Space Flight Center, Alabama

Licensing Opportunity

Scanning X-Ray or Extreme-Ultraviolet Monochromator

The angle of incidence would be varied to change the wavelength of Bragg reflection.

The wavelength of peak transmission of a proposed high-throughput, narrow-band-pass x-ray or extreme-ultraviolet monochromator would be continuously adjustable. The essential filtering and reflecting components of the monochromator would be designed according to the principles described in the preceding article, "Compact X-Ray and Extreme-Ultraviolet Monochromator" (MFS-28499). However, in this case, the angle of the mirrors and, therefore, the wavelength of peak transmission (via Bragg reflection from the mirrors) would be made adjustable.

The scanning monochromator (see figure) could include one or more pairs of parallel mirrors on two or more substrates. The facing surfaces of the substrates in each pair would be coated with identical Bragg-reflecting multilayers. Each mirror would pivot about an axis parallel to its reflecting faces and would be part of a parallelogram linkage that would also include spacer bars. A motor would turn a lead screw in a threaded way on the housing of the monochromator. As the lead screw advanced, it would slide in a grooved way on one of the mirrors and would push or pull on the sides of the grooves, changing the angle of all the mirrors.

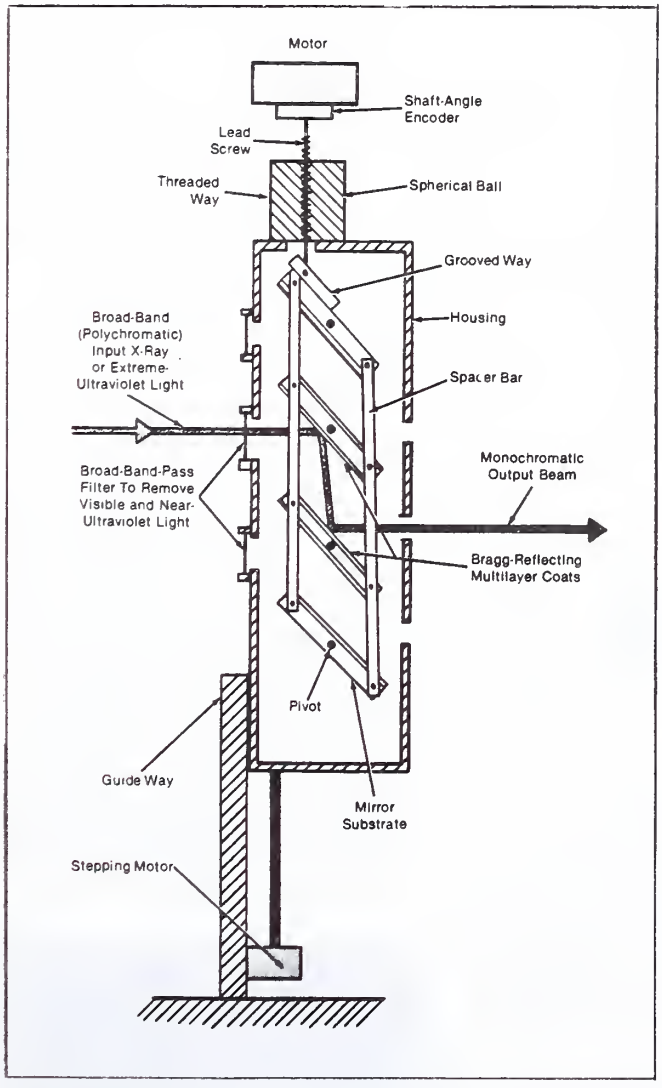

The **Scanning X-Ray or Extreme-Ultraviolet Monochromator** would feature parallel Bragg reflectors on an adjustable parallelogram linkage.

A shaft-angle encoder on the motor would send signals indicating the angle of the lead screw to monitoring and controlling equipment outside the vacuum system in which the monochromator would be operated. The external equipment would compute the angle of the mirrors and the associated peak-transmission wavelength from the encoder outputs and would use these computed values as feedback control signals during a wavelength scan.

Preferably, the mirrors would be scanned through the range of grazing-incidence angles from 30° to 60°, thereby scanning from the shortest wavelength to $\sqrt{3}$ times the shortest wavelength in the range. Because each facing pair of mirror surface could be coated with a different Bragg-reflecting multilayer, each pair of mirrors could cover a different range of wavelengths. The wavelength range would be selected by using a stepping motor to move the monochromator housing vertically along a guideway to the position in which the pair of mirrors for that range would be exposed to the input beam.

This work was done by Richard Hoover of **Marshall Space Flight Center.**

Inquiries concerning rights for the commercial use of this invention should be addressed to the Patent Counsel, Marshall Space Flight Center. Refer to MFS-28492/TN.

George C. Marshall Space Flight Center
Technology Utilization Officer Ismail Akbay
Code AT01
Marshall Space Flight Center,
AL 35812
(205) 544-2223
Patent Counsel
Leon D. Wofford, Jr.
Mail Code CC01
Marshall Space Flight Center,
AL 35812
(205) 544-0024

NASA Tech Brief
National Aeronautics and Space Administration
NASA's Jet Propulsion Laboratory, Pasadena, California

Three-Dimensional Acousto-Optical Spectrum Analyzer

Integration in the third dimension (time) yields superfine resolution.

An experimental acousto-optical Bragg-cell spectrum analyzer achieves subhertz frequency resolution. This system represents an extension to three dimensions of the two-dimensional spectrum-analyzer concept described in the preceding article, "Two-Dimensional Acousto-Optical Spectrum Analyzer" (NPO-18092). In this as in the preceding system, the first and second dimensions are the two spatial dimensions of a charge-coupled-device (CCD) imaging array. The third dimension is time, as sampled at the frame rate of the CCD array.

Figure 1 is a schematic illustration of the three-dimensional spectrum analyzer. As in the two-dimensional version, (1) the signal is first focused in one direction by a Fourier-transform lens (this is called "space integration") onto the CCD array to obtain coarse frequency resolution, then (2) the focused signal is mixed with a reference function in the form of a sampled distributed local oscillator and integrated in time on the CCD array to obtain fine frequency resolution in the perpendicular direction. The fine frequency resolution is typically about 100 Hz.

The three-dimensional spectrum analyzer includes a real-time digital image processor, which "grabs" each frame of the two-dimensional image of the spectrum produced by the space and time integrations on the CCD array. This processor performs a secondary integration in time in each fine-resolution channel over a sequence of frames. A fast Fourier transform is applied to the sequence of values in each picture element. As a result, each fine-resolution channel is resolved further into channels of subhertz width. This three-dimensional operation would be particularly useful in both quickly identifying a narrow-band radio-frequency signal within a wide initial analysis band and analyzing its subhertz spectral features.

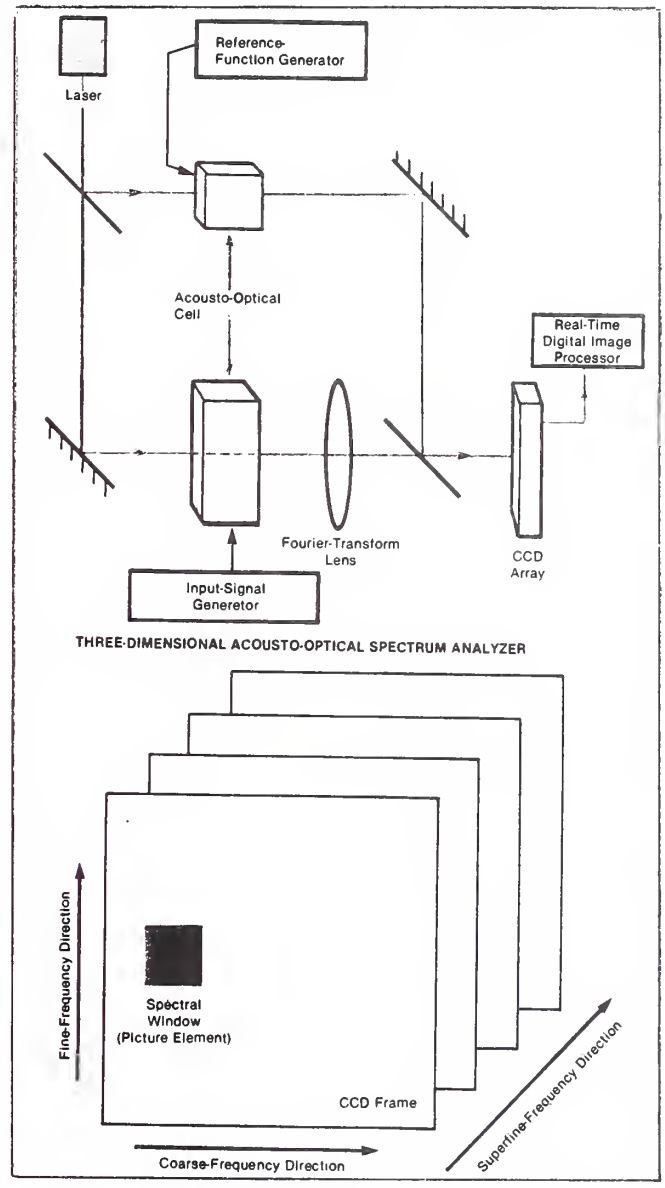

Figure 1. The **Three-Dimensional Acousto-Optical Spectrum Analyzer** is essentially a two-dimensional acousto-optical spectrum analyzer equipped with a real-time digital image processor that performs a secondary integration in time on the output of each picture element in the CCD array.

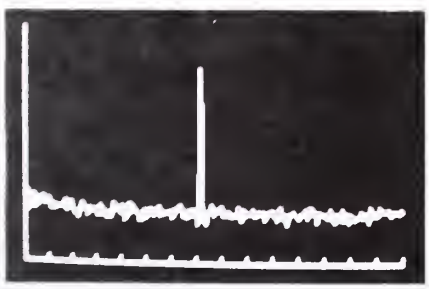

Figure 2. This Spectrum Containing a Peak was obtained by processing a 1,000,941-Hz signal through the three-dimensional acousto-optical spectrum analyzer. The horizontal scale represents frequency at 1 Hz per division.

Figure 2 shows the result of an experiment in which the three-dimensional system was used to analyze a 1,000,941-Hz signal. The CCD frame rate was 30 frames

per second, and the secondary integration in time was performed over 512 frames (about 17 seconds). The output spectral peak has a full width at half maximum of only 0.12 Hz.

This work was done by Homayoon Ansari and James R. Lesh of Caltech for **NASA's Jet Propulsion Laboratory.** *NPO-18122/TN*

FOR ADDITIONAL INFORMATION: *Contact: Director, Technology Transfer Division, P.O. Box 8757, BWI Airport, MD 21240; (301) 621-0100 Ext. 241*
REFER TO THE NUMBER LISTED AT THE END OF THIS ARTICLE

Transportation & Components

0970 Calculating Dynamics of Helicopters and Slung Loads—Motions of multiple lifting helicopters, spreader bars, cables, and loads can be simulated numerically.

0971 Electromagnetic Interference in New Aircraft—Updated standards will reflect a more severe environment and vulnerabilities of modern avionics.

NASA Tech Brief
National Aeronautics and Space Administration
Ames Research Center, Moffett Field, California

Calculating Dynamics of Helicopters and Slung Loads

Motions of multiple lifting helicopters, spreader bars, cables, and loads can be simulated numerically.

General equations have been derived for numerical simulations of the motions of multiple-lift, slung-load systems that consist of two or more lifting helicopters and loads slung from them by various combinations of spreader bars, cables, nets, and attaching hardware. The use of multiple (usually, two) helicopters to lift loads too heavy for one of them has been advocated for decades. However, with the exception of some limited flight tests and a few isolated commercial operations, the dual-lift technique remains largely undeveloped because of the complexity of motion and the consequent difficulty of stabilizing and coordinating the motion, both along the flightpath and in precise hover. New general equations are readily programmable for efficient computation of the motions; thus, they lend themselves well to the analysis and design of control strategies for stabilization and coordination.

In the mathematical model of a multiple-lift system, the helicopters, spreader bar(s), and load are treated as rigid bodies. The attaching hardware and nets are not modeled. The cables are treated as massless straight-line links that can be either inelastic (in the sense of unstretchable) or elastically stretchable. The aerodynamics of the cables are neglected. This model is expected to represent motions adequately at the frequencies up to a few hertz that are of interest in controlling the trajectories of the helicopters.

The derivation begins with the application of the Newton and Euler equations of motion to each rigid body, the definition of vectors that describe the configuration of the system, the introduction of generalized velocity coordinates, and the application of D'Alembert's principle to each body in the system. This approach leads to three formulations, two of which are generalized

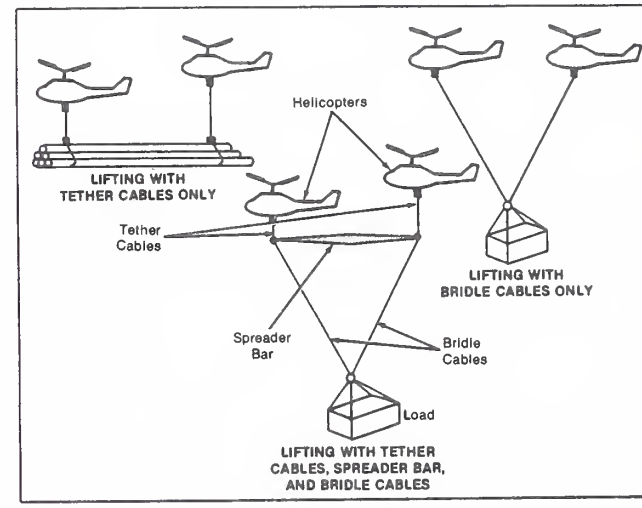

Two Helicopters Lift One Load with the help of cables and, optionally, a spreader bar. The motions of suspension systems like these are complicated and must be simulated numerically for analysis and control.

versions of formulations developed previously for specific cases involving inelastic and elastic cables. The third formulation is a new one obtained by choosing the generalized coordinates in the elastic-cable formulation in such a way that they are partitioned into (1) d coordinates that represent the motion of the system as though the cables were inelastic and (2) c coordinates that describe the component of the motion due to stretching of the cables (where c is the number of constraints that would be imposed by the cables if they were inelastic). For inelastic suspensions, the cable tensions are obtained from the equations governing the stretching-motion coordinates, and this solution is used in the equation for the remaining coordinates. In comparison with the conventional formulation, the new formulation is computationally more efficient.

The new formulation has been applied to obtain equations for the dual-lift system illustrated in the middle of the figure. The other dual-lift systems shown at the left and right can be treated as special cases of the system in the middle by appropriate simplifications of the equations to account for elimination of the bridle cables (left) or elimination of the spreader bar and tether cables (right). In each case, the equations are written in terms of the natural vectors and matrices of the dynamics of three-dimensional rigid bodies and are tractable for both analysis and programming.

This work was done by Luigi Cicolani and Gerd Kanning of **Ames Research Center**. *Further information may be found in NASA TM-102246 [N90-17641], "Equations of Motion of Slung Load Systems with Results for Dual Lift."*

Copies may be purchased [prepayment required] from the National Technical Information Service, Springfield, Virginia 22161, Telephone No. (703) 487-4650. Rush orders may be placed for an extra fee by calling (800) 336-4700.
ARC-12755/TN

FOR ADDITIONAL INFORMATION: *Contact: Director, Technology Transfer Division, P.O. Box 8757, BWI Airport, MD 21240, (301) 621-0100 Ext. 241*
REFER TO THE NUMBER LISTED AT THE END OF THIS ARTICLE

NASA Tech Brief
National Aeronautics and
Space Administration

Electromagnetic Interference in New Aircraft

Updated standards will reflect a more severe environment and vulnerabilities of modern avionics.

A report reviews plans to develop tests and standards to ensure that digital avionics systems in new civil aircraft are immune to electromagnetic interference (EMI). The plans were prompted by trends that make new aircraft more susceptible to EMI than are older aircraft:

- New aircraft incorporate more electronic "fly-by-wire" controls.
- New electronic equipment uses highly integrated circuit chips, which are more easily affected by EMI.
- New aircraft structures are built from composite materials that afford less shielding than metals do.
- Future aircraft will be exposed to increased electromagnetic energy from broadcast, communication, and radar facilities of higher power.

Until now, avionic systems for transport aircraft have been required to meet radio-frequency susceptibility standards set forth in section 20 of the document *Environmental Conditions and Test Procedures for Airborne Equipment*, RTCA DO 160B, published by the Radio Technical Commission for Aeronautics. The document calls for protection against electromagnetic fields of 1 and 2 V/m, whereas a level of 100 V/m is more realistic for such equipment as electronic engine controllers.

Accordingly, the Federal Aviation Administration (FAA) has asked the commission to revise section 20 to reflect current information on the electromagnetic environment and to develop specifications for avionics equipment at the box and system levels. The FAA has also asked the Society of Automotive Engineers to draft an advisory circular and user's manual for certification of commercial aircraft operating in the electromagnetic environment created by incidental emitters. The FAA is coordinating its efforts with those of aviation regulatory authorities in other countries to ensure that the new standards will be internationally accepted.

This work was done by William E. Larsen of **Ames Research Center**. *"Digital Avionics Susceptibility to High Energy Radio Frequency Fields."*
ARC-12161/TN

FOR ADDITIONAL INFORMATION: *Contact: Director, Technology Transfer Division, P.O. Box 8757, BWI Airport, MD 21240; (301) 621-0100 Ext. 241*
REFER TO THE NUMBER LISTED AT THE END OF THIS ARTICLE

U.S. DEPARTMENT OF COMMERCE
National Technical Information Service
Springfield, VA 22161

NTIS ORDER FORM

Use this form ONLY to order reports designated as available from NTIS.

TELEPHONE ORDERS (703) 487-4650 FAX (703) 321-8547 TELEX 89-9405

Rush Service
1-800-553-NTIS

For Subscription Questions
(703) 487-4630

For Tracing an Order
(703) 487-4660

For Editorial Questions
(703) 487-4805

If your address label on this Tech Notes is NOT correct, call the NTIS Subscriptions Department on (703) 487-4630.

1 ADDRESS INFORMATION

Last Name .....

Title .....

Company/Organization .....

Address .....

.....

City/State/ZIP .....

Telephone Number .....

2 METHOD OF PAYMENT

☐ Charge my NTIS Deposit Account .... – .....

☐ Check/Money order enclosed payable to NTIS for $ .....

☐ Purchase order **ADD $7.50 per order** (U.S., Canada, and Mexico only)

Purchase order number .....

Charge my ☐ American Express ☐ VISA ☐ MasterCard

Account Number. ..... Exp. .....

Signature .....
(Required to validate order)

3 ORDER SELECTION (Use only for reports stated as available from NTIS)

NTIS Order Number	*Price**	*Quantity*	*Total Price*
..... /NAC	.....	.....	.....
..... /NAC	.....	.....	.....
..... /NAC	.....	.....	.....
..... /NAC	.....	.....	.....
..... /NAC	.....	.....	.....
		Handling fee	$3.00
		Total	.....

NTIS PRICE SCHEDULE *

This schedule converts into actual prices the price codes cited in those Tech Notes having a report available from NTIS.

Price Code	*Price*
A01	$9.00
A02	12.50
A03	17.00
A04 through A05	19.00
A06 through A09	26.00
A10 through A13	35.00
A14 through A17	43.00
A18 through A21	50.00
A22 through A25	59.00
A99	Contact NTIS for price

These prices are for customers in U.S., Canada, and Mexico. Other addresses should write for the price listing, number PR-360-4.

Prices effective October 1, 1991

10/91

U.S. DEPARTMENT OF COMMERCE
National Technical Information Service
Springfield, VA 22161

NTIS ORDER FORM

Use this form ONLY to order reports designated as available from NTIS.

TELEPHONE ORDERS (703) 487-4650 FAX (703) 321-8547 TELEX 89-9405

Rush Service
1-800-553-NTIS

For Subscription Questions
(703) 487-4630

For Tracing an Order
(703) 487-4660

For Editorial Questions
(703) 487-4805

If your address label on this Tech Notes is NOT correct, call the NTIS Subscriptions Department on (703) 487-4630.

1 ADDRESS INFORMATION

Last Name .....

Title .....

Company/Organization .....

Address .....

.....

City/State/ZIP .....

Telephone Number .....

2 METHOD OF PAYMENT

☐ Charge my NTIS Deposit Account .... – .....

☐ Check/Money order enclosed payable to NTIS for $ .....

☐ Purchase order **ADD $7.50 per order** (U.S., Canada, and Mexico only)

Purchase order number .....

Charge my ☐ American Express ☐ VISA ☐ MasterCard

Account Number..... Exp. .....

Signature .....
(Required to validate order)

3 ORDER SELECTION (Use only for reports stated as available from NTIS)

NTIS Order Number	*Price**	*Quantity*	*Total Price*
..... /NAC	.....	.....	.....
..... /NAC	.....	.....	.....
..... /NAC	.....	.....	.....
..... /NAC	.....	.....	.....
..... /NAC	.....	.....	.....
		Handling fee	$3.00
		Total	.....

NTIS PRICE SCHEDULE *

This schedule converts into actual prices the price codes cited in those Tech Notes having a report available from NTIS.

Price Code	*Price*
A01	$9.00
A02	12.50
A03	17.00
A04 through A05	19.00
A06 through A09	26.00
A10 through A13	35.00
A14 through A17	43.00
A18 through A21	50.00
A22 through A25	59.00
A99	Contact NTIS for price

These prices are for customers in U.S., Canada, and Mexico. Other addresses should write for the price listing, number PR-360-4.

Prices effective October 1, 1991

*U.S. Government Printing Office: 1991 — 311-885/60001

- Agriculture & Food
- Computers
- Electrotechnology
- Energy
- Engineering
- Environmental Science & Technology
- Manufacturing, Machinery, & Tools
- Materials
- Medicine & Biology
- Natural Resources Technology & Engineering
- Physical Sciences
- Transportation & Components

Route To:

PENN STATE UNIVERSITY LIBRARIES
A0000720103961

EPARTMENT OF COMMERCE
nal Technical Information Service
ield, Va. 22161

AL BUSINESS
/ for Private Use, $300

AN EQUAL OPPORTUNITY EMPLOYER

BULK RATE
POSTAGE & FEES PAID
NTIS
Permit No. G-292